Rigorous results in non-equilibrium statistical mechanics

Thibaut Demaerel

Instituut voor Theoretische Fysica, KU Leuven

May 26, 2020

Acknowledgements

I'm grateful to my family for the unwavering support during the years of my PhD: this dissertation would not have been possible without the occasional reassurances of my mother Lieve and the indispensable help of my father and my sisters, Mirthe and Herlinde, in solving many practical and aesthetical household-related problems.

Many thanks are also due to my friends Heleen, Jannes, Martijn for offering encouragement and comfort in my private life. I'm indebted to the A chantar choir for providing welcome musical exomorphism from the burden of work, by allowing me to sing among its ranks.

I'm grateful to my scientific brothers and sisters in the institute for theoretical physics for many stimulating discussions during and outside of the office hours. In particular, I'm indebted to my advisor Christian Maes for displaying an unmatched openness of mind and office during his tutorship of my PhD: it was an honor and delight to work with such an accomplished scientist and to be able to interact with the vast and prolific international network that Christian established and maintained during his career. Next, I want to express my gratitude to Ward Struyve from whom I learned a thing or two about quantum foundations and Bohmian mechanics. He proved an invaluable co-worker in the brief excursion of my research towards quantum gravity, of which a glimpse is reported in chapter 7. Subsequently, I want to thank Wojciech Deroeck, whose clear vision and intellectual versatility would often perplex a mind as humble as mine. Wojciech was a notable co-author of the work reported in Section 5. Finally, I want to thank Karel Netocny for his priceless help in the earlier years of my PhD: I will remember Karel as a subdued, patient but sharp observer and researcher.

Contents

0.1 Commentaar De Bièvre 6
0.2 Commentaar Bert 6
0.3 Commentaar Aernout VE 6
0.4 Commentaar Christ 6

1 Topical introduction **13**

2 Active processes in one dimension **16**
2.1 Introduction 16
2.2 Active diffusion 19
2.2.1 Stationary density of athermal run-and-tumble processes . . . 19
2.2.2 To break or not to break time-reversal symmetry 21
2.2.3 Thermal run-and-tumble processes 24
2.2.4 Equipartition breaking 25
2.2.5 Violation of Sutherland-Einstein relation 26
2.2.6 Higher-order telegraph equation for the spatial density with multiple spin values 28
2.2.7 Arrhenius formula for run-and-tumble processes 29
2.3 Transmission of internal rotation 32

3 Active branching processes **36**
3.1 Introduction 36
3.2 Heuristics about extracting the asymptotic speed: Branched Brownian motion 39
3.3 Thermal run-and-tumble particles 41
3.3.1 The non-thermal case: $D = 0$ 43
3.3.2 Small driving speed: $c^2/b \ll D$ 44
3.4 Active Brownian particles with offspring 44
3.4.1 Effective diffusion constant 45
3.4.2 Propagation speed of front of newborn particles 46

4 Death and resurrection of a current **48**
4.1 Introduction 48

4.2 The sudden death of a current . . . 49
4.3 The effect of disorder along the backbone . . . 49
4.4 Discontinous death . . . 51
4.5 The role of dead-ends for the diffusion of independent particles . . . 58
4.6 Resurrection of a current . . . 60
4.7 Adding interaction . . . 63
4.8 Exclusion enhancing the current . . . 64
4.8.1 Uniformly bounded traps . . . 64
4.8.2 ASEP on random combs . . . 66
4.9 Attractive zero-range process on random combs . . . 68

5 Velocity kappa-distributions 70
5.1 Introduction . . . 70
5.2 Fokker-Planck equation . . . 71
5.3 Diffusive acceleration . . . 73
5.4 Power-law tails in space plasmas . . . 75
5.5 Injecting energy via negative friction . . . 78
5.6 A deterministic model for creating fast particles . . . 81
5.6.1 The non-relativistic dynamic . . . 82
5.6.2 The relativistic dynamic . . . 82
5.6.3 Dynamics including interaction with the plasma bath . . . 84

6 Stabilization of patterns by stirring 86
6.1 Introduction . . . 86
6.2 Model and mathematical setup . . . 88
6.2.1 Forces . . . 88
6.2.2 Spaces . . . 90
6.2.3 Operators . . . 91
6.2.4 Stationary density: construction and uniqueness . . . 92
6.3 The stiffness matrix . . . 93
6.4 Example: linear forces . . . 95
6.5 Smooth dependence on the driving strength . . . 96
6.6 Vector fields and rotation invariance . . . 97

6.7 Stabilization close to equilibrium . . . 98
6.8 Infinite driving limit . . . 99
6.9 Monotonicity of the stabilization for rigid driving . . . 100

7 The dark energy problem through a statistical mechanical lens 102
7.1 Introduction . . . 102
7.2 Noise-induced force: the example of thermophoresis . . . 103
7.3 Adding noise to the Friedmann equations . . . 105
7.4 Mini-superspace with dust . . . 110
7.5 Constraints: boundary conditions and scale . . . 112
7.6 Boundary conditions . . . 112
7.7 Scale . . . 113
7.8 Acceleration as a quantum effect . . . 114
7.8.1 Gaussian superposition with big bang trajectories . . . 114
7.8.2 Gaussian superposition with bouncing trajectories . . . 117
7.8.3 Airy wave train . . . 118
7.8.4 Genericity, decoherence and optics . . . 120

8 Summary and conclusions 122

9 References 125

A Arrhenius formula for run-and-tumble particles 140

B Derivation of the first-hitting time formula 143

C Waiting times on a random comb 145

D Asymptotic speed for thermal active Brownians 146

E The large-M limit 148

F Construction of the Kolmogorov operators and the Feller semi-groups 149

G Proof of Theorem 6.3 159

Commentaar

0.1 Commentaar De Bièvre

0.2 Commentaar Bert

0.3 Commentaar Aernout VE

0.4 Commentaar Christ

Historical introduction: non-equilibrium statistical mechanics towards the 21'st century

"Observe what happens when sunbeams are admitted into a building and shed light on its shadowy places. You will see a multitude of tiny particles mingling in a multitude of ways... their dancing is an actual indication of underlying movements of matter that are hidden from our sight..."

Lucretius, *On the Nature of Things*

The passage above, dating from the first century BC, indicates that the subject now known as statistical mechanics has a long history, certainly when reported observations of Brownian (or *Lucretian*) motion are accepted in the record. The first quantitative theory about a microscopic multi-particle world was submitted in 1738 by Daniel Bernoulli in his *Hydrodynamica*, which laid an early theoretical basis for the kinetic theory of gases. In this work, Bernoulli posited the argument, still used to this day, that gases consist of great numbers of molecules moving in all directions, that their impact on a surface causes the gas pressure that we feel, and that what we experience as heat is simply the kinetic energy of their motion. However, around this time the scientific mainstream diverted to caloric and continuum theories of heat and pressure. Bernoulli's work, together with notable contributions to kinetic theory due to Lomonosov, Le Sage, Herapath and Waterston (most of whom connected their research with the development of mechanical explanations of gravitation) were largely ignored for more than a century.

Jan Ingen-Housz in 1785-1786 and Robert Brown in 1827 repeated and reported extensively on the experimental observation of Brownian motion [1] and although the scientific community did not hurry to find an explanation, it seems that awareness of the phenomenon remained widespread [2]. For a long time, many researchers perceived a biological origin to the jittery motion, a fundamental 'vis viva' propelling nature's constituents. That theory is now long-extinct but in some way it has seen a resurgence by modern applications of stochastic modeling to biophysical systems: Our contribution to this resurgence is presented in Sections 2 and 3 where we show that, in contrast to passive motion, "active" Brownian motion of a particle tends to violate the Markov property, in a trapped environment it has a different escape-time distribution than the Kramers law and if the active particles

branch or reproduce (think of a colony of asexually reproducing bacteria), then the most-outlying particles advance with a speed differing from the celebrated Fisher-Petrovsky-Piskounov-Kolmogorov law [3, 4].

Returning to our chronicle, 1856 and 1857 saw an unprovoked renaissance of kinetic theory with new molecular gas models by August Krönig and Rudolf Clausius respectively. The latter inspired Maxwell to introduce his eponymous distribution for the velocities of a gas of molecules, thus introducing probability theory for the first time in physics (prior development of probability theory focused on applications in the casino, cryptography and coding, economics and Darwin's nascent evolution theory). That being said, observations in outer space have made it apparent that Maxwell's law is very fragile and easily broken when a dilute gas is energized or when it has a far-from-equilibrium history. In Section 5 we explore that issue in depth, stressing the significance of the (paradoxical) dearth in dynamical activity among the faster particles of the gas.

Under the leadership of Maxwell, Boltzmann, Clausius, Thomson, Gibbs and others, the kinetic theorists in the 1860-1905 era developed a framework with the ambition of not only giving a microscopic derivation of the laws of thermodynamics but also giving an account of irreversibility as articulated in a so-called *H-theorem*. Loschmidt's and later Zermelo's objections regarding the apparent clash between the H-theorem on the one hand and the reversibility and recurrence of the fundamental laws of mechanics on the other hand were duly appreciated. Boltzmann developed a reconciliatory explanation that seems to survive scrutiny until today [5]. It emphasizes that, in a large (classical or quantum) many-particle system, (local) equilibrium microstates are overwhelmingly more likely than non-equilibrium microstates. A system's fast exit[1] from a non-equilibrium state into an equilibrium one is then very likely while the waiting-time for a subsequent re-entry into a non-equilibrium state is unfathomable. The research program proposed by Boltzmann therefore urges to confirm this static-geometric picture of a given system's state space while investigations of the system's ergodic properties can wait for another day.

Before 1905, it was largely unresolved how far the atomistic picture and the particle-formalism of kinetic theory had to be taken with regards to actual physical reality.

[1] In a glass, that exit may not happen so fast.

Loschmidt and Maxwell went the furthest, with the latter raising the question [6] of determining the precise value of Avogadro's constant, giving the number of atoms in an agreed macroscopic quantity of matter. Maxwell's guess, aided by Loschmidt's work on liquefaction of gases,[2] was in the right ballpark but was marred by shaky chemistry-related assumptions (about the size of the involved molecules and the filling fraction in the liquid state).

It was therefore a great breakthrough when Einstein and Smoluchowski formulated their proposals in 1905-1906 to put the atomistic hypothesis to a straightforward and clean test: the prevailing kinetic theory, not supplemented by additional assumptions, actually predicted Brownian motion and that the diffusion rate of a pollen would have to be inversely proportional to the viscosity of the solvent-fluid. In a highly-viscous solution, the pollen will respond to individual collisions with atoms of the solution by moving briefly in the direction of collision, before coming to a halt because of the unrelenting viscous dissipation of its differential motion. The random displacement Δx incurred during such a single-collision event is far too short-lived and insignificant to be discernable by the experimenter in 1905. However, the passage of a sufficiently long time t allows a greater number $n(t)$ of collisions to occur at random angles, random unbiased velocity and almost independent of each-other. We learn from the central limit theorem that the net displacement $x(t) - x(0) = \Delta x_1 + ... + \Delta x_{n(t)}$ incurred by the pollen due to those collisions grows like $\sqrt{\langle(\Delta x)^2\rangle n(t)} = \sqrt{\langle(\Delta x)^2\rangle \dot{n} t}$. That quantity grows like $t^{1/2}$, which eventually grows to a macroscopically discernible size. In this form, the proportionality constant $\sqrt{\langle(\Delta x)^2\rangle \dot{n}}$ is not very informative. Einstein and Sutherland cleared that up, getting the relation

$$D := \frac{\langle (x(t) - x(0))^2 \rangle}{t} \approx \frac{RT}{3\pi\eta N_A r}, \qquad \text{(for large } t\text{)} \tag{1}$$

involving the solution's viscosity constant η, which can be independently measured by subjecting the fluid to a very small shear or by measuring the terminal velocity of the pollen in the presence of a gravitational field. So it is that the world was introduced to the paradigm of *fluctuation-dissipation* relations (FDR): systems in thermal equilibrium allow for fluctuations and the amplitude of those fluctuations is inversely proportional to a typical dissipation-coefficient related to the system. In Section 2 and 4 we will discuss when and how stirring or activating a system away from equilibrium may cause its purported FDR to fail. In Section 4 we give an

[2] In honor of Loschmidt's contributions, the German scientific community sometimes speaks of a "Loschmidt constant" in stead of the Avogadro constant.

example of a particle in a random environment in equilibrium whose FDR *ought* to hold at first glance, but it fails nonetheless if we evaluate it at large time in the same way as we did for the historical application of the Einstein-Sutherland-relation (1) to the determination of N_A. The original ambition of extracting or predicting simple-minded relations between macroscopic and slowly-evolving quantities can therefore not always be maintained.

In his famous 1908 paper on critical opalescence, Einstein continued his tour-de-force by laying the foundation of large deviations theory (with earlier notions contributed by Laplace and in the latter half of the 20'th century systematized by Donsker and Varadhan). However, for the purpose of introducing my dissertation I want to skip through to the year 1926, when Einstein hinted to a solution to the "tea-leaf paradox" and attempted to explain the patterns of meandering rivers [7]. A brief consideration of those problems reveals that the force f responsible for creating the patterns (or at least the necessary stability for the preservation of the patterns) will only evoke a reponse $r = O(f^2)$ that starts at second order in the amplitude of the applied force. Einstein's brief entry on the subject was but a grazing of the surface and was not of statistical mechanical nature. Turing submitted a similar-themed entry in 1952, this time on chemical morphogenesis. Again, the relevant equations of motion employed by Turing have a phenomenological and mesoscopic character without a proper microscopic derivation. It is fair to say that, despite notable attempts by Glansdorff, Prigogine, McLennan and others, a systematic account for non-equilibrium stability and pattern-formation remains an open problem to this day. In chapter 6, we contribute to the solution of this problem with a rigorous treatment of a toy-model very similar to the setup considered in the tea-leaf paradox: we find that stirring a certain medium away from equilibrium tends to stiffen it up. In such a circumstance, when a system parameter like a probe position is adjusted, the consequent lack of adjustment in the density of the surrounding stirred medium causes the reaction-force to the parametric adjustment to be smaller than it would have been if the medium was not stirred.

In 1931, Lars Onsager gave a unified explanation for a wide class of phenomena in response theory (e.g. the Peltier-Seebeck effect, uphill diffusion, thermophoresis...) which all carry a flavour of reciprocity: If a force F_A is normally reponsible for pushing a charge of type A (creating a current J_A) also appears to push charge of type B, then the type of force F_B that normally pushes B will also be seen to

push A. When the forces are small, the currents $J_{A,B}$ and forces $F_{A,B}$ are related through a linear response relation of the form

$$\begin{pmatrix} J_A \\ J_B \end{pmatrix} = \begin{pmatrix} L_{AA} L_{AB} \\ L_{BA} L_{BB} \end{pmatrix} \begin{pmatrix} F_A \\ F_B \end{pmatrix}$$

and Onsager specifically pointed out that $L_{AB} = L_{BA}$, i.e. the response matrix L is symmetric, provided the forces are applied to a system in thermal equilibrium (or at least with time-reversal invariance). In fluid dynamics, these reciprocal relations gave an account of the Ludwig-Soret effect, otherwise called thermophoresis: in an environment with a temperature gradient, test-particles will tend to migrate from a region of higher temperature to one with a lower temperature. In mathematical language, that can be seen as a force that results from the presence of a white noise (in the equation of motion) whose amplitude depends on the coordinates of the state-space. Inspired by that observation, we explore in Section 7 how a noise-induced force may alleviate the problem of cosmological dark energy and/or cosmic acceleration. Sticking to that problem, we explore quantum gravity toy models in the reduced minisuperspace formalism where (formally speaking) the addition to the classical equation of motion is no longer a white noise but a so-called quantum force.

Non-equilibrium statistical mechanics has continued to develop at an uneven pace after the 70'ties. The H-theorem for an 'infinitely dilute' gas was put on a rigorous basis by Lanford and Cercignani and on a similar frontier, Villani was able to elucidate the mechanism of energy-cascading in his treatment of Landau damping [8]. Ruelle, Eckman, Sinai and others made great progress in developing a theory of chaos and a somewhat contested "smooth dynamical systems" approach to non-equilibrium physics has been advanced based on those results. Starting in the 90'ties the famous fluctuation-theorems and the Jarzynski work relation were added to the scientific corpus: these results provide a finer-grained picture to irreversibility than provided by entropy-production and they moreover hold sway arbitrarily far from equilibrium. The drawback is that they do not provide much insight or lower bounds to the entropy production for large macroscopic systems, so that their usefulness is usually limited to nano-sized systems.

Throughout all this period, a plethora of models of simple interacting particle systems have been studied in increasing depth, with proofs for and understanding of laws of large numbers, CLT's and large deviation theories when the fluid's spacetime-density profile $\rho_L(x,t)$ is considered the relevant random variable and the system

size $L \to \infty$ [9, 10]. Also, phenomena of glassy behaviour [11] and single-particle (Anderson) localization proved to be ripe for mathematical treatment during this period. Paradoxically then, getting a hold on 'normal' Fourier-like heat-conduction remains quite elusive and the state-of-the-art toy-models developed to emulate it suffer from a unrealistic requirement for stochastic noise throughout the system's bulk [12, 13].

Without further ado, I will conclude this (very incomplete and cherry-picking) historical introduction to delve into the main body of this research.

1 Topical introduction

Chapters 2, 3, which are more-or-less derived from the papers [14] and [15] respectively, concern research on the ongoing exploration of active processes (a.k.a. active diffusion) and active matter. With some abstraction, active particles may be considered objects whose spatial motion is coupled to internal degrees of freedom. We refer to [16, 17] for general reviews. Typical features of the motion include its persistence in direction. Well-known examples are micro-organisms (e.g. driven by flagella, whose orientation gives the direction whereto the spatial motion is biased), Janus particles or self-propelled micro- and nanomotors where the internal degrees of freedom are coupled to a nonequilibrium environment, [18]. The orientation giving "direction" to the particle motion is governed by internal rotational diffusion (in which case we call them "active Brownian particles") or by a Poisson process ("run-and-tumble particles") over different chemo-mechanical states.

In 2, we consider the thermal and athermal overdamped motion of particles in one-dimensional geometries where discrete internal degrees of freedom (spin) are coupled with the translational motion. Adding a driving velocity that depends on the time-dependent spin constitutes the simplest model of active particles (run-and-tumble processes) where the violation of the equipartition principle and of the Sutherland-Einstein relation can be studied in detail even when there is generalized reversibility. We give an example (with four spin values) where the irreversibility of the translational motion manifests itself only in higher-order (than two) time correlations. We derive a generalized telegraph equation as the Smoluchowski equation for the spatial density for an arbitrary number of spin values. We also investigate the Arrhenius exponential law for run-and-tumble particles; due to their activity the slope of the potential becomes important in contrast to the passive diffusion case and activity enhances the escape from a potential well (if that slope is high enough). Finally, in the absence of a driving velocity, the presence of internal currents such as in the chemistry of molecular motors may be transmitted to the translational motion and the internal activity is crucial for the direction of the emerging spatial current. In chapter 3, we study various combinations of active diffusion with branching, as an extension of standard reaction-diffusion processes. We concentrate on the selection of the asymptotic wavefront speed for thermal run-and-tumble and for thermal active Brownian processes in general spatial dimensions. Comparing 1D active branching processes with a passive counterpart (which has the same effective diffusion constant and reproduction rate), we find that the active process has a smaller propagation

speed. In higher dimensions, a similar comparison yields the opposite conclusion.

In chapter 4, which is based on [19], we present our research on the current-field (or current vs. voltage) characteristic for single particles or multi-particle fluids in an environment with randomly positioned obstacles. The latter disorder may cause a first order phase transition concerning the dependence of the current on the applied field: the current drops to zero right-discontinuously when the field strength exceeds a finite threshold. The discontinuity is caused by adding a finite correlation length in the disorder. At the same time the current may resurrect when the field is modulated in time, also discontinuously: a little shaking enables the current to jump up. Finally, in trapping models exclusion between particles postpones or even avoids the current from dying, while attraction may enhance it. This type of phenomenology is sometimes summarized under the nomer "Dynamical phase transitions". Dynamical phase transitions in general refer to abrupt changes in macroscopic dynamical properties when certain applied forcings are cvaried continuously. There is a large literature on such transitions in terms of current fluctuations, especially starting from the nontrivial phase diagram for asymmetric exclusion processes; see [20] and e.g. the recent [21,22] and references therein. The approach that starts from modifying the weight of path-space histories is also closely related and brings the subject to shed light on the nature of glassy dynamics [23] and kinetically constrained dynamics [24,25]. Obviously, to allow for nonanalytic behavior in the current characteristic (e.g. as function of the driving) we need to take some thermodynamic limit, but the dynamical transitions are visible already for sufficiently large systems and as such they should to be observable in real experimental set-ups. In contrast to 1st-order transitions in equilibrium statistical mechanics, we suspect that dynamical phase transitions in the current are not accompanied by the phenomenon of phase co-existence: no "Gibbs phase-rule" for current phase-transitions.

In chapter 2, which is based on the paper [26], we turn our attention to the problem of the observed abundance of high-speed particles in the interstellar gas, relative to the low abundance that is expected at high speeds if a Maxwell or Maxwell-Jüttner distribution were to prevail there. More to the point, we introduce and study effective scenarios for the origin of heavy tails in stationary velocity distributions. A first analysis combines localization with diffusive acceleration. That gets realized in space plasmas to find the so-called kappa-distributions having power-law decay at high speeds. There, localization at high energy already takes place for the reversible

dynamics, but becomes effective by an active diffusion in velocity space. A model for vibrating granular gases and giving rise to stretched exponential tails is also briefly discussed, where negative friction is the energizer. In all cases, the resulting nonMaxwellian velocity distributions are frenetically caused by the dependence on the speed of kinetic parameters.

In chapter 6, which is based on the paper [27], we turn our attention to Einstein's tea-leaf: a dynamics in a confined, 2D, radially-symmetric vessel is considered where a heavy probe (the tea-leaf) is in contact with an overdamped diffusive medium (the surrounding water). Due to that contact, an average or systematic force develops on that probe, with a dependence on the (slowly-evolving) position of the probe. Subsequently, the surrounding diffusive medium can be stirred around the symmetry center of the setup and that affects the systematic force experienced by the probe. We prove that the introduction of the rotational stirring force in general pushes the probe more towards the middle, the symmetry center, of the vessel. This effect kicks in at second-order in the amplitude of the stirring force. When the driving is further enhanced the stabilization occurs for a wide range of rotation profiles and the induced force converges to a universal expression. The model thus provides a rigorous example of stabilization of a fixed point due to contact with a nonequilibrium medium and beyond linear order around equilibrium. This particular research comes in touch with recent efforts to understand the stabilization of fixed points for the dynamics of slow particles in contact with a fast nonequilibrium medium. Applications vary from the induced force on probes in contact with biological tissue or filaments to the motion of dust in atmospheric dynamics. While the context of probes in contact with nonequilibrium media is clearly physically interesting there are currently very few mathematical treatments and even less rigorous results [22, 28–35].

In chapter 7, which is loosely based on [36], we embark on a cosmological journey, trying to address the old and classical problem on finding an explanation for the observed acceleration in the cosmic expansion. While the so-called concordance ΛCDM model agrees to a good extent with the cosmic observations, the jury is still out on the meaning and origin of its acceleration-inducing Λ-parameter [37,38]. Our contribution starts by observing that adding Stratonovich noise to the Friedmann equations of cosmology may significantly boost the expansion of individual sample universes. In reality, this noise could be a consequence of quantum fluctuations and in that light we then quickly turn to a simplified model of quantum gravity using

a mini-superspace description of an isotropic and homogeneous universe with dust. We derive the corresponding Friedmann equations for the scale factor, which now contain a dependence on the wave function. We identify wave functions for which the quantum effects lead to a period of accelerated expansion that is in agreement with the apparent evolution of our universe, all without introducing a cosmological constant. The purpose of the present chapter is to present a clear and explicit case where the quantum contribution to the Friedmann equations can account for the observed expansion of the universe after the decoupling era, possibly even better than the concordance model itself (if the latter would prove insufficient [39]).

2 Active processes in one dimension

2.1 Introduction

In the topical introduction (Chapter 1), we already gave a qualitative description of what active particles represent. A possible quantitative model of such an active particle has its position $x_t \in \mathbb{R}$ and spin $\sigma_t \in \{-1, 1\}$ evolve according to a Markov process described under the Fokker-Planck equation according to the process

$$(\partial_t \rho)(x, \sigma, t) = -c\sigma(\partial_x \rho)(x, \sigma, t) + \eta\left(\rho(x, -\sigma) - \rho(x, \sigma)\right) \tag{2}$$

Qualitatively, this represents a particle moving along the real axis with speed c, aiming to the right whenever its orientation (or spin) $\sigma_t = 1$ and aiming to the left whenever $\sigma_t = -1$. The spin σ_t itself moves autonomously in time, mostly 'remaining constant' but at Poisson-distributed, isolated times it jumps instantaneously and (necessarily) discontinuously to the opposing value. This kind of stochastic process is sometimes called "dichotomous noise" for understandable reasons [40–42]. Of course, analogies of such dichotomous processes on the lattices can be explored as well, where they make for "persistent random walks" or a two-lane random walk. See [43] for elaboration and relevant Master equations.

To continue the present discussion, note that from (2) it follows that the unimodal densities $\rho(x, \pm 1)$ are both annihilated by the differential operator

$$\frac{\partial^2}{\partial t^2} + 2\eta \frac{\partial}{\partial t} - c^2 \frac{\partial^2}{\partial x^2}, \qquad \eta > 0. \tag{3}$$

This operator was first studied by Kelvin for calculating the impedance to be added to a cable to ensure transmission of a signal without changing its shape. Indeed, the

operator is hyperbolic and therefore engenders ballistic transport to the functions that are annihilated by it. On the other hand the limit $c^2, \eta \uparrow \infty$, keeping the ratio c^2/η constant, yields the diffusion equation: the advanced wavefront gets attenuated and its energy is lost in its wake where it spreads out at a slower diffusive pace. We refer to the review [44] for standard material and history related to applications of persistent random walks and the telegraph equation. Various versions or extensions of that telegraph equation (3) are naturally related to active motion as we will show; see also [45, 46]. Similarly, studies in colored noise such as in [47, 48] may be viewed as predecessors of the research into active particles. A more recent version of noise representing activity is in [49].
Finally yet another relation may be found in studies of spin transport; see e.g. [50–52]. There, as in the context of spintronics, spin-orbit coupling is the analogue of the active steering of translational motion through internal degrees of freedom.

In the present chapter, we take the internal degrees of freedom to be discrete, and we call them *spin* for short, so that we imagine spatial point particles that can be in a finite number of internal states (spin values). To be more specific, we introduce the class of models in one dimension that we call *active*. We only deal here with independent particles. The state space is $M = \mathbb{T} \times K$, where $\mathbb{T} \subseteq \mathbb{R}$ can stand for the circle S^1, an interval $[-\ell, \ell]$, the entire line or some discrete (lattice) version thereof. The set K is finite and contains the n possible (spin) values, In any event we call $x \in \mathbb{T}$ the (spatial) position and $\sigma \in K$ the spin. The coupled dynamics (position–spin) in the form of an overdamped diffusion in one dimension is

$$\begin{aligned} \dot{x}_t - v(\sigma_t) &= -\chi(\sigma_t)\, \frac{dU}{dx}(x_t, \sigma_t) + \sqrt{2D(\sigma_t)}\, \xi_t \\ \log \frac{k_x(\sigma, \sigma')}{k_x(\sigma', \sigma)} &= [U(x, \sigma) - U(x, \sigma') + F(x; \sigma, \sigma')]/T \\ \sqrt{k_x(\sigma, \sigma')\, k_x(\sigma', \sigma)} &= \psi(x; \sigma, \sigma') \end{aligned} \tag{4}$$

where we need to add suitable boundary conditions on x depending on the geometry. The first line contains the driving velocity $v(\sigma)$ which depends on the spin σ. A conservative coupling between position x and spin σ goes via the potential $U(x, \sigma)$. The mobility coefficient is $\chi(\sigma) \geq 0$ and $T = D(\sigma)/\chi(\sigma) \geq 0$ (independent of σ) is the temperature of a thermal environment represented by standard white noise ξ_t. (Boltzmann's constant is set to one.) The second and third line of (4) specify the transition rates for the spin. The spin follows a Markov jump process with rate $k_x(\sigma, \sigma')$ for the transition $\sigma \to \sigma'$ at fixed (spatial) position x. There is

the antisymmetric $F(x;\sigma,\sigma') = -F(x;\sigma',\sigma)$ as a possible extra source of nonequilibrium driving in spin-space. The $\psi(x;\sigma',\sigma) = \psi(x;\sigma,\sigma')$ is the symmetric activity part of the rates. The coupling of translational motion and internal spin dynamics combined with the presence of the imposed velocity v and/or of spin-driving F is what makes the motion *active*. Note also the difference with random walkers in a random environment; active particles carry the randomness related to possible bias or traps "on their back."

In the next section we start with active diffusion, both athermal and thermal, and we ask for the stationary density. That analysis intersects with recently reported results in [45]. We also discuss the reversibility or possible irreversibility in the spatial motion. In particular we find an example where the spatial motion shows time–symmetry for all stationary two-time correlation functions, but not for higher–order time–correlations. We continue with the violation of the Sutherland–Einstein relation even when the joint process is generalized reversible. At the end of that Section we give an extension of the Arrhenius law to run-and-tumble particles. The escape rate from a potential well over a barrier is computed and the dependence on the tumble frequency is manifested. In contrast with the case of pure diffusion the slope of the potential constitutes essential information for the exponential law.
In Section 2.3 we start by deleting the explicit velocity field $v(\sigma_t)$ in (4); all nonequilibrium is then caused by the presence of the antisymmetric driving F in spin-space. The natural question is to study the transmission of internal currents (for σ_t) to translational (directed) motion (for x_t), from which a velocity v would emerge. It is interesting and useful at that moment to take into account a possible dependence of the mobility χ on spin σ. In Section 2.2 the mobility $\chi(\sigma) \equiv 1$ in (4) is still constant independent of σ; in Section 2.3 we follow the idea that only at certain values of the spin it is possible for the walker to move forward or backward. In other words, the spin values give kinetic constraints (no motion at σ when $\chi(\sigma) = 0$), which is in fact also similar to what may happen in molecular motors as movement there is only possible at certain chemo-mechanical configurations of the motor. We discuss there the issues of stalling and of the direction of the translational current, and how it depends on the symmetric activity parameters.
As will appear in the next section on active diffusion the telegraph equation (3) is naturally linked to active processes. We give an extension, the thermal telegraph equation, in Section 2.2.3 (see equation (14)). We make a generalization to more than two lanes (general n in (4)) in Section 2.2.6.

Active particles have by now been studied and reviewed from many perspectives and the discussion below has overlap with various other papers to which we refer. The original contributions of the present chapter concern (1) the discussion of (broken) time-reversal invariance (Section 2.2.2), (2) the violation of the Sutherland-Einstein relation as compatible with the fluctuation–dissipation relation for generalized reversible processes (Section 2.2.5), (3) the derivation of a generalized telegraph equation for run-and-tumble processes with more than two driving velocities (Section 2.2.6), (4) the discussion on the Arrhenius law for run-and-tumble processes (Section 2.2.7), and (5) the phenomenon of stalling for kinetically constrained active particles (Section 2.3).

2.2 Active diffusion

To start we consider a single particle with position x pushed with velocity field $c_\sigma(x)$ depending on spin $\sigma = \pm 1$. In other words, we take (4) with $[v(\sigma) - \chi(\sigma)\, U'(x,\sigma)] = c_x(\sigma)$ and $k_x(\sigma, -\sigma) = k_\sigma(x)$:

$$\dot{x} = c_\sigma(x), \qquad \text{and jumps } \sigma \longrightarrow -\sigma \text{ at rate } k_\sigma(x) \tag{5}$$

where the $c_\sigma(x)$ are smooth in x with $c_+ \geq 0 \geq c_-$, $c_+ > c_-$, while the transition rates $k_\sigma(x) \geq \varepsilon > 0$ are piecewise continuous in x. The model is athermal for the moment, with $D = 0 = T$ in (4).
The evolution of the joint probability density $(\rho_+(x,t),\, \rho_-(x,t))$ is

$$\begin{aligned}(\partial_t \rho_+)(x,t) &= -\partial_x(c_+(x)\rho_+(x,t)) \\ &+k_-(x)\rho_-(x,t) - k_+(x)\rho_+(x,t)\end{aligned} \tag{6}$$

$$\begin{aligned}(\partial_t \rho_-)(x,t) &= -\partial_x(c_-(x)\rho_-(x,t)) \\ &+k_+(x)\rho_+(x,t) - k_-(x)\rho_-(x,t)\end{aligned}$$

The standard telegraph process (3) for the total density $\rho = \rho_+ + \rho_-$ corresponds to $c_\sigma = c\,\sigma$ for amplitude $c > 0$ and activity parameter $k_\sigma = a = \eta/2$ and is then easily obtained from (6).

2.2.1 Stationary density of athermal run-and-tumble processes

Stationary distributions for independent active particles have been obtained in various cases; see e.g. [16, 17]. While completing this chapter a very similar study

appeared as [45], dealing with run-and-tumble particles in one dimension. In particular, a complementary treatment of the stationary density was given there at least in the thermal case. We continue here first with the athermal case (5), which was already considered in [41, 42].

The stationary density (ρ_+, ρ_-) for (6) solves

$$\begin{cases} 0 = -(c_+\rho_+)' + k_-\rho_- - k_+\rho_+ \\ 0 = -(c_-\rho_-)' + k_+\rho_+ - k_-\rho_- \end{cases} \tag{7}$$

where boundary conditions ought to be added depending on the geometry. For example these equations are impossible to verify on the circle unless $\oint k_-\,\rho_- = \oint k_+\,\rho_+$. On the line, from adding the two equations in (7) and integrating over x,

$$c_+\rho_+ + c_-\rho_- = \text{constant } \ J \tag{8}$$

where J has the interpretation of being the total current in the direction of x. Combining (8) with (7) we get

$$-(c_\sigma\rho_\sigma)' + \frac{k_{-\sigma}}{c_{-\sigma}}\,(J - c_\sigma\rho_\sigma) - k_\sigma\rho_\sigma = 0$$

with general solution

$$\rho_\sigma(x) = \frac{e^{\phi(x)}}{c_\sigma(x)}\left[\frac{J}{2} + \sigma\,A + J\int_0^x \frac{k_{-\sigma}(x')}{c_\sigma(x')c_{-\sigma}(x')}e^{-\phi(x)}\mathrm{d}x'\right] \tag{9}$$

where A is an integration constant and ϕ is defined through

$$\phi(0) = 0, \qquad \phi' = -\frac{k_+}{c_+} - \frac{k_-}{c_-} \tag{10}$$

where boundary conditions will of course matter again for their (possible) solution. For the infinite line there may not be any stationary density.

For the dynamics on $[-\ell, \ell]$ we should let c_+ vanish at $x = \ell$ while c_- should vanish at $x = -\ell$. Then, requiring that the densities ρ_σ have a finite mass, the stationary density from (9) must have translational current $J = 0$ and we get

$$\rho_\sigma(x) = \sigma\,\frac{A}{c_\sigma(x)}e^{\phi(x)},\ A^{-1} = \int_{-\ell}^{\ell} dx\, e^{\phi(x)}\,[\frac{1}{c_+(x)} - \frac{1}{c_-(x)}] \tag{11}$$

Note that wherever $c_+(x) = -Ec_-(x) > 0$ for some constant $E > 0$ (while the k_σ remain arbitrary), the densities given by (11) are proportional to each other:

$$\rho_+(x) = \frac{A}{c_+(x)}e^{\phi(x)} = \frac{1}{E}\rho_-(x)$$

We can for example take constant $k_\sigma = a > 0$ and

$$c_\sigma(x) = \begin{cases} 0 \text{ when } x = \sigma\,\ell \\ \sigma\,c \text{ otherwise} \end{cases}$$

Then, we find

$$\rho_+(x) = \frac{1}{2 + 4\ell a/c}\left\{\delta(x-\ell) + \frac{a}{c}\right\}$$
$$\rho_-(x) = \frac{1}{2 + 4\ell a/c}\left\{\delta(x+\ell) + \frac{a}{c}\right\}$$
$$\rho(x) = \frac{1}{2 + 4\ell a/c}\left\{\delta(x-\ell) + \delta(x+\ell) + \frac{2a}{c}\right\}$$

in agreement with equation (17) in [45].

On the other hand, if we add a harmonic potential $V(x) = \kappa x^2/2$ by taking

$$\begin{cases} c_+(x) = c - \kappa x = c - V'(x) \\ c_-(x) = -c - \kappa x = -c - V'(x) \\ k_+(x) = k_-(x) = a \end{cases}$$

we must fix $\kappa = c/\ell$ for c_σ to vanish at $\sigma\ell$. Integrating (10) and plugging the result into (11) yields

$$\rho_\sigma(x) \propto \frac{(c^2 - (\kappa x)^2)^{a/\kappa}}{c - \sigma\,\kappa x} \tag{12}$$

Notice that the $\sigma = +1$ particles pile up around $\ell = c/\kappa$ while the $\sigma = -1$ particles pile up at the other side of the interval, as expected. That is an instance of breaking of Boltzmann statistics even for the position variable alone; see again under Section 2.2.4.

2.2.2 To break or not to break time-reversal symmetry

Various questions can be asked about the time-reversibility of active processes. In particular, we can ask for the entropy production, cf. [53], as will also appear at the end of Section 2.2.5. Yet, it is important to first specify precisely the question on reversibility, as we now indicate for the athermal processes above.

The simplest question is to ask whether the coupled Markov process (5) is reversible in its stationary distribution (11). That amounts to asking detailed balance for the

coupled process, which is in general not true of course. A formal but instructive proof (of that irreversibility) goes via the calculation of the generator L^* of the time-reversed process. Note that the backward generator L of the Markov process (5) acts on a function $f_\sigma(x)$ as

$$(Lf)_\sigma(x) = c_\sigma(x) f'_\sigma(x) + k_\sigma(x)\,(f_{-\sigma}(x) - f_\sigma(x))$$

Consider now the forward generator $L^\dagger$, the adjoint of L. For stationary distribution ρ in (11) and any smooth function f, e.g. with $\sigma = +$,

$$\begin{aligned}
(L^\dagger(\rho f))_+ &= -(c_+\rho_+ f_+)' + k_-\rho_- f_- - k_+\rho_+ f_+ \\
&= -c_+\rho_+ f'_+ - (c_+\rho_+)' f_+ + k_-\rho_- f_- - k_+\rho_+ f_+ \\
&= -c_+\rho_+ f'_+ - (k_-\rho_- - k_+\rho_+) f_+ + k_-\rho_- f_- - k_+\rho_+ f_+ \\
&= -c_+\rho_+ f'_+ + k_-\rho_-[f_- - f_+] \\
&= \rho_+ \left[-c_+ f'_+ - \frac{c_+ k_-}{c_-}[f_- - f_+] \right]
\end{aligned} \tag{13}$$

where (7) was used in the third step and (11) in the last step. From $L^\dagger$ we find the expression of the forward generator L^* of the time-reversed Markov process via the formula $L^\dagger(\rho f) = \rho L^* f$ when we take ρ to be the stationary density $\rho_\sigma(x)$ of (11). From (13) we thus get

$$(L^* f)_\sigma = -c_\sigma f'_\sigma - \frac{c_\sigma k_{-\sigma}}{c_{-\sigma}}(f_{-\sigma} - f_\sigma)$$

Therefore, $L \neq L^*$ in general which means that the stationary Markov process (5) is indeed not reversible.

On the other hand, the system does satisfy a *generalized* detailed balance if the velocities are antisymmetric, where we flip the spin as part of the kinematical time-reversal. Define the involution $\mathcal{I}(x,\sigma) = (x,-\sigma)$, and by extension $(\mathcal{I}f)_\sigma(x) = f_{-\sigma}(x)$. Then,

$$(\mathcal{I}L^*\mathcal{I}f)_\sigma = -c_{-\sigma} f'_\sigma - \frac{c_{-\sigma} k_\sigma}{c_\sigma}(f_{-\sigma} - f_\sigma)$$

so that $\mathcal{I}L^*\mathcal{I} = L$ when $-c_- = c_+$. In that sense, when indeed $c_\sigma = E(x)\sigma$, then the joint position-spin process is time-reversal invariant in the same way a Hamiltonian dynamics is.

Another aspect is to look at the stationary stochastic process of positions $X(t)$ (only) obtained by integrating out the spin σ. Then, the resulting or induced process is reversible, at least for the two-lane set-up treated so far. That does not need to

remain like that for $n > 2$.

To illustrate that most easily, we take a model with $n = 4$ (four lanes for spin $\sigma \in \{-2-1, 1, 2\}$) and with position on a (discrete) ring with N sites. The evolution is in discrete time given by

$$X(t+1) = X(t) + \sigma(t) \mod N$$

$$\sigma(t+1) = \begin{cases} \sigma(t) \text{ with probability } 1-\epsilon \\ G(\sigma(t)) \text{ with probability } \epsilon \text{ for} \end{cases}$$

$$G(-2) = 1,\ G(1) = 2,\ G(2) = -1,\ G(-1) = -2$$

Note that in the stationary process all states (X, σ) occur *a priori* with probability $\frac{1}{4N}$. One can also check that the probability of spin-history $\{(t, \sigma(t))\}_{0 \le t \le \mathcal{T}}$ over time $[0, \mathcal{T}]$ is the same as the probability of $\{(t, -\sigma(t))\}_{0 \le t \le \mathcal{T}}$. That implies that the probability to move forward a certain distance — starting from X_0 – in time $\mathcal{T}$ is the same as for moving backward the same distance, and in fact does not depend on that initial position X_0. Therefore, all the two-time correlations in the stationary process associated to that evolution satisfy

$$\begin{aligned} &\text{Prob}[X(t_0) = X_0,\ X(t_1) = X_1] \\ &= \underbrace{\text{Prob}[X(t_0) = X_0]}_{=\frac{1}{N}} \text{Prob}[X(t_1) = X_1 | X(t_0) = X_0] \\ &= \underbrace{\text{Prob}[X(t_0) = X_1]}_{=\frac{1}{N}} \text{Prob}[X(t_1) = X_0 | X(t_0) = X_1] \\ &= \text{Prob}[X(t_0) = X_1,\ X(t_1) = X_0] \end{aligned}$$

Looking at two-time correlations therefore, the irreversibility of the original process goes unnoticed. At the level of three-point temporal correlations however, we have e.g.

$$\text{Prob}[X(t_0) = X_0,\ X(t_0+1) = X_0+1,\ X(t_0+2) = X_0+3] = \frac{1}{4N}\epsilon$$

while for the reversed process

$$\text{Prob}[X(t_0) = X_0+3,\ X(t_0+1) = X_0+1,\ X(t_0+2) = X_0] = 0$$

That example can be mimicked in the continuous space and/or continuous time setting. To the best of our knowledge it is the most simple example of a diffusive process not showing any time-reversal breaking on the level of two-time correlations and yet being irreversible. Remark that four is the minimal number of lanes where

this higher-order irreversibility manifests itself; in a three-lane setting one seemingly again obtains a fully reversible process after integrating out the spin.

2.2.3 Thermal run-and-tumble processes

We now look at a finite temperature (T) version of (5), which corresponds to the run-and-tumble processes of [45] with $\sigma = \pm 1$. In other words we look now at (4) with $v(\sigma) - \chi(\sigma)U'(x,\sigma) = \sigma\, c$, $k_x(\sigma,-\sigma) = k_\sigma(x)$ and $D(\sigma) = T$:

$$\dot{x} = \sigma\, c + \sqrt{2T}\xi_t, \qquad \sigma \longrightarrow -\sigma \text{ at rate } k_\sigma(x) \equiv a$$

taking thus $c_+ = c \geq 0, c_- = -c$. Equation (16) in [45] gives the stationary density on a finite interval. In the transient case we have the Smoluchowski equation for the spatial density ρ which satisfies

$$(\partial_t - T\partial_x^2)^2\rho - c^2\partial_x^2\rho = -2a(\partial_t - T\partial_x^2)\rho \tag{14}$$

The derivation of (14) goes as follows:
The Fokker-Planck equation for the probability density (we still write $\rho_+(x,t) := \rho(x,\sigma=+1,t)$ and $\rho_-(x,t) := \rho(x,\sigma=-1,t)$) is given by

$$\begin{cases} \partial_t\rho_+ = \partial_x\left(-c\rho_+ + T\partial_x\rho_+\right) + a(\rho_- - \rho_+) \\ \partial_t\rho_- = \partial_x\left(c\rho_- + T\partial_x\rho_-\right) + a(\rho_+ - \rho_-) \end{cases}$$

That can be written equivalently as $L_+\rho_+ = a(\rho_- - \rho_+) = -L_-\rho_-$, where we defined the operators $L_\pm$ as

$$L_\pm\nu = \partial_t\nu - \partial_x\left(\mp c\nu + T\partial_x\nu\right) \tag{15}$$

One has

$$L_-L_+\nu = L_+L_-\nu = (\partial_t - T\partial_x^2)^2\nu - c^2\partial_x^2\nu$$

So then

$$\begin{gathered} L_-L_+\rho_+ = aL_-(\rho_- - \rho_+) \\ = a^2(\rho_+ - \rho_-) + aL_+\rho_+ - 2a(\partial_t - T\partial_x^2)\rho_+ \\ = -2a(\partial_t - T\partial_x^2)\rho_+ \end{gathered}$$

from which we conclude that

$$(\partial_t - T\partial_x^2)^2\rho_+ - c^2\partial_x^2\rho_+ = -2a(\partial_t - T\partial_x^2)\rho_+ \tag{16}$$

and one can verify that ρ_- solves it as well. So the total density $\rho = \rho_+ + \rho_-$ solves (14).

There is another instructive way to write that thermal telegraph equation. The equation (14) is equivalent to the following system for functions $\pi(x,t), \rho(x,t)$,

$$\begin{cases} (\partial_t - T\partial_x^2)\rho = \pi \\ (\partial_t - T\partial_x^2)\pi = c^2\partial_x^2\rho - 2a\,\pi \end{cases} \tag{17}$$

Defining the energy functional

$$\mathcal{H}[\pi,\rho] := \frac{1}{2}\int dx \left(\pi^2 + c^2(\partial_x\rho)^2\right)$$

one can rewrite (17) and thus also (14) as an equation of motion for (ρ,π) with a Hamiltonian plus a dissipative part,

$$\begin{cases} \partial_t\rho = \frac{\delta\mathcal{H}}{\delta\pi} - \frac{T}{c^2}\frac{\delta\mathcal{H}}{\delta\rho} \\ \partial_t\pi = -\frac{\delta\mathcal{H}}{\delta\rho} - (2a - T\partial_x^2)\frac{\delta\mathcal{H}}{\delta\pi} \end{cases}$$

One now easily verifies for example that $\mathcal{H}$ is a Lyapunov functional.
One obtains the athermal telegraph equation of the previous subsection in the limit $T = 0$.

2.2.4 Equipartition breaking

We can try to capture the active particle in a harmonic potential

$$V(x) = \frac{\kappa\, x^2}{2}$$

Recall that a particle performing a detailed-balance dynamics would assume the density $\rho(x) \propto e^{-V(x)/T}$ and would therefore have its variance converging in time to $\langle x^2\rangle_{\text{eq}} = \frac{T}{\kappa}$. The environment temperature T therefore is equal to $\kappa\,\langle x^2\rangle_{\text{eq}}$, an instance of the equipartition theorem.
For the active particle the stationary equation of motion now becomes

$$\begin{cases} 0 = \partial_x\left(-[c - \kappa\, x]\rho_+ + T\partial_x\rho_+\right) + a\,(\rho_- - \rho_+) \\ 0 = \partial_x\left([c + \kappa\, x]\rho_- + T\partial_x\rho_-\right) + a\,(\rho_+ - \rho_-) \end{cases} \tag{18}$$

One obtains three pairs of equations by multiplying (18) with $1, x$ and x^2 and integrating over $x \in \mathbb{R}$. From those six equations, one finds

$$\kappa\,\langle x^2\rangle = T + \frac{c^2}{\kappa + 2a} =: T_{\text{eff}}(\kappa) \tag{19}$$

which we can call an effective temperature, which is always greater than T as expected. For the first moments on the two lanes (so for fixed $\sigma = +1$ and $\sigma = -1$ respectively),

$$\langle x \rangle_+ = \frac{c}{\kappa + 2a} = -\langle x \rangle_-$$

which signals again that the stationary density in a symmetric trap acquires a bimodal character as a result of the activity, or shows non-Boltzmann statistics as mentioned with formula (12). Non-Boltzmann distributions have of course been observed in active particles; cf. [17,54,55], and equivalence with other *effective* equilibrium potentials is discussed in [49].

2.2.5 Violation of Sutherland-Einstein relation

To obtain the diffusion constant $\mathcal{D}$ we release the process with initial data concentrated at $x = 0$ and track $\langle x^2 \rangle(t)$ for t large. The relative probability of starting with $\sigma = 1$ or $\sigma = -1$ is not important. Multiplying equation (14) by x^2 and integrating, one gets

$$\langle \ddot{x^2} \rangle - 2c^2 = -2a \langle \dot{x^2} \rangle + 4aT$$

For $t \to +\infty$, one then obtains $\langle x^2 \rangle - (2T + \frac{c^2}{a})t \to$ Const. and the diffusion constant is

$$\mathcal{D} := \lim_{t \to \infty} \frac{\langle x^2 \rangle(t)}{2t} = T + \frac{c^2}{2a} \tag{20}$$

reproducing Eq. (12) in [45] which is obtained there from the exact expression for the time-dependent density $\rho(x,t) = \rho_+(x,t) + \rho_-(x,t)$. The expression (20) implies that there is already diffusion at zero temperature $T = 0$, making the situation reminiscent of the one in quantum mechanics; see e.g. [56]. Furthermore, comparing with (19), (20) implies

$$T \leq T_{\text{eff}}(\kappa) \leq T_{\text{eff}}(0) = \mathcal{D} \tag{21}$$

The effective temperature $T_{\text{eff}}(V)$ associated to an arbitrary confining potential V probably always falls between the same limits T and $\mathcal{D}$. The inequalities (21) then hint that the validity of a Sutherland-Einstein relation may depend on the interpretation of temperature. When taking the original temperature T it will not be met for this system, and that is easy to verify now by calculating the mobility.

To see the mean velocity (or current) $\nu = \lim_{t \to \infty} \frac{\langle x \rangle(t)}{t}$ resulting from the application of an extra electric field $\mathcal{E}$, we modify the drift $c_\sigma = \sigma\, c$ to $c_\sigma = \sigma\, c + \mathcal{E}$. A trivial

calculation then yields that $\nu = \mathcal{E}$. The mobility defined as $\mu := \frac{\nu}{\mathcal{E}}$ is thus 1. Plugging in the calculated values, one obtains

$$\frac{\mathcal{D}}{\mu T} = \frac{\mathcal{D}}{T} = 1 + \frac{c^2}{2a\,T} > 1 \tag{22}$$

so that the Sutherland-Einstein relation is broken [57]. Active particles are relatively more diffusive than their passive counterparts. (21) reveals that in (22) an ad-hoc replacement of T by an effective temperature would not have changed that verdict. Paradoxically however there is a way to argue that the fluctuation-dissipation relation still has sway, as we show next.

There is an exact expression for the mobility at finite time t. Suppose we add the field $\mathcal{E}$ at time zero, then to linear order in $\mathcal{E} \downarrow 0$,

$$\frac{1}{\mathcal{E}} \langle x_t - x_0 \rangle^{\mathcal{E}} = \frac{1}{2T} \langle (x_t - x_0)^2 \rangle^0 - \frac{c}{2T} \int_0^t ds \, \langle (x_t - x_0)\, \sigma_s \rangle^0 \tag{23}$$

That can be obtained via standard path-integration techniques; cf. [58]. We see that the last term of (23) is not zero and is responsible for the violation of the Sutherland-Einstein relation. Yet the reference distribution (where $\mathcal{E} = 0$) is generalized reversible (cf. Section 2.2.2) and for the involution $\mathcal{I}$ that was used there, the term

$$\frac{1}{T} \int_0^t ds\, \mathcal{E}\ (\dot{x}_s - c\sigma_s) \tag{24}$$

is anti-symmetric under time-reversal. The path-quantity (24) is in fact nothing else than the path-dependent entropy flux during the time $[0, t]$ in the thermal environment at temperature T due to the perturbation with $\mathcal{E}$. Observe now that the linear response (23) is given as a correlation between the observable $x_t - x_0$ and that entropy flux (24). Hence, while the Sutherland–Einstein relation is broken, at the same time we keep (23) expressing the standard fluctuation–dissipation relation as valid close-to-equilibrium. If, on the other hand, we interpret the spin as symmetric under kinematical time-reversal, then the last term in (23) corresponds to the frenetic contribution in the linear response around steady nonequilibrium, and we find the breaking of the Sutherland–Einstein relation much as expected, [58].
As a final remark here we note that we can easily calculate the second term in (23),

$$\begin{aligned} \langle (x_t - x_0)\, \sigma_s \rangle^0 &= \int_0^t du\, \langle \Big(\sigma_u\, c + \sqrt{2T}\xi_u \Big)\ \sigma_s \rangle^0 \\ &= c \int_0^t du\, \langle \sigma_u\, \sigma_s \rangle^0 \end{aligned}$$

which in the limit $t \uparrow \infty$ yields

$$\frac{1}{t}\int_0^t du \int_0^t ds\, \langle \sigma_u \sigma_s \rangle^0 = \frac{1}{t}\int_0^t du \int_0^t ds\, e^{-2a|u-s|} \to \frac{1}{a}$$

Hence, the $t \to \infty$ limit of (23) gives $\mu = \mathcal{D}/T - c^2/(2Ta)$ in accordance with (22).

2.2.6 Higher-order telegraph equation for the spatial density with multiple spin values

So far we have concentrated on run-and-tumble processes that have $n = 2$ in (4). We can however take that dynamics also with multiple lanes, $n \geq 2$. It means that the driving velocities can take more than two values but we stick to the homogeneous case where they do not depend on position and where the potential $U = 0$.

Suppose $\rho(x, \sigma; t)$ denotes the probability density for finding spin σ and position x at time t. They obey a coupled system of Kolmogorov forward-equations,

$$(P\rho)(., \sigma; .) := \sum_{\sigma'} P_{\sigma\sigma'}(\partial_t, \partial_x)\rho(., \sigma'; .) = 0 \tag{25}$$

where $P_{\sigma\sigma'}$ is a polynomial in derivatives to time t and position x and P is the $n \times n$ matrix with the operator-entries $P_{\sigma\sigma'}$. The evolution equation (25) is what you get for the densities of model (4) when $U = 0$ and $k_x(\sigma, \sigma')$ does not depend on x: with $k_x(\sigma, \sigma') = a(\sigma, \sigma')$ and escape rate $\sum_{\sigma'} a(\sigma, \sigma') = \zeta(\sigma)$, we have

$$P_{\sigma\sigma'}(G, H) = \delta_{\sigma,\sigma'}[G + v(\sigma)H - TH^2 + \zeta(\sigma)] - a(\sigma, \sigma')$$

in (25).

The $P_{\sigma\sigma'}$ are linear maps on the space of smooth spatio-temporal densities and they mutually commute under map composition, so they generate a commutative algebra. Therefore the characteristic polynomial $q(\lambda) := \det(\lambda I - P) = c_n\lambda^n + \ldots + c_0$ is well defined. When we plug the matrix P itself into that polynomial, the result is the zero matrix (as stipulated by the Cayley-Hamilton theorem [59]): $q(P) = 0$. Hence, for all smooth functions $v(x, t, \sigma)$

$$0 = q(P)v = c_n(P^n v) + \ldots + c_1 Pv + c_0 v$$

But (25) implies that $P\rho = 0$. Therefore,

$$\begin{aligned} 0 = q(P)\rho &= [c_n P^{n-1} + \ldots + c_1] \circ \underbrace{P\rho}_{=0} + c_0\rho \\ &= c_0\rho = q(0)\rho \\ &= (-1)^n(\det P)\rho \end{aligned}$$

So, for each σ,

$$[(\det P)(\partial_t, \partial_x)]\, \rho(., \sigma; .) = 0 \tag{26}$$

(provided one ascertains that densities solving (25) remain smooth if given smooth initial data). By taking the sum, for the spatial density $\rho(x,t) = \sum_\sigma \rho(x, \sigma; t)$, we thus get

$$[(\det P)(\partial_t, \partial_x)]\, \rho = 0 \tag{27}$$

If the diagonal entries $P_{\sigma\sigma'}$ in (25) are first-order in ∂_t (as is the case when the joint process is Markovian) while the off-diagonal entries are zeroth-order, then the ∂_t-order of equation (27) is equal to n, the number of spin values. The equation (27) is the generalization of the telegraph equation for general (finite) spin space.
For clarity let us illustrate it for $n = 2$ and $a(\sigma, \sigma') = a\,(1 - \delta_{\sigma,\sigma'})$ as in thermal run-and-tumble processes. Then,

$$P_{\sigma\sigma'}(G, H) = \delta_{\sigma,\sigma'}[G + c\sigma H - TH^2 - a] + a(1 - \delta_{\sigma,\sigma'})$$

and $\det\, P(G,H) = (G + cH - TH^2 + a)(G = cH - TH^2 + a) - a^2 = (G - TH^2)^2 + 2a(G - TH^2) - c^2H^2$. Putting $G = \partial_t, H = \partial_x$ we check that (27) reproduces (14). Comparing to the derivation (15)-(16), the proof of (26) really amounts to an abstraction of the process of Gaussian elimination (e.g. eliminating ρ_- to get a closed equation for ρ_+), with the only curiosity being that the relevant coëfficients are mutually commuting linear operators instead of complex numbers.

2.2.7 Arrhenius formula for run-and-tumble processes

An interesting question is to estimate the time for active particles to traverse a potential barrier. It is related to first-passage problems as considered also in [45]. Here we look at the escape time from a local minimum in the potential. The more general theory is known today as Kramers' escape rate theory but very few results are available for nonequilibrium systems. Recall that in passive diffusive systems, without driving, the expected escape time τ_p is of the form

$$\tau_p \approx C\, \exp \frac{\Delta}{T}, \qquad \text{in the regime where } \Delta/T \gg 1 \tag{28}$$

to overcome a potential-barrier of height Δ at temperature T, and C is some pre-factor which may depend on more details of the potential shape and on temperature. In this Subsection we are only after the exponential form, the so-called Arrhenius behavior, ignoring the pre-factor. However in contrast with that case of pure/passive diffusion now and naturally the shape of the potential becomes important: the

local slope must be compared with the strength of the velocity driving c. That is especially clear in the athermal case: if the slope of the potential exceeds c on the right side of a potential well and dips below $-c$ on the left side, then at $T = 0$ the particle remains localized inside the well whereas it will eventually escape when the slope remains below those thresholds. Obviously, in the passive athermal case $c = T = 0$, the particle never escapes.

To concentrate on the slope and for further simplicity we consider a linear potential $V(x) = \mathcal{E}\,|x|$ on the interval $[-h, h]$ where the potential height $V(h) = \mathcal{E}\,h$ will be taken very large while the slope $\mathcal{E} > 0$ is fixed. The dynamics for the position $x_t > 0$ of the active particle is

$$\dot{x}_t - c\sigma_t = -\mathcal{E} + \sqrt{2T}\,\xi_t$$

while σ_t is a Markov jump process on $\{+1, -1\}$ with rate $a_\pm$ for the transition $\pm 1 \to \mp 1$. There is a hard wall at the origin $x = 0$ upon which the particle reflects without having a σ-transition (In appendix A it is clarified how this is precisely implemented). At time zero $x_0 = 0$ with random initial spin $\sigma_0 = \pm 1$ and we estimate the time τ required to reach $\pm h$ where the potential has height $\Delta := \mathcal{E}h$. We show in the Appendix A that, for fixed slope $\mathcal{E} > 0$,

$$\tau(\Delta) = C\,\exp\left(\lambda_2\,\frac{\Delta}{\mathcal{E}}\right), \qquad \Delta \uparrow \infty \tag{29}$$

with $\log C$ sublinear in Δ and where, for the case $a_\pm = a$,

$$\lambda_2 = \frac{2\mathcal{E}}{3T} + 2\sqrt{p}\cos\left(\frac{1}{3}\left[\arccos\left(-q\,p^{-3/2}\right) - 2\pi\right]\right) \tag{30}$$

with

$$\begin{cases} p = 4\mathcal{E}^2/(9T^2) - B/3 \\ q = -\frac{8}{27}\mathcal{E}^3/T^3 + \frac{1}{3}B\,\mathcal{E}/T + a\,\frac{\mathcal{E}}{T^2} \\ B = (\mathcal{E}^2 - c^2)/T^2 - 2a/T \end{cases}$$

We check immediately here that for $c = 0 = a$ (passive diffusion), we get $\lambda_2 = \mathcal{E}/T$ letting (29) to reproduce the Arrhenius law (28). The general qualitative behavior can be seen from Figs. 1 and 2.

The escape time is governed by the behavior of λ_2. We can show that λ_2 decreases with temperature T and increases with $\mathcal{E}/c$. In fact $\lambda_2 \uparrow \mathcal{E}/T$ as $a \uparrow \infty$, and $\lambda_2 \downarrow [\mathcal{E} - c]/T$ as $a \downarrow 0$ when $\mathcal{E} \geq c$. In general λ_2 remains between those two limits.

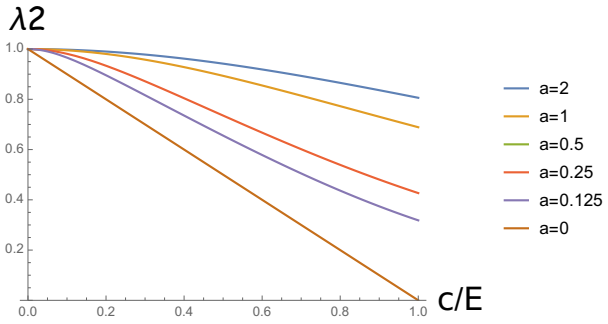

Figure 1: See formula (29). The plot gives λ_2 for $\mathcal{E} = T = 1$ as function of the driving $c/\mathcal{E}$ for various amounts of persistence. The escape time (29) decreases with $c/\mathcal{E}$, and faster for larger persistence $\propto 1/a$. The ordering of the graphs (from top to bottom) agrees with the order of the labels in the legend.

They correspond to the values where the barrier height is either $\Delta_- := (\mathcal{E} - c)h > 0$ or is $\Delta = \mathcal{E}h$ for passive diffusion (again, for h large and $\mathcal{E}$ fixed):

$$\tau_T^p(\Delta_-) \leq \tau(\Delta) \leq \tau_T^p(\Delta)$$

with the superscript "p" refers to passive diffusion (at temperature T). Especially the upper bound is not evident, as it says that activity helps the escape from a potential well and is also illustrated in greater details in Figs. 1 and 2.
If we take a passive diffusion with effective temperature $T_{\text{eff}} = T + \frac{c^2}{2a}$ as suggested by (20) and (22), it always yields a smaller escape time than for the active diffusion at the physical temperature, but giving a good approximation for small persistence times ($a \to \infty$):

$$\tau_{T_{\text{eff}}}^p(\Delta_-) \leq \tau(\Delta), \qquad \lambda_2 - \frac{\mathcal{E}}{T_{\text{eff}}} = O\left(\frac{\mathcal{E}c^4}{a^2T^3}\right)$$

as is illustrated in the lowest curve in Fig.2.

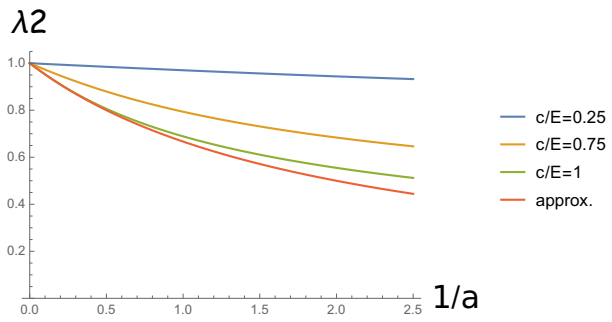

Figure 2: λ_2 as function of persistence $1/a$ for several driving amplitudes $c/\mathcal{E}$ while again $\mathcal{E} = T = 1$. Larger driving decreases the escape time (29) for all values of persistence. The lower curve is $1/a \mapsto \frac{\mathcal{E}}{T+\frac{c^2}{2a}}$, in good agreement for small persistence, here compared with λ_2 for $c = 1$. For large persistence the asympotic values are $(\mathcal{E} - c)/T$. The ordering of the graphs (from top to bottom) agrees with the order of the labels in the legend.

The result (29) remains valid when $a_+ \neq a_-$ with λ_2 being the middle (real) root of the polynomial

$$p(\lambda) = \lambda^3 - 2\frac{\mathcal{E}}{T}\lambda^2 + \left[\frac{\mathcal{E}^2 - c^2}{T^2} - \frac{a_+}{T} - \frac{a_-}{T}\right]\lambda + \frac{1}{T^2}\left[a_+(\mathcal{E} + c) + a_-(\mathcal{E} - c)\right]$$

Formula (30) gives that root in the case $a_- = a_+ = a$.
If the transition rates comes to favour more the "faster" lanes and penalizes more the slower ones, then the escape time τ gets smaller. On the other hand, if the slope gets $\mathcal{E}$ gets too small in the sense that

$$0 < \frac{\mathcal{E}}{c} \leq \frac{a_- - a_+}{a_- + a_+}$$

then the escape becomes ballistic (i.e $\tau \propto h$) and $\lambda_2 \downarrow 0$. That slope dependence in the Arrhenius exponential is of course impossible for passive diffusion.

2.3 Transmission of internal rotation

So far we have been following mostly the set-up of run-and-tumble processes. The model (4) is however richer. All the nonequilibrium driving can for example be delegated to the spin space. In that case we delete the driving velocity, putting $v(\sigma) = 0$, and we hope it emerges effectively. We are then dealing with model (4)

taking the form

$$\dot{x}_t = -\chi(\sigma_t)\,\frac{dU}{dx}(x_t,\sigma_t) + \sqrt{2\chi(\sigma_t)\,T}\,\xi_t \tag{31}$$
$$\log\frac{k_x(\sigma,\sigma')}{k_x(\sigma',\sigma)} = \frac{1}{T}\,[U(x,\sigma) - U(x,\sigma') + F(x;\sigma,\sigma')]$$
$$\sqrt{k_x(\sigma,\sigma')\;k_x(\sigma',\sigma)} = \psi(x;\sigma,\sigma')$$

We repeat that the F may break global detailed balance, by introducing an internal rotation in spin space. In the simplest situation, for $n > 2$, we may take $\sigma \in \mathbb{Z}_n$ (discrete ring) and put

$$F(x;\sigma,\sigma\pm 1) = \pm\varepsilon, \qquad F(x;\sigma,\sigma') = 0 \text{ if } \sigma' \neq \sigma \pm 1$$

for nonequilibrium amplitude $\varepsilon > 0$. Similarly for the symmetric activity parameter we may put

$$\psi(x;\sigma,\sigma') = \phi_\pm(\sigma,\varepsilon) > 0, \qquad \text{for } \sigma' = \sigma \pm 1$$

and zero otherwise. The first main question is then to understand if and how the internal rotation (on the spin ring $\mathbb{Z}_n$) gives rise to a spatial rotation for $x \in S^1$ on the circle. An easier case is obtained under the quasi-static limit where the spin-relaxation (for fixed x) to its (nonequilibrium) stationary distribution is much faster than the spatial motion. For simplicity let us put still mobility $\chi(\sigma) = 1$ constant and assume that $\phi_\pm(\sigma,\varepsilon) \gg 1$. In the limit where the spin relaxes much faster than the position x_t, the equation of motion (31) for the position becomes

$$\dot{x}_t = f(x_t) = -\sum_\sigma \frac{dU}{dx}(x_t,\sigma)\;\rho(\sigma|x_t) + \sqrt{2\,T}\,\xi_t$$

for effective force $f(x)$, and $\rho(\sigma|x)$ is the stationary distribution on the spin σ for a given position x on the circle. For $\varepsilon = 0$ (equilibrium case) that effective force is derivable from a potential and the particle moves in a free energy landscape $\mathcal{F}(x) = -T\log\sum_\sigma \exp -U(x,\sigma)/T$. In general however (with $\varepsilon \neq 0$), the effective force is not derivable from a potential and has a rotational part $\oint f(x)dx \neq 0$. In that case the steady spatial motion (on the circle) will show a current, transmitted from the rotation in spin-space. The characteristics of that motion, e.g. direction and stability of fixed points, is strongly dependent on the choice of the activity parameter $\phi_\pm$ and how it varies with the driving ε. We do not pursue that line here and some examples are given in [60, 61].

Instead we simplify the model mathematically to observe the effect beyond the quasi-static limit. At the same time we take serious the possible influence of spin-dependent mobility $\chi(\sigma)$. The point is that spatial motion often (in the so called power stroke for molecular motors) is possible at all only from certain internal states, i.e., $\chi(\sigma) = 0$ for most spin states σ. To make the point more clearly we put the position x_t also on a discrete ring and we study motion on structures which resemble necklaces as in Fig.3, [62]. There we see heptagons of internal spin states, $\sigma \in \mathbb{Z}_6$. To

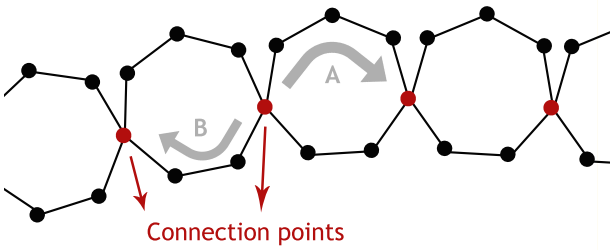

Figure 3: Internal states making the pearls on a necklace. Here 6 internal states are associated to each discrete position. Trajectory A expends as much entropy as trajectory B, leaving it undecided by the Second Law whether the spatial motion will be towards the right or towards the left. Here 6 internal states are associated to each discrete position. [Courtesy M. Stichelbaut, [62].]

be specific and referring to Fig.3 for the general situation, we think of the connection points being the possible spatial positions and there are exactly three internal states (out of the 6 in Fig.3) allowing movement to another spatial position. Let us now fix the Markov jump process by giving the transition rates over each bond in Fig.3. Supposing that there are ℓ bonds in trajectory A and m bonds in trajectory B, we put for all bonds in trajectory A, the jump rate $k(\sigma, \sigma \pm 1) = \exp(\pm m\varepsilon)$ and for all bonds in trajectory B, $k(\sigma, \sigma \pm 1) = \varphi \exp(\pm \ell\varepsilon)$. Note that the entropy flux for a journey along trajectory A is equal to the one associated to trajectory B:

$$\frac{k(x,0,1)k(x,1,2)\cdots k(x,\ell-1,\ell)}{k(x,\ell,\ell-1)\cdots k(x,2,1)k(x,1,0)} = \exp \varepsilon$$

for the trajectory A and a similar calculation for the trajectory B.

At every vertex, any outflow through some bond is exactly compensated by an inflow through a bond on the opposite side. As a consequence, the stationary density ρ is

uniform. The physical current (say to the right in Fig.3) is then given by

$$\begin{aligned} J_{\rightarrow}(\varphi,\varepsilon) &= \rho\left\{\exp(m\varepsilon)-\exp(-m\varepsilon)\right\} \\ &-\rho\left\{\varphi[\exp(\ell\varepsilon)-\exp(-\ell\varepsilon)]\right\} \\ &= 2\rho\left\{\sinh(m\varepsilon)-\varphi\sinh(\ell\varepsilon)\right\} \end{aligned}$$

It is clear from that expression that

1. When $\ell = m$, (symmetric pearls), $J_{\rightarrow}$ is only zero when $\varepsilon = 0$ (equilibrium) or $\varphi = 1$, ε arbitrary.

2. When $\ell > m$, the current vanishes when either $\epsilon = 0$ or otherwise when $\varphi = \frac{\sinh(n\varepsilon)}{\sinh(m\varepsilon)}$. Inverting the latter relation, we see that for all φ strictly between 0 and 1, there exists a $\varepsilon_{crit}(\varphi)$ such that $J_{\rightarrow}(\varphi, \varepsilon_{crit}(\varphi)) = 0$ (stalling).

We thus see that for fixed driving ε the direction of the spatial current reverses as a function of the symmetric activity rate φ. A similar dependence on the activity parameter has been shown in the model 3C in [63].

3 Active branching processes

3.1 Introduction

Speed selection in reaction-diffusion processes has been studied since more than 70 years. The best-known example occurs in the Fisher–KPP equation, [3, 4],

$$\partial_t u = D\,\partial_{xx}^2 u + \alpha\, u(1-u) \tag{32}$$

for the density $u(x,t)$ of particles as a function of position $x \in \mathbb{R}$ and time $t \geq 0$. The parameter α couples the diffusion with the nonlinear reaction part. A standard set-up has the process starting from $u(x,0) = 1$ for $x < 0$ and $u(x,0) = 0$ for $x > 0$. Then, the nonlinear reaction part ensures the convergence asymptotically in time to a traveling wave solution of (32), $u(x,t) \to w(x - v^* t)$, where for $\alpha > 0$ the front of particles invades the unstable empty state with a deterministic speed v^* appearing in the large time limit. That front speed v^* can be calculated as the minimum possible speed in the linearized equation around the unstable state; see e.g. [64–68]. Given the context of reaction–diffusion processes however, it is natural to ask what happens when also the diffusion part of the particle motion becomes *active* as understood in nonequilibrium statistical mechanics and as was recently studied in a variety of problems such as including [14, 16–18, 45, 69]. By 'active' we indeed mean the presence of an internal degree of freedom which couples with the translation degree of freedom in such a way as to break time-reversal invariance of the process. Such processes have been studied in a large variety of contexts, e.g. for stochastic models underlying the telegraph equation [40, 44], and are also known as (continuous time) correlated random walks; see also the references in [70]. Studies have been made both on the mathematical and on the physical side of the question, cf. [71–75], and the mathematical modeling has for example also been used in epidemics and biology, cf. [70, 76]. Many results on generalizing reaction-diffusion systems beyond the classical Brownian diffusion processes are found in [77]. The new results we add here in the context of active reaction-diffusion processes are for thermal run-and-tumble particles in one dimension, and for active Brownians in all dimensions. Each time we compare the asymptotic speed with the one for passive reaction–diffusion processes running with the same effective diffusion constant. For 1-dimensional processes we find that the asymptotic speed is generally lower, except when the dynamics becomes Gaussian as in activated Ornstein-Uhlenbeck processes. On the other hand, in higher dimensions (a case pioneered in [78]) the speed turns out to be higher. Such results are quite general as can be seen also in the cases studied

e.g. in [74, 75].

A priori the combination of active diffusion and chemistry can be done in many ways. Purely on the level of differential equations for the density profile but physically *ad hoc* we could replace the (passive) diffusion part in (32) with its *active* counterpart as for example copied from the telegraph equation,

$$\frac{1}{2\varepsilon}\,\partial_{tt}^2 u + \partial_t u = D\,\partial_{xx}^2 u + \alpha\, u\,(1-u) \tag{33}$$

For $\alpha = 0$ we have here the telegraph equation, [44, 79]. The extra parameter ε is an inverse persistence time. When the persistence time goes to zero, $\varepsilon \uparrow \infty$ keeping α and D fixed, we are back to the case of (32). There is indeed bio-mathematical work done on this equation; see e.g. [40]. However, (33) is not the equation one naturally obtains when starting from a biophysical process on the more mesoscopic level which motivates the problem originally. The reason is that for the active processes we have in mind here, the particles are carrying internal degrees of freedom, like what is called a spin or a rotation angle etc. Only jointly, taking position and internal degrees of freedom (extra dimensions) together, is the dynamics autonomous in terms of a Markov process or a first order in time Smoluchowski-Fokker-Planck equation. When integrating out the extra degrees of freedom, the additive structure between diffusion and reaction as in (33) may disappear. To illustrate that, we take a binary spin degree $\sigma = \pm 1$ for simplicity. The stochastic Markov dynamics involves independent particles each with position $x_t \in \mathbb{R}$ and (internal) spin $\sigma_t \in \{+1, -1\}$. Each of the particles moves independently with

$$\dot{x}_t = c\,\sigma_t, \qquad \text{and} \;\; \sigma_t \to -\sigma_t \text{ at rate } \epsilon \tag{34}$$

where $c > 0$ and $\epsilon \geq 0$ are parameters. Furthermore each particle (whatever its spin) at exponential time with rate $\alpha \geq 0$ creates a new particle at the same position and with (new) spin ± 1 with equal probability. The time-dependent density of noninteracting particles at x with spin σ is denoted by $\rho_\sigma(x,t)$. The evolution of the joint particle density $(\rho_+(x,t),\, \rho_-(x,t))$ is therefore

$$\begin{aligned}(\partial_t \rho_+)(x,t) &= -c\partial_x \rho_+(x,t) + \epsilon\,(\rho_-(x,t) - \rho_+(x,t)) + \alpha\rho(x,t)\\ (\partial_t \rho_-)(x,t) &= c\,\partial_x \rho_-(x,t) + \epsilon\,(\rho_+(x,t) - \rho_-(x,t)) + \alpha\rho(x,t)\end{aligned}$$

In the right-hand of (3.1), the first term is the ballistic transport with driving speed c and the second term refers to the flipping of the spin at rate ϵ. The last term in

each of the two equations is a pure birth (no death) at rate α out of the total local density $\rho(x,t) = \rho_+(x,t) + \rho_-(x,t)$.
By summing and subtracting the two equations and taking another time-derivative we readily obtain the closed equation,

$$(\partial_{tt}^2\rho)(x,t) + 2(\epsilon - \alpha)\,\partial_t\rho(x,t) = c^2\partial_x^2\rho(x,t) + 4\epsilon\,\alpha\,\rho(x,t) \tag{35}$$

As in (33), for $\alpha = 0$ that is the telegraph equation. Since the chemistry for (35) is trivial, -unsurprisingly- the equation lacks a non-linear contribution. More importantly however, we see that the chemistry of the initial model (35) (births with rate α) influences the effective persistence in (35). For small persistence, $\epsilon \uparrow \infty$, and with $c^2 = 2\epsilon\,D$ we get back the linearized F–KPP equation (32) with birth rate 2α. For large persistence however we see that the prefactor $\epsilon - \alpha$ becomes negative. Interactions between particles and more chemistry can even change the equations more drastically. We refer here also to [80] for the derivation of active reaction–diffusion processes.

With $\alpha = 0$ the evolution (3.1) describes active diffusion with effective diffusion constant

$$D_{\text{eff}} := \lim_{t\to\infty} \frac{\langle (x_t - x_0)^2\rangle}{2t} = \frac{c^2}{2\varepsilon}$$

as understood in the telegraph equation and its relation with correlated random walk [44, 79]. With $\alpha > 0$ there is a large class of positive traveling wave solutions $\rho(x,t) = w(x - vt) = e^{\lambda(v)(x-ct)}$, where the infimum for the possible values of v is found to be

$$v_{\min} = \begin{cases} \frac{2c}{\alpha+\varepsilon}\sqrt{\alpha\,\varepsilon} \text{ when } \alpha \le \varepsilon \\ c \text{ when } \alpha > \varepsilon \end{cases}$$

Notice then that

$$v_{\min} < 2\sqrt{D_{\text{eff}}\alpha} \tag{36}$$

which (by virtue of the F-KPP-result where $v_{\text{FKPP}} = 2\sqrt{D\,\alpha}$) means that the active diffusion with reproduction has a smaller overall propagation speed than the corresponding passive diffusion with diffusion constant $D = D_{\text{eff}}$; see e.g. [14]. The inequality (36) is already known since longer; see e.g. [77].
We will see that (36) remains true for thermal run-and-tumble processes in one dimension (Section 3.3), but the inequality gets reversed for active Brownian motion in dimension $d \ge 2$ as shown in Section 3.4.

As a side-note, notice that (36) approaches equality in the limit where $\varepsilon \to \infty$, keeping $\frac{c}{\sqrt{\varepsilon}}$ and $\alpha =$ constant. In this limit, the system approaches a Gaussian branching process (branching Brownian motion). It is easy to see that for Gaussian processes the equality $v_{\min} = 2\sqrt{\alpha D_{\text{eff}}}$ always holds, as can be verified readily for example for Ornstein-Uhlenbeck-activated particles that branch at a rate α and whose offspring inherit the same position and velocity as the parent at the time of birth. The global branch density $u(x, v, t)$ then evolves according to

$$\partial_t u = -v\partial_x u + D_x \partial_x^2 u + \partial_v \left(\gamma v u + D_v \partial_v u\right) + \alpha u$$

This dynamics possesses Gaussian solutions with marginal $\overline{u}(x,t) := \int_{-\infty}^{+\infty} u(x,v,t)dv$ of the form

$$\overline{u}(x,t) = \frac{1}{\sqrt{2\pi\sigma^2(t)}} \exp\left(-\frac{x^2}{2\sigma^2(t)}\right) \exp(\alpha t)$$

for some time-dependent variance $\sigma^2(t)$. The wave-front position $x_C(t)$ defined by

$$\overline{u}(x_C(t), t) = C$$

shows the asymptotic speed

$$v_\infty = \lim_{t\to\infty} \frac{|x_C(t)|}{t} = 2\sqrt{D_{\text{eff}}\,\alpha} \tag{37}$$

We start in the next Section with general ideas about speed selection including the issue of linearization and of taking different definitions for the speed, as we encountered already above. Sections 3.3–3.4 give explicit results about the minimal speed of the traveling wave for linearized active reaction-diffusion models with small driving speed.

3.2 Heuristics about extracting the asymptotic speed: Branched Brownian motion

This section continues the introduction but adds some technical clarifications on method or strategy. We aim here to make the chapter 3 self-contained; more details and more references in this context can be obtained from [77].

For understanding speed selection in reaction-diffusion processes, we can rely on various definitions. As mentioned under Eq. (32) we are interested in the speed of a moving front of newborns, but there are different options that nevertheless often coincide to leading order in time. To be more specific we remind ourselves of a well-studied case; many things remain formally unchanged from then on. E.g. the

nonlinearity in the equation (32) (and others to come) may be due to applying saturation or interaction effects; yet, the density of newborns at any moment remaining very small, we are allowed to ignore the nonlinearity for the purpose of speed selection.

A branching Brownian particle starts alone at $x = 0$ at time $t = 0$. The diffusion constant is D and the reproduction rate is α. Newborn particles are always spawned at the instantaneous position of the parent and they will diffuse and reproduce under the same evolution law.
Then the global branch density ρ, defined by demanding that the expected number of branches in the arbitrary interval $[a, b]$ equals $\int_a^b \rho(x,t)\mathrm{d}x$, solves

$$\partial_t \rho = D\partial_x^2 \rho + \alpha\rho \tag{38}$$

subject to the initial condition $\rho(x, t = 0) = \delta(x)$.
Hence,

$$\rho(x,t) = \frac{1}{\sqrt{4\pi D t}} e^{-\frac{x^2}{4Dt}+\alpha t} = \sqrt{\frac{\alpha}{4\pi D}} e^{-\frac{x^2}{4Dt}+\alpha t-\frac{1}{2}\log(\alpha t)}$$

and the density ρ acquires the constant value $\sqrt{\frac{\alpha}{4\pi D}}e^C$ along the line $t \mapsto (\pm x_C(t), t)$ where

$$x_C(t) = \pm\sqrt{4\alpha D t^2 - 2Dt\log(\alpha t) - Ct} \underset{t \text{ large}}{\approx} 2\sqrt{\alpha D}\, t - \frac{1}{2}\sqrt{\frac{D}{\alpha}}\log(\alpha t)$$

It provides a first definition of a speed $x_C(t)/t$. Yet it compares well to the speed of (random) position $x_{\max}(t)$ of the rightmost branch; see [3, 4, 64–66]. In particular, it gives the correct asymptotic velocity

$$v_\infty := \text{a.s.} \lim_{t\to\infty} \frac{x_{\max}(t)}{t} = 2\sqrt{\alpha D} \tag{39}$$

We can even correctly guess that the correction to the linear term in t is logarithmic, although the pre-factor turns out to be too small by a factor of 3 [66].
Another method how we could have extracted (39) is by looking for a running-wave solution $\rho(x,t) = e^{-\lambda(x-vt)}$ to (38). Plugging in, we get the possibilities

$$\lambda_\pm = \frac{v \pm \sqrt{v^2 - 4\alpha D}}{2D}$$

If $v < 2\sqrt{\alpha D} =: v_{\text{FKPP}}$, we are then unable to construct a positive traveling-wave solution. If $v > v_{\text{FKPP}}$, there are $\lambda_+ > \lambda_{\text{crit}} := \frac{v_{\text{FKPP}}}{2D} = \sqrt{\frac{\alpha}{D}}$ and $\lambda_- < \lambda_{\text{crit}}$. There is indeed a way to understand why in both cases, either for small λ or for large λ in the initial pattern $\rho(x, 0)$ the traveling-wave solutions have a velocity greater than v_{FKPP}:

- Small λ: in this case the initial density profile has a heavy tail at large $x > 0$. The higher velocity finds its origin in the offspring of those particles that started off in a relatively advanced position to begin with, without requiring a particularly large fraction of particles to move faster than v_{FKPP}.

- Large λ: in this case the initial density profile has a heavy tail for $x < 0$. The offspring there is so numerous that the exceptional particles which move forward faster than v_{FKPP} are still numerous. Moreover, these pioneers enter regions which are very sparsely populated and therefore they cause a large relative increase in the density there. Together, this allows for an overall velocity greater than v_{FKPP}.

From that line of thinking, one could expect more generally that the minimal speed $v_{\min}$ attainable within the class of positive traveling wave solutions is always going to be larger than or equal to the propagation speed v_∞ of the descendants of one single particle. For the simple case of passive diffusion that we just discussed, we arrive at the surprise that $v_{\min} = v_\infty$. We therefore still advance the hypothesis that the asymptotic velocity v_∞ of the rightmost branch in a Markovian branching process may be found by calculating the minimal value $v_{\min}$ for which we can find a positive running-wave solution for the global branch density ρ. That will be our main method to proceed in the case of active diffusion, although for now we lack a physical derivation of that hypothesis.

3.3 Thermal run-and-tumble particles

To go beyond (3.1) and to add new results we consider here first the case of thermal run-and-tumble particles. The temperature adds noise in the jump rates of the particles, which means that (34) gets replaced by

$$\dot{x}_t = c\,\sigma_t + \sqrt{2D}\xi_t, \qquad \text{and} \;\; \sigma_t \to -\sigma_t \text{ at rate } \epsilon \tag{40}$$

where ξ_t is standard white noise and D is a measure of thermal fluctuations. As before, the state space S of a single particle is $\mathbb{R} \times \{+, -\}$. The (time-dependent) probability density is denoted by $\rho(x, \sigma) = \rho_\sigma(x)$, and it satisfies

$$\begin{cases} \partial_t \rho_+ = -c\partial_x \rho_+ + D\partial_x^2 \rho_+ + \epsilon(\rho_- - \rho_+) \\ \partial_t \rho_- = c\partial_x \rho_- + D\partial_x^2 \rho_- + \epsilon(\rho_+ - \rho_-) \end{cases}$$

where c is the driving speed and ε^{-1} is the persistence time. Compared to (3.1) we added a (passive) diffusion term referring to the presence of thermal fluctuations. One easily verifies, [14], that the effective diffusion constant D_{eff} is given by

$$D_{\text{eff}} := \lim_{t\to\infty} \frac{\int_{-\infty}^{+\infty}(\rho_+(x,t)+\rho_-(x,t))x^2\mathrm{d}x}{2t} = D + \frac{c^2}{2\epsilon} \tag{41}$$

When we extend the diffusion to include (Markovian) replication and termination of particles, this system of evolution equations for the global branch-density is altered to

$$\begin{cases} \partial_t\rho_+ = -c\partial_x\rho_+ + D\partial_x^2\rho_+ + \epsilon(\rho_- - \rho_+) \\ +(\alpha_{++}^+ - \alpha_{--}^+ - \delta)\rho_+ + (2\alpha_{++}^- + \alpha_{+-}^- + \alpha_{-+}^-)\rho_- \\ \partial_t\rho_- = c\partial_x\rho_- + D\partial_x^2\rho_- + \epsilon(\rho_+ - \rho_-) \\ +(\alpha_{--}^- - \alpha_{++}^- - \delta)\rho_+ + (2\alpha_{--}^+ + \alpha_{+-}^+ + \alpha_{-+}^+)\rho_- \end{cases} \tag{42}$$

where we introduced the birth matrix $\alpha_{\sigma_2\sigma_3}^{\sigma_1}$: a parent with spin σ_1 gives birth to a descendant with spin σ_2; the spin of the parent after the birth becomes σ_3. The parameter δ determines the rate at which a branch with (either) spin is terminated. The first question is to find the speeds $v \geq 0$ for which there are running-wave solutions

$$(\rho_+(x,t),\rho_-(x,t)) \equiv (f_+(x-vt),\ f_-(x-vt))$$

to the equation (42). For simplicity we assume that the birth matrix enjoys the symmetry

$$\alpha_{\sigma,\sigma'}^{+} = \alpha_{-\sigma,-\sigma'}^{-}$$

We start by constructing the solution in its tail $x \to +\infty$ where $u_\pm(x,t) \to 0+$. There, one can remove terms which are quadratic in $u_\pm$ (linearization), and propose a solution of the form $u_\pm(x,t) = f_\pm(x-vt) = v_\pm^0\exp(-\lambda(x-vt))$. *A priori*, such an *Ansatz* is indeed a solution provided $\lambda > 0$ is a root of the polynomial

$$P_v(\lambda) := \det\begin{pmatrix} D\lambda^2 - (v-c)\lambda + a & b \\ b & D\lambda^2 - (v+c)\lambda + a \end{pmatrix}$$

where $a = -\epsilon + \alpha_{++}^+ - \alpha_{--}^+ - \delta, \quad b = \epsilon + \alpha_{+-}^- + \alpha_{-+}^- + 2\alpha_{++}^-$. In other words,

$$P_v(\lambda) = (D\lambda^2 - v\lambda + a)^2 - (c\lambda)^2 - b^2$$

Requiring that the coefficients $v_\pm^0$ are non-negative, yields the additional constraint

$$D\lambda^2 - (v-c)\lambda + a \leq 0 \tag{43}$$

The positive roots λ^* of P_v that obey the constraint (43) satisfy

$$D\lambda^{*2} - v\lambda^* + a = -\sqrt{b^2 + (c\lambda^*)^2} \tag{44}$$

3.3.1 The non-thermal case: $D = 0$

When $D = 0$, the condition that $P_v(X) = (v^2 - c^2)X^2 - 2avX + a^2 - b^2$ has real roots at all requires that its discriminant is non-negative:

$$v^2 \geq \frac{b^2 - a^2}{b^2} c^2 \tag{45}$$

On the other hand, the inequality (43) (which now reads $-(v - c)\lambda^* + a \leq 0$) and the requirement that $\lambda^* > 0$ implies the additional requirement

$$\lambda^* \geq \frac{a}{v - c} \text{ when } v > c \text{ and } a \geq 0 \tag{46}$$

$$\lambda^* \leq \frac{-a}{c - v} \text{ when } v < c \text{ and } a \leq 0 \tag{47}$$

All $\lambda^* > 0$ fine when $v \geq c$ and $a \leq 0$,

otherwise no $\lambda^* > 0$ satisfy the inequality.

We now consider 4 disjoint cases:

- $a < 0$ and $b^2 - a^2 > 0$: we set v equal to $c\sqrt{\frac{b^2-a^2}{b^2}}$ (so that (45) reduces to an equality) and we find that P_v has a double positive root at $X = \frac{|b|}{|a|c}\sqrt{b^2 - a^2}$ which is less than or equal to $\frac{|a|}{c-v} = \frac{|ab|}{c(|b|-\sqrt{b^2-a^2})}$ so that also (47) is fulfilled. Hence $v_{\min} = c\sqrt{\frac{b^2-a^2}{b^2}}$

- $a < 0$ and $b^2 - a^2 \leq 0$: For $v = 0$, P_v has the roots $\pm\frac{\sqrt{a^2-b^2}}{c}$ of which the greatest one is non-negative, yet smaller than $\frac{|a|}{c} = \frac{|a|}{c-v}$: hence the condition (46) is met and we conclude that $v_{\min} = 0$ in this case.
  Remember that for e.g. the model (3.1), $a = \alpha - \varepsilon$ and $b = \alpha + \varepsilon$ so that $b^2 - a^2 = 4\alpha\epsilon$ can never be negative.

- $a \geq 0$: Let us put $v = c(1 + \delta)$ (with the purpose of letting $\delta \to 0+$), the largest root of P_v diverges to $+\infty$ approximately as $\frac{4av}{2(v^2-c^2)} \sim \frac{a}{c\delta}$. As far as the bound (43) is concerned, we have to meet (45) wherein the right-hand-side $\frac{a}{v-c} = \frac{a}{c\delta}$. Plugging $X = \frac{a}{c\delta}$ into P_v yields the result $-b^2 \leq 0$. Hence P_v has a root λ^* larger than X, so that (45) is fulfilled. Hence $v_{\min} = \inf_{\delta>0} c(1+\delta) = c$ (although that minimal velocity may not by strictly attained in this case)

(45) and (46) combined yield the result

$$v_{\min} = \begin{cases} 0 \text{ when } a < 0 \text{ and } b^2 > a^2 \\ c\sqrt{\frac{b^2-a^2}{b^2}} \text{ when } a < 0 \text{ and } a^2 \geq b^2 \\ c \text{ when } a \geq 0 \end{cases}$$

3.3.2 Small driving speed: $c^2/b \ll D$

Condition (44) requires that the function $p(x) := Dx^2 - vx + a + \sqrt{b^2 + (cx)^2}$ has a root ($x = \lambda^*$). Such a root certainly exists if there is a polynomial $q(x)$ greater than $p(x)$ that also has a real root. The inequality $\sqrt{1+x} \leq 1 + \frac{1}{2}x$ implies that $q(x) := Dx^2 - vx + a + b\left(1 + \frac{(cx)^2}{2b^2}\right)$ is such a polynomial exceeding p, with the difference between q and p small when c is small, and q has real roots iff

$$v^2 \geq 4\left(D + \frac{c^2}{2b}\right)(a+b)$$

So the positive wave-front in this range of velocities certainly exists and therefore the minimal speed satisfies

$$v_{\min}^2 \leq 4\left(D + \frac{c^2}{2b}\right)(a+b)$$

The important remark now is that, because $b \geq \epsilon$, we have by (41) that $D + \frac{c^2}{2b} \leq D_{\text{eff}}$ and hence the minimal traveling-wave speed is less than the effective F-KPP speed:

$$v_{\min}^2 \leq 4 D_{\text{eff}} \alpha_{\text{eff}} \tag{48}$$

where $\alpha_{\text{eff}} = \alpha_{++}^{+} + \alpha_{+-}^{+} + \alpha_{-+}^{+} + \alpha_{--}^{+} - \delta = a + b$.

3.4 Active Brownian particles with offspring

With active Brownian particles one refers to Brownian motion where the particles have a fluctuating rotational degree of freedom which determines the direction of the drift velocity. For two-dimensional active Brownian particles, [69], we have two coordinates for spatial location and one angle for the orientation of the propagation speed. In dimensions $d \geq 2$ and for independent active Brownian particles the Fokker-Planck equation for the probability density $\rho(x_1, ..., x_d, \theta_1, ..., \theta_{d-1}, t)$ relative to the volume element $\left(\prod_{j=1}^{d-1} \mathrm{d}x_j \, \sin^{d-j-1}(\theta_j) d\theta_j\right) \mathrm{d}x_d$ is given by

$$\partial_t \rho = -\mathbf{c}(\theta) \cdot \nabla_x \rho + D_x \nabla_x^2 \rho + D_\theta \nabla_\theta^2 \rho \tag{49}$$

where the velocity $\mathbf{c}$ is defined in terms of the hyperspherical angles θ_j through its components $c_1(\theta) = c\cos(\theta_1)$, $c_j(\theta) = c\left(\prod_{k=1}^{j-1}\sin(\theta_k)\right)\cos(\theta_j)$ for $2 \leq j \leq d-1$, and $c_d(\theta) = c\left(\prod_{k=1}^{d-1}\sin(\theta_k)\right)$. The last term in (49) gives the rotational diffusion. In that way the dynamics (49) which is very similar to (40) except that now the internal degree of freedom is not a two-valued spin but is rotational. Note that the the angular Laplacian is defined as

$$\nabla_\theta^2 := \sin^{2-d}(\theta_1)\frac{\partial}{\partial\theta_1}\sin^{d-2}(\theta_1)\frac{\partial}{\partial\theta_1} + \sum_{j=2}^{d-1}\frac{\sin^{1+j-d}(\theta_j)}{\prod_{k=1}^{j-1}\sin^2(\theta_k)}\frac{\partial}{\partial\theta_j}\sin^{d-j-1}(\theta_j)\frac{\partial}{\partial\theta_j}$$

We want the projection of the equation of motion on the direction of propagation. The marginal density

$$\rho_m(x_1,\theta_1,t) := \int_{\mathbb{R}^{d-1}}\left(\prod_{j=2}^{d}\mathrm{d}x_j\right)\int_{(0,\pi)^{d-2}\times(0,2\pi)}\left(\prod_{j=2}^{d-1}\sin^{d-j-1}(\theta_j)d\theta_j\right)\rho(x,\theta,t)$$

can easily be shown to evolve according to the following much simpler evolution equation

$$\partial_t\rho_m = -c\cos(\theta_1)\frac{\partial\rho}{\partial x_1} + D_x\frac{\partial^2\rho}{\partial x_1^2} + D_\theta\sin^{2-d}(\theta_1)\frac{\partial}{\partial\theta_1}\left(\sin^{d-2}(\theta_1)\frac{\partial\rho}{\partial\theta_1}\right) \tag{50}$$

3.4.1 Effective diffusion constant

Multiplying (50) with x_1^2 respectively with $x_1\cos(\theta_1)$ and applying the integration $\int_{-\infty}^{+\infty}\mathrm{d}x_1\int_0^\pi\sin^{d-2}(\theta_1)d\theta_1$ yields the equations

$$\begin{cases}\frac{d}{\mathrm{d}t}\langle x_1^2\rangle_t = 2c\langle x_1\cos(\theta_1)\rangle_t + 2D_x\\ \frac{d}{\mathrm{d}t}\langle x_1\cos(\theta)\rangle_t = c\langle\cos^2(\theta_1)\rangle_t - (d-1)D_\theta\langle x_1\cos(\theta_1)\rangle_t\\ \frac{d}{\mathrm{d}t}\langle\cos^2(\theta_1)\rangle_t = 2D_\theta\left(1 - d\langle\cos^2(\theta_1)\rangle_t\right)\end{cases} \tag{51}$$

From the last equation, $\langle\cos^2(\theta_1)\rangle_t \to \frac{1}{d} = \frac{\int_0^\pi\sin^{d-2}(\theta_1)\cos^2(\theta_1)d\theta_1}{\int_0^\pi\sin^{d-2}(\theta_1)d\theta_1}$ as $t\to\infty$. Inserting that in the second equation of (51), we see that

$$\langle x_1\cos(\theta_1)\rangle_t \to \lim_{t\to\infty}\frac{c}{D_\theta(d-1)}\langle\cos^2(\theta_1)\rangle_t = \frac{c}{D_\theta}\frac{1}{d(d-1)}.$$

Therefore, the first equation of (51) finally implies that $\langle x^2\rangle_t \to 2(D_x + \frac{c^2}{d(d-1)D_\theta})$. The effective diffusion constant is therefore given by

$$D_{\text{eff}} := \lim_{t\to\infty}\frac{\langle x_1^2\rangle_t}{2t} = D_x + \frac{c^2}{d(d-1)D_\theta} = \lim_{t\to\infty}\frac{\left\langle\sum_{j=1}^d x_j^2\right\rangle_t}{2d\,t}$$

3.4.2 Propagation speed of front of newborn particles

We add a growth-term $\alpha\rho$ to (49) to describe the global density for active Brownians with branching at rate α. That addition corresponds to an extra term $\alpha\rho_m$ in (50):

$$\partial_t\rho_m = -c\cos(\theta)\partial_x\rho_m + D_x\partial_x^2\rho_m + D_\theta \sin^{2-d}(\theta)\partial_\theta\left(\sin^{d-2}(\theta)\partial_\theta\rho\right) + \alpha\rho_m \tag{52}$$

New particles inherit the orientation θ of the parent-particle. To estimate the velocity of the newborns, we need the *positive* traveling-wave solution $\rho_m(x,\theta,t) = e^{-\lambda(x-vt)}f(\theta)$ (writing x,θ instead of x_1,θ_1) to (52). Plugging in the traveling-wave Ansatz, we get

$$\begin{aligned} 0 &= [\alpha + (c\cos(\theta) - v)\lambda + D_x\lambda^2]f(\theta) + D_\theta\sin^{2-d}(\theta)\left(\sin^{d-2}(\theta)f'(\theta)\right)' \\ &=: (\alpha - v\lambda + D_x\lambda^2)f(\theta) - (Lf)(\theta) \end{aligned} \tag{53}$$

where the differential operator L is Sturm-Liouville for the desired boundary condition $f'(0) = f'(\pi) = 0$ and in the Hilbert space defined by the inner product

$$\langle g, h\rangle = \int_0^\pi d\theta \sin^{d-2}(\theta)\,\overline{g(\theta)}\,h(\theta)$$

Equation (53) forces us to find a positive function f that is an eigenvector of L. A standard result of Sturm-Liouville theory confirms that there is precisely one such eigenvector and it is the one corresponding to the lowest eigenvalue κ of L and is the infimum of the Rayleigh-Ritz quotient:

$$\begin{aligned} Q(f) := \frac{\langle f, Lf\rangle}{\langle f, f\rangle} &= \frac{\int_0^\pi d\theta\ \sin^{d-1}(\theta)\left(-c\lambda\cos(\theta)|f(\theta)|^2 + D_\theta|f'(\theta)|^2\right)}{\int_0^\pi d\theta\ \sin^{d-1}(\theta)|f(\theta)|^2} \\ \kappa = \inf_{f>0} Q(f) &= \alpha - v\lambda + D_x\lambda^2 \end{aligned} \tag{54}$$

where the fact that $\kappa = \alpha - v\lambda + D_x\lambda^2$ follows from (53).
Plugging the trial function $\tilde{f} \equiv 1$ into the Rayleigh-Ritz quotient yields the bound $\kappa \le 0$. The equation (54) then reduces to the inequality $0 \le \alpha - v\lambda + D_x\lambda^2$ which requires a non-negative discriminant, or equivalently $v \ge 2\sqrt{\alpha D_x}$. Therefore also $v_{\min} \ge 2\sqrt{\alpha D_x}$: the active component of the particle diffusion certainly speeds up the wave relative to the case where the driving c is set to zero.
The more interesting question however is whether

$$v_{\min} \overset{?}{\ge} 2\sqrt{\alpha D_{\text{eff}}} = 2\sqrt{\alpha(D_x + \frac{1}{D_\theta}\frac{c^2}{d(d-1)})}.$$

That is shown to hold in Appendix D, at least for small c, by plugging better trial functions $\tilde{f}$ in the Rayleigh-Ritz quotient. (By "better," we mean that $\tilde{f}$ has to

better approximate the actual leading eigenvector of L). We calculate there that, up to order c^4,

$$v_{\min}^2 = 4\alpha D_{\text{eff}} + \frac{4\alpha^2 c^4}{d^3(d-1)^3(d+2)D_\theta^3 D_{\text{eff}}} \tag{55}$$

In other words, at least for sufficiently small driving c, the minimal speed $v_{\min}$ exceeds the effective F-KPP speed, in contrast with the situation for run-and-tumble processes in $d = 1$; see (48). In high dimensions $d \uparrow \infty$ the Gaussian equality (37) is restored. Our computations in several dimensions are summarized in Fig. 4.

Figure 4: The dependence of the propagation speed $v_{\min}$ on the bias c. We used the parameters $\alpha = \alpha_{\text{eff}} = 1$, $b = 3/2$, $D = D_x = D_\theta = 1$ throughout. The fraction $\frac{v_{\min}}{\sqrt{\alpha D_{\text{eff}}}}$ is in 1 dimension generally smaller than the passive value (=2) while that fraction is higher for reproducing active brownians in higher dimensions. In dimension 3, we are already very close to the passive value (=2).

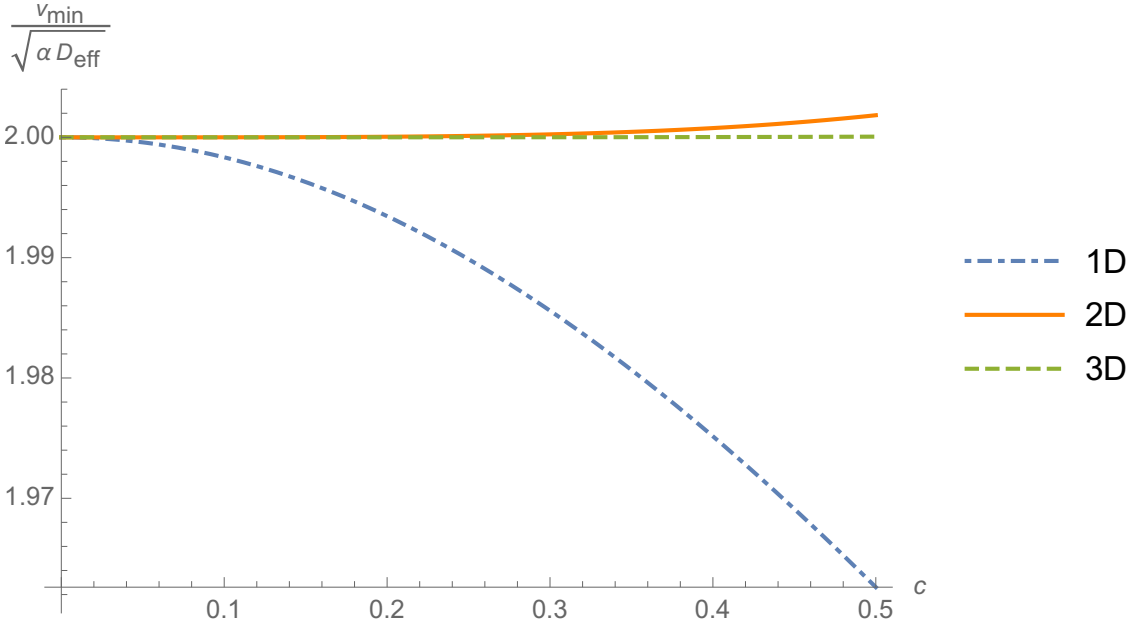

4 Death and resurrection of a current

4.1 Introduction

In the following subsection we present random walk models (in a random environment) where the current or speed shows a first order phase transition: strictly above a threshold in the driving field, the current tumbles to zero in a discontinuous way. In Section 4.6 we show how adding activity via a time-dependence in the field ("shaking") may make the current nonzero in regimes where it vanishes otherwise. Then, in Section 4.7 we consider the effect of particle interactions and specifically the influence of exclusion *versus* inclusion on the behavior of the current. Clearly many-body effects do have an influence on localization, see e.g. [81, 82].
In all cases, proofs can be made mathematically rigorous but in the bulk of the present chapter we mostly sketch the more heuristic arguments for the claims. Appendices B and C are adding more technical details.

Clearly, both the general context and detailed models have been considered before for a multitude of reasons. Random walks or diffusions in random media is of course a famous subject covering a vast range of domains, see e.g. [83–85], and we cannot even start giving a proper introduction or a more complete list of references. The question of biased transport in complex or branched structures has been considered in many areas of statistical physics; see for example [68, 75, 82, 86–90]. We will come back to specific results later. Another very related connection is to glassy behavior, ageing and/or anomalous diffusion in trapping models. Again the literature is immense and we only recall some aspects in the beginning of Section 4.6. This chapter discusses the aspect of dynamical phase transition in a number of simple models where the novelty is mostly (1) in the example of an overdamped diffusion in a random potential with a first–order transition as function of the field, (2) in the idea of resurrection of the current as function of the dynamical activity, here induced by (even a little) shaking, and (3) how all that may be modified depending on the nature of repulsive *versus* attractive interaction between the particles. One of the main aspects here is that the models allow a complete mathematical treatment.

4.2 The sudden death of a current

One of the first theoretical physics examples where a particle current was seen to die beyond a threshold value for the external field is in [86]. That paper deals mainly with a two-dimensional set-up where the square lattice is diluted via independent bond removal. When there is percolation of bonds a particle is driven through the (infinite) percolation cluster and it is argued that the current (strictly) dies, i.e., vanishes to become zero, when pushing too hard, subsequently confirmed by Monte Carlo simulations, [82, 91]. The situation is of course reminiscent of the Lorentz gas with randomly placed obstacles, where, for the same physical reasons, a negative differential conductivity can be observed on finite graphs. By now there is a large literature on such phenomena; see e.g. [92–98].

Still in [86], two different mechanisms are identified as responsible for the suppression of the current: first there is the possibility that the traversable "backbones", i.e., the paths that remain open after the completion of the bond-removal process, display kinks or bends. A particle will have a hard time to move beyond such a bend since such a structure represents a trap, a local minimum in the potential energy coming from the external bias. We revisit that effect in the following two subsections. In particular we show how the distribution of the disorder may lead to a *discontinuous* vanishing of the current (in Section 4.4). Second, there are dead-ends attached to the backbones, i.e. paths with only one entrance. Particles may waste some time there before resuming the useful part of their journey. That brings us in Section 4.5 to the widely studied transport on comb-like structures, as for example studied already in [87] in the same context of field-induced trapping due to branches in the infinite percolation cluster.

4.3 The effect of disorder along the backbone

To probe the effect of the kinks, Dhar and Barma, in Section 3.2 of [86], consider a simpler version of the process by removing all branches (dead ends). The model lives on the one-dimensional lattice and can be considered to be part of a larger class of examples as e.g. extensively explored in [68, 98]. We give a typical example.

Let $w = (w_x, x \in \mathbb{Z})$ be independent $\{0, 1\}$-random variables, where $w_x = 1$ with probability ρ, and $w_x = 0$ with probability $1-\rho$, for fixed density $\rho \in [1/2, 1]$. Given

a realization of that field w, we introduce the driving parameter $p \in [1/2, 1]$ and we consider the discrete–time nearest–neighbor random walk X_t on $\mathbb{Z}$ with transition probabilities

$$\text{Prob}[X_{t+1} = x + 1 | X_t = x] = (2p - 1)\, w_x + (1 - p)$$
$$\text{Prob}[X_{t+1} = x - 1 | X_t = x] = (1 - 2p)\, w_x + p$$

Since $\rho \geq 1/2$ there is a bias to the right when $p > 1/2$. That is a typical example of a random walk in a random environment in dimension 1 as studied by Solomon [98] for which the speed

$$v(\rho, p) = \lim_t \frac{1}{t}\, X_t$$

exists and is explicit. The result is that when $1/2 < p < \rho$, there is the nonzero speed

$$v(\rho, p) = \frac{(2p - 1)(\rho - p)}{\rho(1 - p) + p(1 - \rho)} > 0$$

while, if $p \geq \rho$, then $v(\rho, p) = 0$. In other words, the current dies (continuously) at $p = \rho$. There remains the linear response regime where $v(\rho, p) \simeq \varepsilon(2\rho - 1)$ is increasing for small $\varepsilon = p - 1/2 > 0$ and $\rho > 1/2$, but then, for higher values of p, the current reaches a maximum and decreases to zero at $p = \rho$.
A detailed study of the diffusion and current in periodic one-dimensional discrete time hopping models can be found in [68]. The current is calculated there also in the random case for the infinite one-dimensional lattice, and, as in the above, regions are identified where the current vanishes.

Note that the opposite phenomenon is also possible, as in depinning transitions [99–101], or as in the case of a yield stress where a solid starts to show plastic deformation and flows only beyond a certain stress. In such and other similar cases, the corresponding diffusion constant remains zero then for small but finite driving, and the system only starts to "move" for large enough external field where also the Sutherland-Einstein relation between mobility and diffusion constant strictly fails [102]. See also [103] for a discussion on anomalous diffusion due to disorder and/or interaction.
Observe also that *a priori* the disorder can work both on the bond or on the site variables. Below, starting from equation (56), we work with the bond version, where the "force" is random (entropic disorder). In that case (bond disorder), there does need to be a correlation between going forward and backward; for site disorder it is

the local escape rate which is variable (frenetic disorder).

4.4 Discontinous death

The one-dimensional model in Section 3.2 of [86] is on the lattice. There are also simple examples of overdamped diffusive systems with a current that goes to zero at some value of the external force. Here however and as a new aspect to the theory and to the phenomena introduced above, we present a case, as in the title of the present section, where the current goes to zero with a jump (discontinuously). Our model is an argument for predicting that the vanishing of the high-field driven current in the supercritical percolation regime, cf. [86], is in fact discontinuous when taking into account the backbone only.

Consider $x_t \in \mathbb{R}$ and the overdamped diffusion at times $t \geq 0$,

$$\dot{x}_t = F(x_t) + \sqrt{2}\,\xi_t, \qquad x_0 = 0 \tag{56}$$

for standard white noise ξ_t. We put $k_B T = 1$ with T the temperature as energy reference, and the friction $\gamma = 1$ also for convenience. The force $F = -V'$ and the potential V is a random, continuous and piecewise smooth potential on $\mathbb{R}$ in such a way that its increments $V(x+\Delta x) - V(x)$ have a distribution that does not depend on x. For the sake of simplicity we continue here with one specific choice, while the mathematical treatment allows a much larger class of examples. That point is made visible in the Appendix B. The conceptual setting is very much similar to Section 3.2 in [86] however.

We take a parameter $w \in (0,1)$ to make a Bernoulli sequence $z_i = 1$ with probability w and $z_i = -1$ with probability $1 - w$ for $i \in \mathbb{Z}_0$. When $z_i = +1$ we associate to it a length $\ell_i > 0$ which is i.i.d. drawn from a probability measure μ_+ with the property that $\mathbb{E}_{\mu_+}[e^{-\xi \ell_i}]$ is finite for all $\xi \in [-\nu, +\infty)$ (where $0 \leq \nu < +\infty$) and $\mathbb{E}_{\mu_+}[\ell_i] < +\infty$. An example of such a measure could be $d\mu_+(\ell) = \rho_+(\ell) d\ell$ where

$$\rho_+(\ell) = \frac{1}{\ell_0\, \mathcal{L}(\nu \ell_0)} \frac{e^{-\nu \ell}}{1 + (\ell/\ell_0)^\alpha}, \quad \mathcal{L}(s) = \int_0^{+\infty} \frac{e^{-s\,u}}{1+u^\alpha}\, \mathrm{d}u$$

provided $\alpha > 1$, $\nu \geq 0$ and $\ell_0 > 0$. Such behavior where the exponential decay is corrected with a power law decay $(\ell/\ell_0)^{-\alpha}$ with $\alpha = (d-1)/2$ depending on the

dimension d, is often dubbed an Ornstein-Zernike behavior, [104], and it will play a crucial role for having a discontinuous current-field characteristic.

The potential V on $\mathbb{R}$ is obtained from associating to i a slope $E > 0$ and length ℓ_i when $z_i = 1$, and a slope $-E$ and length L (a fixed number strictly greater than $\frac{w}{1-w}\mathbb{E}_{\mu_+}[\ell]$) when $z_i = -1$. By fixing $V(0) = 0$ we can construct the whole potential that way, and the force $F = -V'$ is defined by joining the successive patches. For large w (close to one) there will be long intervals where the slope in V is upward and the force points to the left. More explicitly, we define $x_0 = 0$ and

$$x_i = \sum_{j=1}^{i} [\ell_j \, \delta_{z_j,1} + L \, \delta_{z_j,-1}], \quad i = 1, 2, \dots$$

$$x_i = -\sum_{j=i}^{-1} [\ell_j \, \delta_{z_j,1} + L \, \delta_{z_j,-1}], \quad i = -1, -2, \dots$$

so that the force equals

$$F(x) = E \quad \text{when} \quad x \in (x_{i-1}, x_i) \ \text{ for } \ z_i = 1, i = 1, 2 \dots$$

$$F(x) = -E \quad \text{when} \quad x \in (x_{i-1}, x_i) \ \text{ for } \ z_i = -1, i = 1, 2, \dots$$

and similarly for $x < 0$.

Because $L > \mathbb{E}_{\mu_+}[\ell]$, the potential V tilts downward on average in the direction of increasing x. The average force to the right is indeed

$$\langle F \rangle = E \, \frac{(1-w)L - w\mathbb{E}_{\mu_+}[\ell]}{(1-w)L + w\mathbb{E}_{\mu_+}[\ell]} > 0$$

The interpretation where the randomness is associated to the geometry of a one-dimensional channel is displayed in the lower part of Fig.5. This clarifies also the link with the kinks considered in [86]. The intervals $[x_{i-1}, x_i]$ are either pointing to the right (in the direction of the external field $E > 0$) when $z_i = -1$, or pointing to the left (against the external field) when $z_i = +1$. In that picture, the external field always points to the right with amplitude E but by the geometry of the channel, particles need to move against the field on some (random) stretches of length ℓ_i during their journey. In other words, the points x_i become traps when $z_i = +1, z_{i+1} = -1$, and more so for large E. Trapping may of course also happen on a larger scale, in a combination or sequence of smaller traps as in Fig. 5. It is then not so surprising that the current (to the right) dies for large E or for small ν. As we will show the current in fact is zero for $E > \nu$. There are two sub-cases:

1. When $\nu > 0$, then the current has a jump-discontinuity at $E = \nu$.

2. When $\nu = 0$, then the current is zero for all $E \geq 0$. Note the apparent violation of the Einstein-Sutherland relation here: the diffusion rate at $E = 0$ is non-zero, but the particle responds to an external field as though it were held back by an infinite viscosity.

The argument can be sketched as follows (with Appendix B adding details): If the expected length of the random intervals $[x_j, x_{j+1}]$ is bounded (as it is), then using the law of large numbers one can prove that the asymptotic speed

$$v = \limsup_{t\to\infty} \frac{x(t)}{t} \overset{a.s.}{=} \frac{\langle x_1 - x_0\rangle}{\langle \Delta t_0\rangle} = \frac{\langle x_1\rangle}{\langle \Delta t_0\rangle} \tag{57}$$

where $\langle \Delta t_0\rangle$ is the average time required for the particle to hit x_1 if it starts at $x_0 = 0$.

It is therefore essential to compute the expected time -or "first passage time"- $\langle \Delta t_j\rangle$ for the process to travel from x_j to x_{j+1} (thereby allowing the process to go backwards and re-enter the interval $(-\infty, x_j)$). Averaging only over the dynamics we have the following "Dynkin formula" [105, 106],

$$\langle \Delta t_j\rangle = \int_{x_j}^{x_{j+1}} \mathrm{d}y \int_{-\infty}^{y} \mathrm{d}z\, e^{V(y)-V(z)}$$

(See Appendix B.) Note that the right-hand side has the dimension of length-squared = time, as one can see from the equation of motion (56) where the diffusion constant is taken dimensionless.

We rewrite this as

$$\begin{aligned}\langle \Delta t_j\rangle &= \int_{x_j}^{x_{j+1}} \mathrm{d}y \left\{ e^{V(y)-V(x_j)} \underbrace{\int_{-\infty}^{x_j} \mathrm{d}z\, e^{V(x_j)-V(z)}}_{\kappa_j} + \int_{x_j}^{y} \mathrm{d}z\, e^{V(y)-V(z)} \right\} \\ &= \kappa_j \underbrace{\int_{x_j}^{x_{j+1}} \mathrm{d}y\, e^{V(y)-V(x_j)}}_{=:B_j} + \underbrace{\int_{x_j}^{x_{j+1}} \mathrm{d}y \int_{x_j}^{y} \mathrm{d}z\, e^{V(y)-V(z)}}_{=:C_j}\end{aligned}$$

Here $(B_j)_j$ and $(C_j)_j$ are iid, $(\kappa_j)_j$ is stationary, and κ_j and B_j are mutually independent.

Next we take the expectation over the disorder,

$$\overline{\langle \Delta t_j\rangle} = \kappa B + C$$

To determine κ, note that

$$\kappa_{j+1} = \int_{-\infty}^{x_{j+1}} \mathrm{d}z\, e^{V(x_{j+1})-V(z)}$$
$$= \underbrace{e^{V(x_{j+1})-V(x_j)}}_{=:c_j} \int_{-\infty}^{x_j} \mathrm{d}z\, e^{V(x_j)-V(z)} + \underbrace{\int_{x_j}^{x_{j+1}} \mathrm{d}z\, e^{V(x_{j+1})-V(y)}}_{=:A_j}$$
$$= c_j\kappa_j + A_j$$

where c_j and A_j are iid, and c_j and κ_j are mutually independent. Taking expectations on both sides yields $\kappa = c\kappa + A$. Hence (since κ_j is a positive random variable),

$$\kappa = \begin{cases} \frac{A}{1-c} \text{ when } c < 1 \\ +\infty \text{ otherwise} \end{cases}$$

We conclude that

$$\overline{\langle \Delta t_j \rangle} = \begin{cases} \frac{AB}{1-c} + C \text{ when } c < 1 \\ +\infty \text{ otherwise.} \end{cases} \tag{58}$$

To see where the asymptotic speed is nonzero, we thus need to check where $c < 1$, and to verify when A, B, C are bounded:

$$\begin{cases} c(E) = (1-w)\, e^{-EL} + w \int_0^\infty \mathrm{d}\ell \rho_+(\ell)\, e^{E\ell} \\ A = \frac{1-w}{E} e^{-EL}(e^{EL}-1) + \frac{w}{E}\int_0^\infty \mathrm{d}\ell \rho_+(\ell) e^{E\ell}(1-e^{-E\ell}) \\ B = A \\ C = (1-w)\,(\frac{e^{-EL}-1}{E^2} + \frac{L}{E}) + \frac{w}{E}\int_0^\infty \mathrm{d}\ell \rho_+(\ell)[\frac{1}{E}(e^{E\ell}-1) - L] \end{cases} \tag{59}$$

We see that $c(E) < 1$ for E small enough. In fact,

$$c(E) = \begin{cases} (1-w)\, e^{-EL} + \frac{w}{\ell_0 \mathcal{L}(\nu\ell_0)} \int_0^\infty \frac{e^{(E-\nu)\ell}}{1+(\ell/\ell_0)^2}\, \mathrm{d}\ell \text{ when } E \le \nu \\ +\infty \text{ otherwise} \end{cases}$$

For fixed ν and ℓ_0 we can choose $w > 0$ very small and L sufficiently large so that $c(E) < 1$ on the interval $[0, \nu]$. Also A, B and C are, as a function of E, bounded on the interval $[0, \nu]$. We conclude that the speed goes to zero at $E = \nu$ in a right-discontinuous way (see Fig. 6). It is also clear from the calculation (1) why it goes to zero at all, and (2) why it goes to zero with a jump. Ad (1) there is little new except that there are few and simple diffusion models where the death of a current is shown in that generality. Ad (2) there is something new here and the origin of

the jump (and first-order transition) can be traced back to the finite exponential moment

$$\mathbb{E}_{\mu_+}[e^{\nu\ell}] < \infty \tag{60}$$

as we already stressed before. To reiterate: (60) tells that the disorder deciding the length of the positive slopes in the potential V is not entirely multiplicative: the (more microscopic) steps in the disorder are not independent and the large $\ell-$decay of the length of the "bad" domains follows a type of Ornstein–Zernike law (polynomial correction to exponential decay), [104].

Figure 5: Top picture: The random potential discussed in the text. Here $z_1 = z_3 = z_6 = 1$ and $z_2 = z_4 = z_5 = -1$. Lower picture: the channel-interpretation corresponding to the potential above.

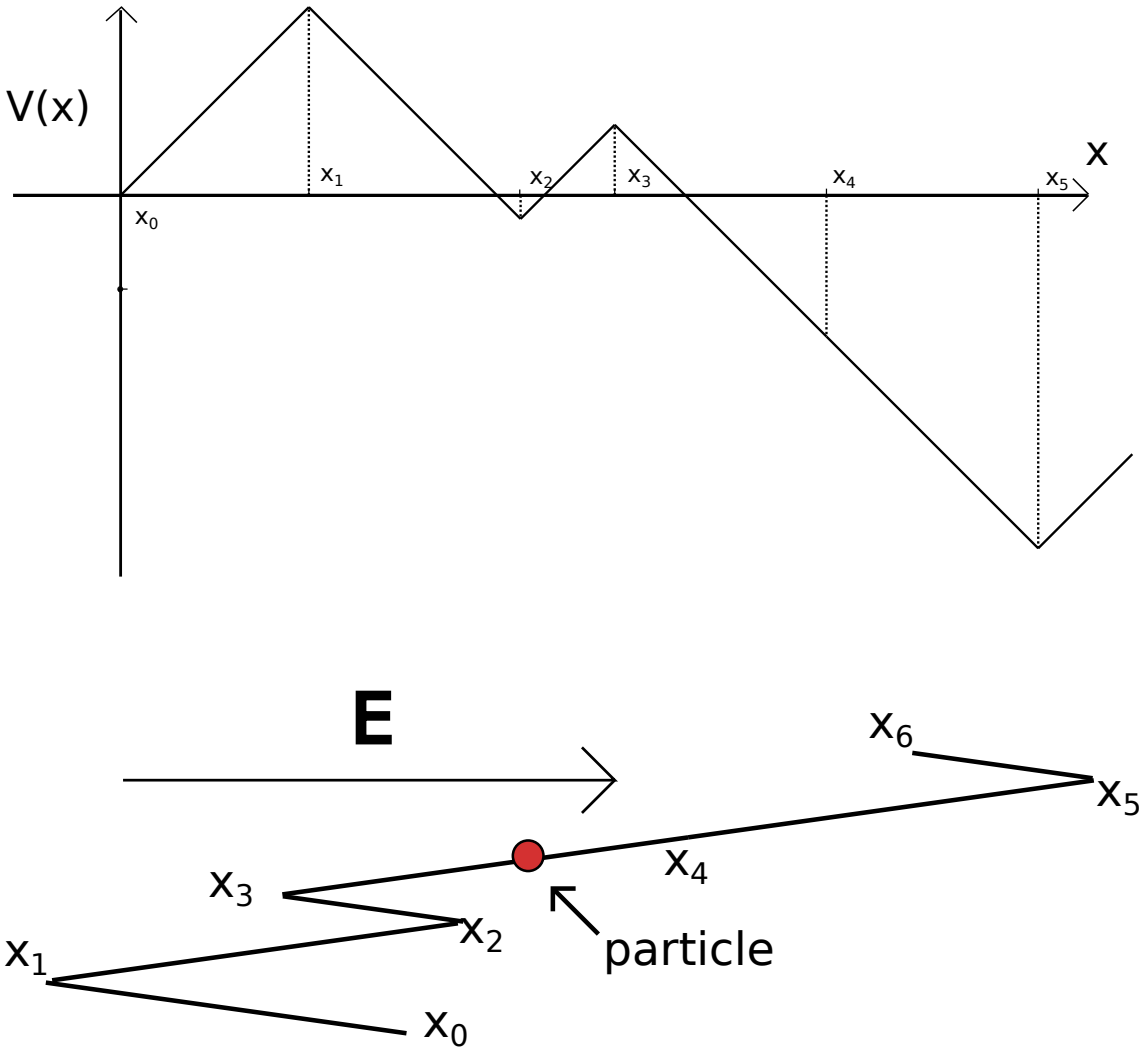

Figure 6: The speed-field-characteristic for $w = 0.005,\ 0.05,\ 0.1,\ 0.3$ resp. and $L = \nu = \ell_0 = 1$. Computed via (57), (58), (59)

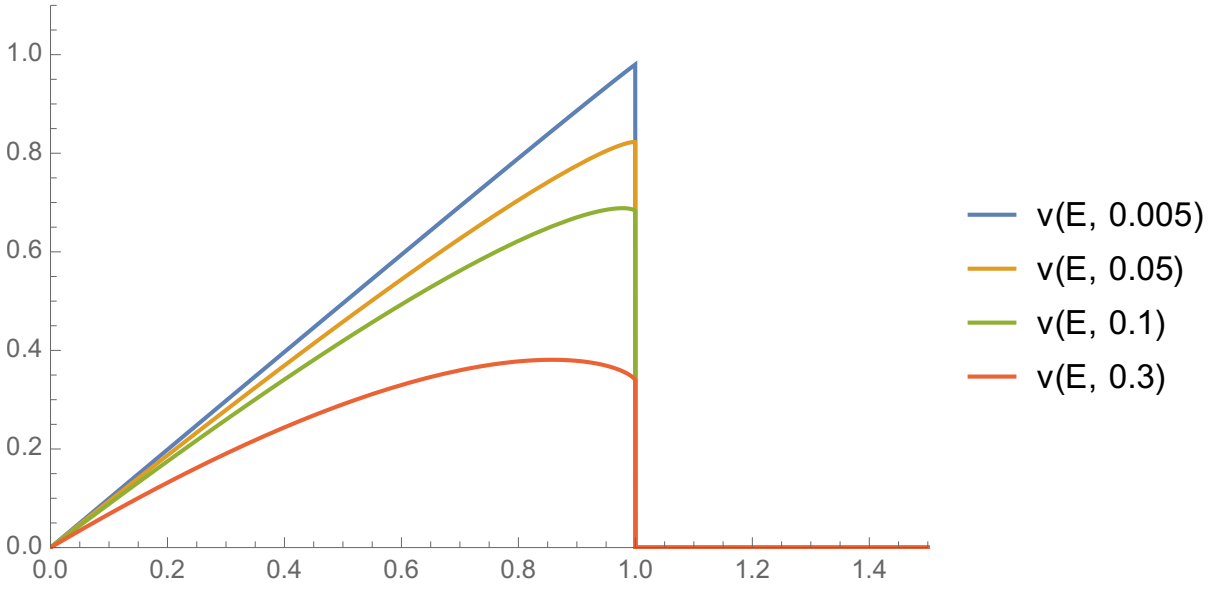

4.5 The role of dead-ends for the diffusion of independent particles

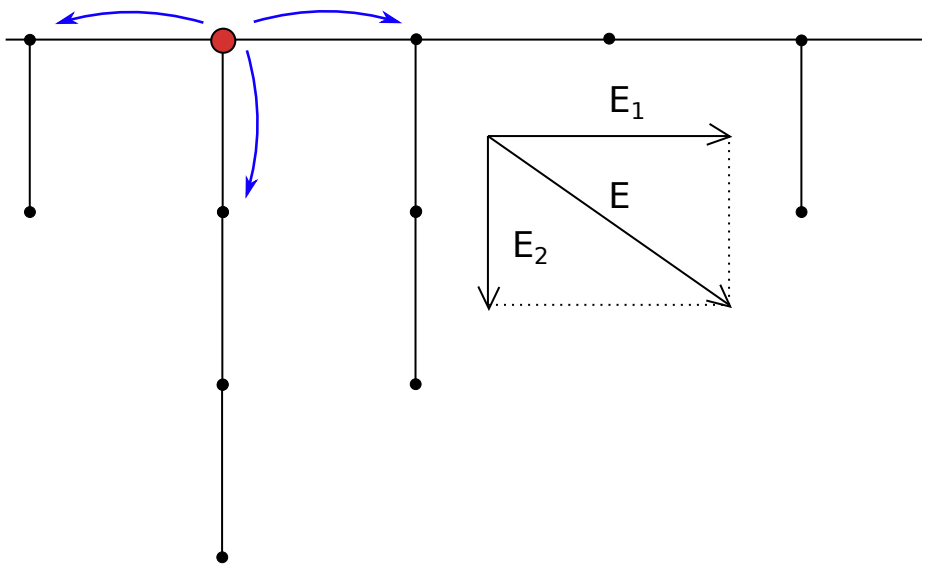

Figure 7: Walking on a random comb

Since [87] the problem of field-induced transport on the infinite percolation cluster related to dead ends has been considered on random combs. The literature on diffusion and currents on random combs is of course vast, including especially for our purposes the work in [75, 82, 89, 90]. In Section 4.3 we already outlined a scenario how kinks in the backbone may give rise to a first-order transition in the speed of the particle. That is also true for dead ends and for the same basic reason. Eg. in [90] the problem of transport on a comb is reduced to that of a continuous time random walk where the waiting times are induced by the dent disorder. The current vanishes for power-law and stretched-exponential distributions of branch lengths on the comb, whatever be the biasing field strength. In the present subsection we ask what aspect in the distribution could lead to a first-order phase transition in the current, and we find back the result of the previous discussion in Section 4.4 but in a much simpler setting. The new thing follows in Section 4.6 for the resurrection of the current via shaking.

In this section, we look at a continuous time-discrete space RW. The state space is

arranged in a "comb"-geometry, as a cartoon for a backbone with dead-ends. We refer to Fig. 7. More precisely, the sites are on $M := \{(n,m) \in \mathbb{Z}^2 \,|\, 0 \leq m \leq L_n\}$ where the $(L_n)_n$ are positive integers, independent and identically distributed with finite expectation, $\mathbb{E}[L_n] < \infty$.
The inter-site jump rates are

- $e^{\pm E_1/2}$ for jumps from site $(n,0)$ to $(n \pm 1, 0)$;
- $e^{E_2/2}$ for jumps from site (n,m) to $(n, m+1)$ (provided $m \leq L_n - 1$);
- $e^{-E_2/2}$ for jumps from site (n,m) to $(n, m-1)$(provided $m > 0$);
- All other inter-site jumps are forbidden.

We then define the speed (or current)

$$v = \limsup_{t\to\infty} \frac{n(t)}{t}$$

Basically one proceeds by proving the three successive equalities for the speed (almost surely with respect to the disorder):

$$v = \frac{1}{\langle \Delta t_0 \rangle} = \tanh(E_1/2) \frac{1}{\langle \widetilde{\Delta t_0} \rangle} = 2\sinh(E_1/2) \frac{e^{E_2} - 1}{e^{E_2} \langle e^{L_0 E_2} \rangle - 1} \tag{61}$$

where Δt_0 is the time required for the walker to reach the site $(1,0)$ for the first time when it starts at the site $(0,0)$ and the average $\langle ... \rangle$ is both over the random comb-geometry and the jump dynamics. Likewise, $\langle \widetilde{\Delta t_0} \rangle$ is the average time required for the walker to reach either $(-1,0)$ or $(1,0)$ given that it started at $(0,0)$. The first equality of (61) is a consequence of the law of large numbers (for stationary processes). The second equality follows from the following argument:

- The average time for the walker to reach either $(-1,0)$ or $(1,0)$ given that it started at $(0,0)$ is $\langle \widetilde{\Delta t_0} \rangle$ as said before
- The probability for the walker to first jump to $(\pm 1, 0)$ is resp. $\frac{e^{E_1/2}}{e^{E_1/2} + e^{-E_1/2}}$ and $\frac{e^{-E_1/2}}{e^{E_1/2} + e^{-E_1/2}}$.
- In the former case, we had $\widetilde{\Delta t_0} = \Delta t_0$. In the latter case, the particle jumped to $(-1,0)$ after a time $\widetilde{\Delta t_0}$. From there, it has to wait (on average) a time $\langle \Delta t_{-1} \rangle = \langle \Delta t_0 \rangle$ to jump back to $(0,0)$ and then an additional time $\langle \Delta t_0 \rangle$ to finally jump to $(1,0)$. Therefore

$$\langle \Delta t_0 \rangle = \langle \widetilde{\Delta t_0} \rangle + \frac{e^{-E_1/2}}{e^{E_1/2} + e^{-E_1/2}} 2 \langle \Delta t_0 \rangle,$$

or

$$\langle \Delta t_0 \rangle = \frac{\widetilde{\langle \Delta t_0 \rangle}}{\tanh(E_1)}.$$

The third equality in (61) is shown through a straightforward exercise in the theory of average escape times in a Markov jump process with finite state space. We refer to Appendix C for more details on the calculation.
Inspecting (61), we see again that the speed is zero either when E_1 is zero or when $\langle e^{L_0 E_2} \rangle$ (which is a function E_2) is zero. Very much similar as in Section 4.3 we find that when L_0 is distributed in a non-multiplicative way, e.g. with

$$\text{Prob}\,[L_0 = L] = \frac{1}{\mathcal{L}(\nu, L_0)} \frac{e^{-\nu L}}{1 + (L/L_0)^2} \tag{62}$$

then the current goes to zero in a discontinuous way at $E_2 = \nu$. Note that a breaking of multiplicativity such as in (62) is quite likely when considering the length-distribution of dead-ends in percolation clusters: simply the conditioning on a dead-end being a dead-end rather than a backbone does the job, cf [104] for a rigorous result.

4.6 Resurrection of a current

Given the importance of dynamical activity in nonequilibrium physics [107], we may wonder if shaking (an AC field) may resurrect the current. We proceed with additional features related to the phenomenon that we discussed already in [108].
At the same time we stick to the the realm of trapping models which since many years (cf [28,109]) have been central in questions of glassy behavior, ageing behavior or anomalous transport. The trapping will here be realized by a crystalline comb-geometry such as in [75, 82, 89, 90].

We consider a continuous time random walk on the comb-like configuration space $\mathbb{Z}_n \times \{a, s\}$ where a stands for "active" and s for "sleeping" (a trapped state) and $\mathbb{Z}_n$ is the ring with n sites; see Fig. 8 for a portion of that ring. The dynamics is a time-dependent Markov process. The transitions are $(j, a) \to (j, s)$ at rate $q(t)$, $(j, s) \to (j, a)$ at rate $p(t)$. Furthermore, to get a current we choose $\lambda > 0$ and let $(j, a) \to (j + 1, a)$ at rate $q^\lambda(t)$, $(j + 1, a) \to (j, a)$ at rate $p^\lambda(t)$ for all $1 \leq j \leq n$ (periodic). The fact that the vertical and horizontal transition rates are coupled must be interpreted via the presence of an external field for which the angle with the vertical is quantified with λ. We take $p(t)q(t) = 1 = p^\lambda(t)q^\lambda(t)$ to have a

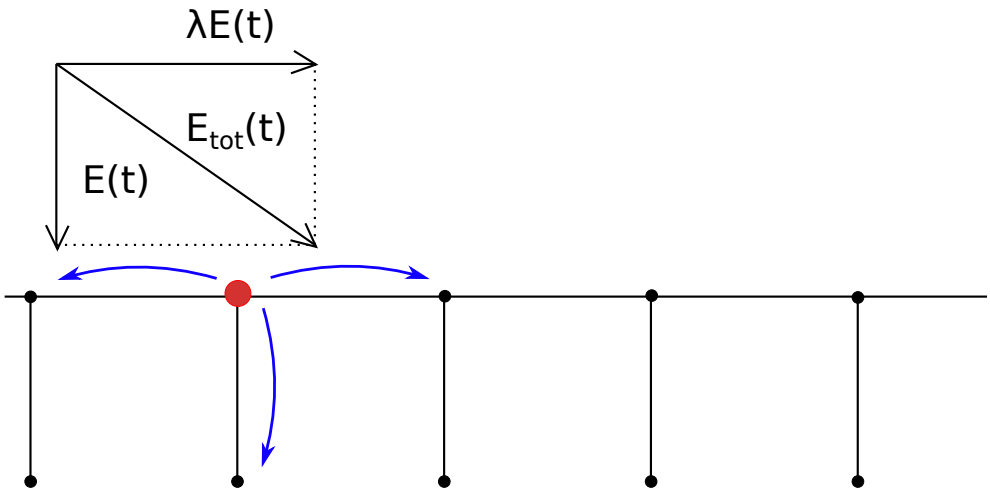

Figure 8: The active a-states are represented by the black dots on the backbone of the comb, while the sleeping s-states are represented by the black dots on the dents. The arrows on the upper left illustrate the applied force: its magnitude and direction may change in time, but its angle remains fixed. That is: the ratio of its horizontal and vertical components is λ at all times.

constant activity parameter.
With $\rho_a(t)$ the total probability (at time t) to be in an active state and $\rho_s(t) = 1 - \rho_a(t)$ the probability to be sleeping,

$$\begin{cases} \dot{\rho}_a(t) = p(t)\rho_s(t) - q(t)\rho_a(t) = p(t)[1 - \rho_a(t)] - q(t)\rho_a(t) \\ \dot{\rho}_s(t) = q(t)\rho_a(t) - p(t)\rho_s(t) = q(t)[1 - \rho_s(t)] - p(t)\rho_s(t) \end{cases} \tag{63}$$

The instantaneous macroscopic current over the ring $J(t)$ is

$$J(t) = \rho_a(t)[q^\lambda(t) - p^\lambda(t)]$$

The time-dependence is chosen such that $p(t) = q^{-1}(t)$ is periodic with period $\tau = t_1 + t_2$,

$$p(t) = \begin{cases} p_1 \text{ when } t \in [0,\, t_1) \\ p_2 \text{ when } t \in [t_1,\, t_1 + t_2) \end{cases}$$

Writing the escape rates and jump probabilities as

$$\Lambda_1 = p_1 + q_1, \quad \Lambda_2 = p_2 + q_2$$
$$\rho_1 = \frac{p_1}{\Lambda_1}, \qquad \rho_2 = \frac{p_2}{\Lambda_2}$$

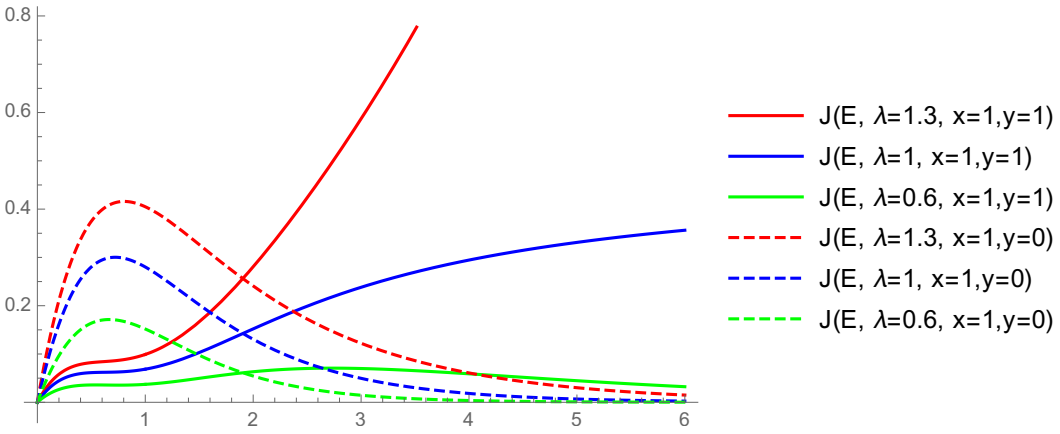

Figure 9: The shaken and unshaken currents $\mathcal{J}(E, x = 1, y = 1)$ resp. $\mathcal{J}(E, x = 1, y = 0)$ as a function of E for $\lambda = 1.3, \lambda = 1$ and $\lambda = 0.6$ (the ordering in the legend agrees with the top-down order of the graphs at $E = 6$).

one easily checks that ρ_a solving (63) converges for large t to the periodic function

$$\rho_a(t) = \begin{cases} \frac{(\rho_2-\rho_1)(1-e^{-\Lambda_2 t_2})}{1-e^{-\Lambda_1 t_1-\Lambda_2 t_2}} e^{-\Lambda_1 t} + \rho_1 \text{ when } t \in [0, t_1] \mod t_1 + t_2 \\ \frac{(\rho_1-\rho_2)(1-e^{-\Lambda_1 t_1})}{1-e^{-\Lambda_1 t_1-\Lambda_2 t_2}} e^{-\Lambda_2 (t-t_1)} + \rho_2 \text{ when } t \in [t_1, t_1 + t_2] \mod t_1 + t_2 \end{cases}$$

In the steady state the average current $\mathcal{J} = \frac{1}{\tau}\int_0^\tau J(t)$ is given by ($x := \Lambda_1 t_1$, $y := \Lambda_2 t_2$)

$$\mathcal{J} = \frac{1}{t_1+t_2}\left\{\int_0^{t_1} \rho_a(t')[q_1^\lambda - p_1^\lambda]\mathrm{d}t' + \int_{t_1}^{t_1+t_2} \rho_a(t')[q_2^\lambda - p_2^\lambda]\mathrm{d}t'\right\}$$

$$= \frac{1}{(t_1+t_2)(1-e^{-(x+y)})}\left\{\frac{(\rho_2-\rho_1)(1-e^{-x})(1-e^{-y}) + \rho_1 x(1-e^{-(x+y)})}{\Lambda_1}[q_1^\lambda - p_1^\lambda]\right.$$
$$\left. + \frac{(\rho_1-\rho_2)(1-e^{-x})(1-e^{-y}) + \rho_2 y(1-e^{-(x+y)})}{\Lambda_2}[q_2^\lambda - p_2^\lambda]\right\}$$

If we put $q_1 = p_1^{-1} = e^E$ and $p_2 = q_2 = 1$, we have $\Lambda_1 = 2\cosh E$, $\Lambda_2 = 2$, $\rho_1 = \frac{e^{-E}}{2\cosh E}$ and $\rho_2 = \frac{1}{2}$. The expression for the average current $\mathcal{J} = \mathcal{J}(E, x, y)$ reduces to

$$\mathcal{J} = \frac{\sinh(\lambda E)}{(x + 2y\cosh E)(1-e^{-(x+y)})\cosh E}\left\{(\cosh E - e^{-E})(1-e^{-x})(1-e^{-y}) + e^{-E}x(1-e^{-(x+y)})\right\} \tag{64}$$

Putting $y = 0$ in this result brings us to the result of the time-independent system where $\mathcal{J}(E, x, 0) = e^{-E}\sinh(\lambda E)/\cosh E$, or

$$\mathcal{J}(E, x, 0) \simeq e^{E(\lambda-2)}, \qquad E \uparrow \infty$$

We see the familiar behavior of a current going to zero for large E provided $0 < \lambda < 2$. The physical reason is that as E increases the walker also goes to sleep more

often.
However, if we keep $x, y > 0$ fixed in (64), one finds

$$\mathcal{J}(E, x, y) \simeq e^{E(\lambda-1)} \frac{(1-e^{-x})(1-e^{-y})}{2y(1-e^{-(x+y)})}, \qquad E \uparrow \infty$$

so shaking can indeed "resurrect" the current for $\lambda \geq 1$; see Fig. 9. For $\lambda \in (1, 2)$ the current is exponentially smaller in E compared to the case when activity is added in terms of shaking. Of course the limit of $E \uparrow \infty$ cannot be exchanged with that of $y \downarrow 0$, and even for very small shaking (small y) the effect of resurrecting the current is immediately there. Methods of enhancing flow or of restoring current are obviously of much practical importance. Here and in [108] we propose that a little shaking can do a lot; see also [110] in the case of granular suspensions.

Note that in the above example specific choices were made for the rates. More specifically: one can make other choices regarding the amount of traffic between the different states and how that depends on the external field. For virtually all choices one comes to the conclusion that some amount of shaking can significantly boost the current and overall activity.
Secondly, the resurrection (as the vanishing) of the current here plays at large E; mathematically in the limit $E \uparrow \infty$ only. That is however the result of the uniform boundedness of the depth of the traps, i.e. of the dents in Fig. 8.
In the next section we concentrate on the influence of interaction but we also make the comb random. In other words we will make the sleeping state more dynamical and resolve its microscopics.

4.7 Adding interaction

So far we have studied the influence of disorder and activity on the current characteristic. Here we show how the nature of the interaction can also dramatically and differently influence the current. Such a study with very similar results has been given already in [82] especially for the fermionic case where exclusion between particles enters. We estimate however that our analysis is more succinct and rigorous. Additionally we compare with an bosonic particle model in Section 4.9, where the driven zero range process [111] with constant rates is put on a random comb.

4.8 Exclusion enhancing the current

4.8.1 Uniformly bounded traps

Before we make the comb random we consider the set-up of [95, 97], but with exclusion. Consider therefore a system of N mutually excluding particles in Fig. 10. A cell has address $c = (\ell, n)$ where $1 \leq \ell \leq L$ and $1 \leq n \leq 4$. This asymmetric exclusion process on a random comb has been studied earlier in [82].

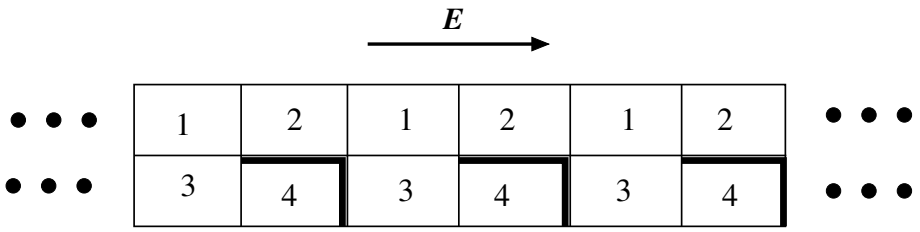

Figure 10: A comb like in Fig. 8 where the dents are bent inward. Figure courtesy of [95].

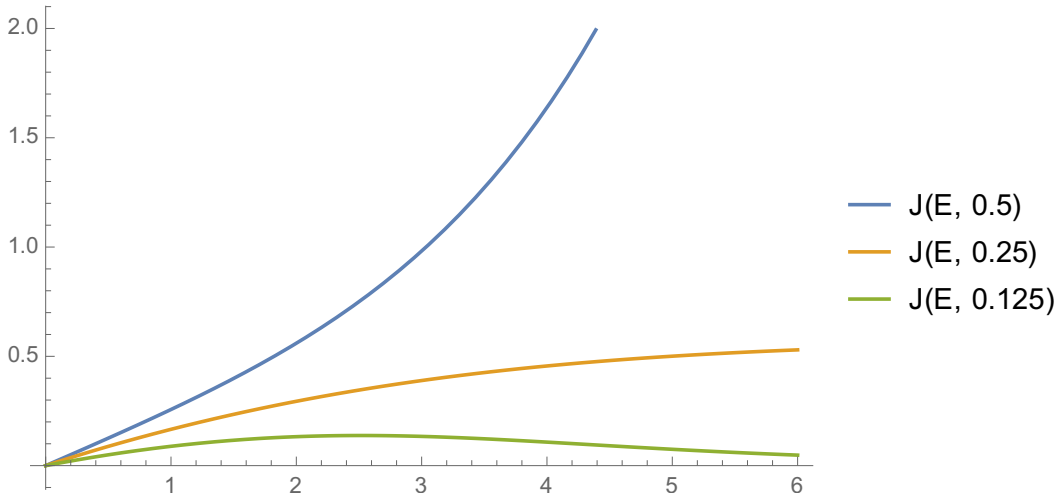

Figure 11: Plot of the current (66) for the values $\rho = 0.5$, 0.25 and 0.125 respectively.

The particles have labels (are distinguishable) and the state of the system is therefore $x = (x_1, \ldots, x_N)$ with each x_i being some cell c. For the current that will not matter. The dynamics is by exchanging the occupation between neighboring cells. Horizontal exchanges (if permitted) have rates $\exp \pm E/2$; vertical transitions (if permitted) have rate 1. The permission depends on there being a "wall" or not between adjacent cells; see the thick lines in Fig. 10. When there would be no exclusion and the particles are independent, the current would become vanishingly small for large

E. This compares very well with results (and the similar figures) in [82].

The stationary distribution is given by

$$\mathrm{Prob}(x) = \frac{1}{\mathcal{Z}} \exp\left(- \sum_{j=1}^{N} \phi(x_j) \right)$$

where the potential $\phi(c)$ in a cell c is defined by

$$\phi(c) = \phi((\ell, n)) = \begin{cases} 0 \text{ when } n \in \{1,2,3\} \\ -E \text{ otherwise.} \end{cases}$$

That stationary measure is a (Fermi-Dirac) product measure in the open finite system or in the thermodynamic limit. Suppose indeed that particles are introduced both at $(1,1)$ and $(L,2)$ at rates $\frac{1}{1+\theta} e^{E/2}$ and $\frac{1}{1+\theta} e^{-E/2}$ respectively, at least when those cells are not occupied by a particle already. Likewise, for the exit of particles at $(1,1)$ and at $(L,2)$ we take the rate $\frac{1}{1+\theta}$. Then the stationary distribution is the grand-canonical one,

$$\mathrm{Prob}(x) = \frac{1}{\Xi} \prod_{\text{cell } c} [\theta^{-1} e^{-\phi(c)}]^{\delta_{c \in x}} \tag{65}$$

The correct normalization is

$$\Xi = \prod_{\text{cell } c} [1 + \theta^{-1} e^{-\phi(c)}]$$

so that we can rewrite (65) in the familiar Fermi-Dirac form:

$$\mathrm{Prob}(x) = \prod_{\text{cell } c} \frac{[1 + \theta e^{\phi(c)}]^{1 - \delta_{c \in x}}}{1 + \theta e^{\phi(c)}}.$$

In the thermodynamic limit, a similar product distribution is stationary. In that setting, one adjusts the chemical potential θ to fit that measure to the desired average particle density. We will now use that stationary distribution to compute the current explicitly.

In the 4-cell system, the $n = 1, 2, 3$-cells are occupied by a particle with probability $\frac{1}{1+\theta}$. The cell $n = 4$ is occupied with probability $\frac{1}{1+\theta e^{-E}}$. Since the measure is a product-measure, the expected total number 4ρ of particles in one macroscopic unit is the sum of the expected number of particles in each sub-cell, i.e.,

$$4\rho = \frac{3}{1+\theta} + \frac{1}{1+\theta e^{-E}}$$

If we now adjust E while the density ρ is to remain constant, θ becomes a function of E:

$$\theta(E) = \frac{[e^E + 3 - 4\rho(e^E+1)] + \sqrt{[e^E + 3 - 4\rho(e^E+1)]^2 + 4(4-4\rho)4\rho e^E}}{8\rho}$$

When $\rho < 1/4$, one has $\theta(E) \sim \frac{1-4\rho}{4\rho} e^E$ when $E \to +\infty$. When $\rho = 1/4$, it is $\theta(E) \sim \sqrt{3}\, e^{E/2}$. Finally, when $1 < 4\rho < 4$, $\theta(E) \to \frac{4-4\rho}{4\rho-1}$ when $E \to +\infty$. For the current J, one has

$$\begin{aligned} J(E) &= \text{Prob(cell } n=1 \text{ occupied)Prob(cell } n=2 \text{ unoccupied)}\, e^{E/2} \\ &\quad - \text{Prob(cell } n=2 \text{ occupied)Prob(cell } n=1 \text{ unoccupied)}\, e^{-E/2} \\ &= \frac{2\theta(E)}{(1+\theta(E))^2} \sinh(E/2) \end{aligned} \tag{66}$$

Therefore,

$$\lim_{E\to\infty} J(E) = \begin{cases} 0 \text{ when } \rho < 1/4, \\ \sqrt{1/3} \text{ when } \rho = 1/4, \\ +\infty \text{ when } 1/4 < \rho < 1 \end{cases} \tag{67}$$

In other words, when the density becomes sufficiently elevated, the exclusion prevents the current from dying. Note however that the current also depends on the choice of rates and would change if the "time-scale" would also depend on E. For example, the dynamical activity or traffic in a cell also changes with E. The sharp transition in (67) is on one specific time-scale, but the general feature of exclusion promoting current seems more universal.

4.8.2 ASEP on random combs

We continue with the study of an asymmetric exclusion process on a comb whose dents have a random (integer) length. We refer to Fig. 12. More precisely, the sites are on $M := \{(n,m) \in \mathbb{Z}^2 \,|\, 0 \le m \le L_n\}$ where the $(L_n)_n$ are positive integers, independent and identically distributed with finite expectation, $\mathbb{E}[L_n] < \infty$.
The jump rates imposed on individual particles are identical to those considered for the random walk in section 4.5, but of course we now impose that such jumps are annulled in case the destination-site of the jump is already occupied by a particle.

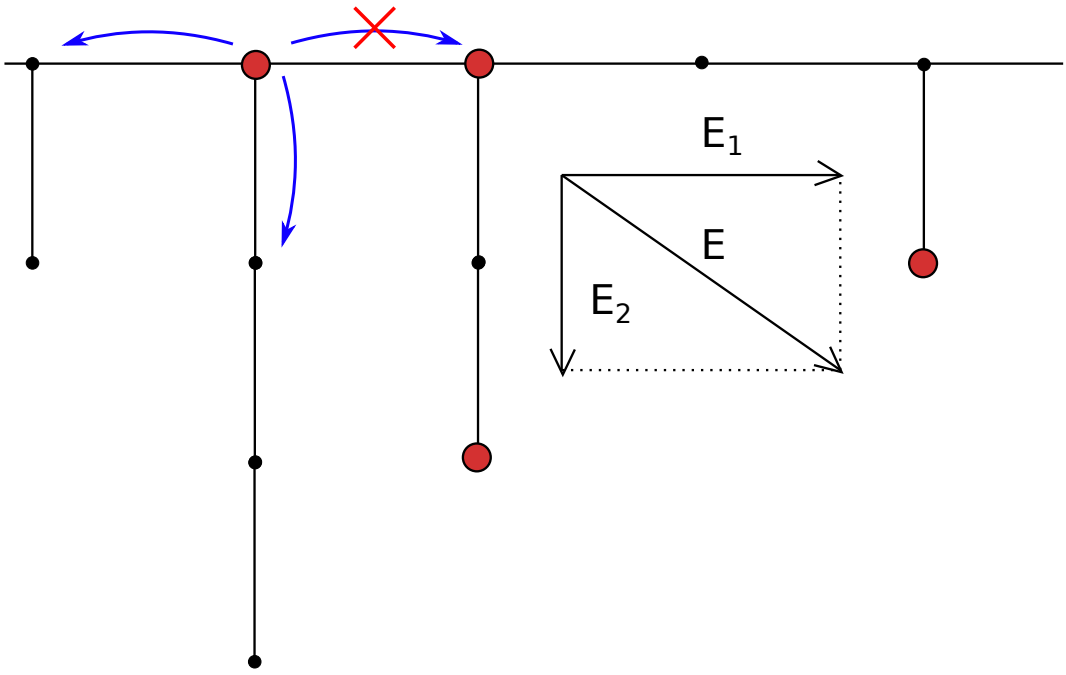

Figure 12: The asymmetric simple exclusion process on a random comb.

Consider the single site occupation densities ν^s_{θ,E_2} defined as

$$\nu^s_{\theta,E_2}[s=(n,m) \text{ is occupied by a particle}] = \frac{1}{1+\theta e^{-mE_2}}$$
$$\nu^s_{\theta,E_2}[s=(n,m) \text{ is not occupied by a particle}] = \frac{\theta e^{-mE_2}}{1+\theta e^{-mE_2}},$$

One can show that the product probability measure $\mu_{\theta,E_2} = \otimes_{s\in M}\nu^s_{\theta,E_2}$ is invariant under the dynamics.

The fugacity θ determines the overall particle density

$$\rho(\theta,E_2) = \frac{\langle \text{ number of particles on the sites } \cup_{m=0}^{L_0}(0,m)\rangle}{\mathbb{E}[L_0]}$$
$$= \frac{1}{\mathbb{E}[L_0]}\sum_{j=0}^{\infty}\text{Prob}[L_0=j]\sum_{m=0}^{j}\frac{1}{1+\theta e^{-mE_2}}$$

One can indeed verify that this notion of density agrees with the empirical density, i.e.

$$\frac{\text{number of particles on the sites } \cup_{j=-n}^{n}\cup_{m=0}^{L_0}(n,m)}{\sum_{j=-n}^{n}(L_n+1)} \overset{a.s.}{\to} \rho(\theta,E_2) \text{ as } n\to\infty$$

The translational (horizontal) current is

$$\begin{aligned} J_\theta(E_1) &= \text{Prob[site } (0,0) \text{ occupied and site } (1,0) \text{ unoccupied}]e^{E_1/2} \\ &- \text{ Prob[site } (0,0) \text{ unoccupied and site } (1,0) \text{ occupied}]e^{-E_1/2} \\ &= \frac{\theta}{(1+\theta)^2}(e^{E_1/2} - e^{-E_1/2}) \end{aligned}$$

The current vanishes in the limits $\theta \to 0$ and $\theta \to +\infty$. The first limit corresponds to the density approaching 1 (mathematically as a consequence of the monotone convergence theorem); the other limit corresponds to the density going to zero (by the dominated convergence theorem). To understand that $J_\theta(E_1) > 0$ for all $E_1 > 0$, we need to see that for nontrivial densities $0 < \rho < 1$ there is a nonzero and finite fugacity. To arrive at that we notice that $\theta \mapsto \rho(\theta, E_2)$ is differentiable with respect to θ to any order. The inverse function theorem implies that the strictly decreasing function $\rho(\theta, E_2)$ can be inverted with respect to θ to obtain a strictly decreasing function $\theta(\rho, E_2)$. Hence, if $0 < \rho < 1$, then $0 < \theta(\rho, E_2) < \infty$ and therefore $J_{\theta(\rho,E_2)}(E_1) > 0$ provided $E_1 > 0$. We conclude that the exclusion between the particles assures that an external field *always* gives rise to a nonzero current. When there is no such exclusion (independent particles) and the dents have for example an exponential distribution, there is a threshold in the external field above which the current strictly vanishes.

4.9 Attractive zero-range process on random combs

Suppose now that particles are allowed to jump to already occupied sites. The so called zero-range process allows that and there one imagines particles jumping to nearest neighbor sites at a rate which only depends on the number of particles at the site of departure; see [111] for detailed definitions of the model. We take a zero range process with constant rates: particle jump to nearest neighbor sites at a rate which is independent of the number of particles at the departure (or target) site. That means that the dynamics of the previous section described in 2(a)–(b) still applies for precisely one particle on every occupied site; additional particles, if present, are inactive until said particle has left the site.

In that case the product probability measure $\mu_{\theta,E_2} = \otimes_{s\in M}\nu^s_{\theta,E_2}$ is invariant under the dynamics, where ν^s_{θ,E_2} is defined as

$$\nu^s_{\theta,E_2}[s = (n,m) \text{ is occupied by } k \in \mathbb{N} \text{ particles}] = \left(\theta e^{mE_2}\right)^k \left[1 - \theta e^{mE_2}\right]$$

Note however that that is ill-defined unless $\theta\, e^{mE_2} < 1$ for all m. Since m can take values in a random range, depending on the length of the dent we must require that the random variable $L_j \sim L_0$ has a finite support. So consider the above described asymmetric zero range process on a random comb where the dents are uniformly bounded by length $L_{\max}$: for every fixed E_2 we have that μ_{θ,E_2} is well-defined for all $\theta < e^{-L_{\max}E_2}$.

The translation (horizontal) current is

$$\begin{aligned} J_\theta(E_1) &:= \mathbb{E}_{\theta,E_2}[\text{Number of particles at site } (0,0)]e^{E_1/2} \\ &\quad -\mathbb{E}_{\theta,E_2}[\text{Number of particles at site } (1,0)]e^{-E_1/2} \\ &= \sum_{j=0}^{\infty} \left(j\theta^j(1-\theta)\right)(e^{E_1/2} - e^{-E_1/2}) \\ &= \frac{\theta}{1-\theta}(e^{E_1/2} - e^{-E_1/2}) < \frac{1}{e^{L_{\max}E_2} - 1}(e^{E_1/2} - e^{-E_1/2}) \end{aligned}$$

We see that the current converges to zero if we let $L_{\max} \to \infty$: the current gets vanishingly small as the support of the length distribution becomes infinite, for all fields E_1 and allowed densities. That is of course in sharp contrast with the exclusion process of the previous section where the current (67) or (4.8.2) will keep away from zero, uniformly in any cut-off $L_{\max}$.

5 Velocity kappa-distributions

5.1 Introduction

How do Maxwellians originate? Consider a classical gas of N point particles of mass m. We fix the total energy E which we assume is totally kinetic. Every particle has a velocity $\mathbf{v}_i$ with only constraint that $\sum_i mv_i^2/2 = E$. We ask what fraction of particles has a velocity $\mathbf{v}_i \simeq \mathbf{u} \pm \delta$ approximately equal to a given $\mathbf{u}$; the $\delta > 0$ gives some small margin. Denote that proportion by

$$p(\mathbf{u}) := \frac{1}{N} \left| \{ i = 1, \ldots, N : \mathbf{v}_i \in \Delta(\mathbf{u}) \} \right|$$

where $\Delta(\mathbf{u})$ is a cube of volume δ^3 around $\mathbf{u} \in (\delta\mathbb{Z})^3$. The main observation is that for very large N,

$$p(\mathbf{u}) \simeq \frac{e^{-\beta m|\mathbf{u}|^2/2}}{(2\pi m k_B T)^{3/2}}$$

Here T is the absolute temperature (and $\beta = 1/(k_B T)$) for which $E = 3Nk_BT/2$. More precisely, no matter how small we choose some $\varepsilon > 0$, we can make N large enough so that for almost all $(\mathbf{v}_1, \ldots, \mathbf{v}_N)$ on the E-surface,

$$\left| p(\mathbf{u}) - \frac{e^{-\beta m|\mathbf{u}|^2/2}}{(2\pi m k_B T)^{3/2}} \right| \leq \varepsilon$$

Obviously there is the assumption here of an *a priori* uniform distribution, the microcanonical one on phase space, which we take for granted as it is dynamically natural. Given that hypothesis of equidistribution on the energy-surface, we conclude that in thermal equilibrium the Maxwell distribution is just what you would expect, i.e., it is the *typical* velocity distribution, as taught by Boltzmann (1896):

> The Maxwell distribution is in no way a special singular distribution which is to be contrasted to infinitely many more non-Maxwellian distributions; rather it is characterized by the fact that by far the largest number of possible velocity distributions have the characteristic properties of the Maxwell distribution.

There are of course also dynamical "derivations" of the Maxwell distribution. We could e.g. use the Boltzmann equation for dilute gases with hard core interaction to find that the Maxwellian is stationary. Or, for open systems (Brownian motion) we can consider the Langevin equation and derive the Maxwellian as the stationary distribution. Those derivations are in no way independent but in fact consequences,

be it indirectly, of the counting argument above.

The above has a relativistic version (in the so called Jüttner distribution) but that is of no concern for the present chapter. The general question here is to get a simple understanding of the presence of nonMaxwellians in nature. Going for even more sensation, we wish to understand the possible origin of heavily occupied tails in the velocity distribution of dilute gases or other classical macroscopic systems. While one may imagine various possible mechanisms we concentrate on a single idea formalized in Section 5.3: the original reversible dynamics shows localization in energy and when combined with active diffusion in velocity space, the high velocity tails get overpopulated. What matters most is the dependence on the speed of escape rates and of activity parameters, which are addressed as frenetic contributions or non-dissipative aspects in nonequilibrium statistical mechanics, [107].
In Section 5.4 we illustrate the scenario for the origin of power-law decay in space plasmas. Interestingly, the active velocity diffusion there can be related to Taylor dispersion in velocity space [112], and we borrow the insight of [113] to set up a simple model relating it to the telegraph process. Similarly, in Section 5.5 we connect with driven granular gases for the understanding of stretched exponential decay. There we add negative friction to model the macroscopic impact of a vibrating plate which is another version of stochastic acceleration. Both applications are not original and for each of those cases (multiple) analyses and reasons have been given in the literature. E.g. in [114, 115] one finds a convincing explanation of power law tails in the velocity distribution in space plasmas by means of whistler-mode wave stochastic acceleration. For granular gases a very similar analysis is contained in [116, 117]. There may even be other physical explanations, differing in various details. The simplicity of our reasoning may allow to unify those many versions. The point of departure in the next section are Markov diffusion processes in velocity space.

5.2 Fokker-Planck equation

In view of the counting argument presented in the beginning of the Introduction it is natural to ask how then it can still be the case that suprathermal tails physically arise in velocity distributions. It must of course be a nonequilibrium effect, where a driving and the compensation in dissipation gives rise to a stationary condition for an open system dynamics that does not satisfy detailed balance.

In the simplest of worlds we assume a three-dimensional effective Markov diffusion dynamics in an isotropic and homogeneous environment for independent particles of mass m: in Stratonovich convention,

$$m\dot{\mathbf{v}} = -\gamma(v)\,\mathbf{v} + \sqrt{2D(v)}\,\xi_{\mathbf{t}}, \qquad |\mathbf{v}| = v \geq 0$$

where the functions $\gamma(v)$ (friction or rate at which the particle decelerates) and $D(v)$ (diffusion in velocity space) will need to be derived in some limiting regime or under some approximations as e.g. discussed in the next sections. The noise ξ_t is standard white noise in three dimensions. We assume that the initial velocity distribution is isotropic so that the corresponding Fokker-Planck equation for the density $\rho(\mathbf{v},t), t \geq 0$, with respect to $d^3\mathbf{v}$ is given by

$$\frac{\partial\rho}{\partial t}(\mathbf{v},t) = \frac{1}{v^2}\frac{\partial}{\partial v}\left(\frac{\gamma(v)}{m}\,v^3\,\rho(\mathbf{v},t)\right) + \frac{1}{v^2}\frac{\partial}{\partial v}\left(v^2\,\frac{D(v)}{m^2}\frac{\partial\rho}{\partial v}(\mathbf{v},t)\right) \tag{68}$$

The Maxwellian for particles of mass m in a thermal environment at temperature T is the probability density $\rho_{\rm eq}(\mathbf{v}) = \frac{1}{Z}\exp[-mv^2/2k_BT]$. It solves the stationary Fokker-Planck equation (68)$= 0$, whenever $D(v) = k_B\,T\,\gamma(v)$ (Einstein relation in velocity space). Note that the dependence on v of the kinetics hidden in $\gamma(v) = D(v)/(k_BT)$ does not matter at all then for the stationary density.

That Einstein relation gets violated, [118,119], and the dependence of the parameters $\gamma(v), D(v)$ on v becomes in fact crucial when the environment is out-of-equilibrium. In the minimal formal version we still consider in this section it means simply that the function $\gamma(v)$ is no longer proportional to $D(v)$, and then, as is easy to verify, we get the following velocity distribution as stationary solution to (68),

$$\rho_s(\mathbf{v}) \sim \exp -M(v) \tag{69}$$

where $M'(v) = \frac{m\,\gamma(v)\,v}{D(v)}$ or

$$M(v) = m\int_0^v du\,\frac{\gamma(u)\,u}{D(u)} \tag{70}$$

if the integral makes sense. That function $M(v)$ will contain the coupling strength of the particle with its environment and it will depend on further nonequilibrium features of that environment as well. Note however that the spatial extension of the system is not involved, nor do we employ the position of the particle to apply the nonequilibrium driving; there will be no systematic force but in the shaking of the velocities — see below.

The conclusion on the shape of the speed distribution (69) is directly reached by inspecting the exponent α in the large speed behavior of the integrand in (70),

$$\frac{\gamma(v)}{D(v)} = \frac{1}{k_B T} \left(\frac{v}{v_0}\right)^{\alpha-1} \tag{71}$$

(where $k_B T$ sets the thermal energy scale and v_0 is a corresponding reference speed). If $\alpha = 1$ we get $M(v) \propto v^2/2$ and a Gaussian (thermal) decay in the speed distribution. Suprathermal tails are found when $\alpha < 1$ (understanding (71) for $v/v_0 \uparrow \infty$). For $\alpha = 0$ we get an exponential decay. The case $1 > \alpha > -1$ implies compressed to stretched exponential decay ending in $\alpha = -1$ where a power-law decay arises in the speed distribution. For $\alpha < -1$ the set-up does not make sense for obtaining stationary distributions.

Mathematically there are two equivalent ways to get away from $\alpha = 1$ in (71), either to modify $D(v)$ or to modify $\gamma(v)$. Physically, they are arising from different mechanisms possibly, as we discuss in the next sections.

5.3 Diffusive acceleration

The scenario here is to move from the equilibrium dynamics by changing $D(v)$ without changing $\gamma(v)$. In other words we consider (68) in the version of a sum

$$\frac{\partial \rho}{\partial t}(\mathbf{v},t) = \frac{1}{v^2}\frac{\partial}{\partial v}\left(\frac{\gamma(v)}{m}\, v^2 \left[v\,\rho(\mathbf{v},t) + \frac{k_B T}{m}\frac{\partial \rho}{\partial v}(\mathbf{v},t)\right]\right) + \frac{1}{v^2}\frac{\partial}{\partial v}\left(v^2\,\frac{B(v)}{m^2}\frac{\partial \rho}{\partial v}(\mathbf{v},t)\right) \tag{72}$$

which is exactly the same equation as (68) but with $D(v) = k_B T\gamma(v) + B(v)$ and where the left-hand side of (71) is changed into

$$\frac{\gamma(v)}{k_B T\gamma(v) + B(v)} = \frac{1}{k_B T + B(v)/\gamma(v)}$$

The exponent α in (71) is decided by

$$\frac{B(v)}{\gamma(v)} \propto v^{2\eta}, \quad v \uparrow \infty, \qquad \alpha = 1 - 2\eta, \quad 0 \leq \eta \leq 1 \tag{73}$$

to give the stationary nonequilibrium speed distribution (69),

$$\rho_s(\mathbf{v})\, d^3\mathbf{v} = 4\pi\, v^2\, \rho_s(v)\, dv \propto \frac{dv}{v^{2\kappa}}\, \exp -b\, v^{2(1-\eta)}, \qquad v \uparrow \infty \tag{74}$$

with power-law exponent κ getting important (only) for $\eta = 1$, and with $b > 0$ also being determined by further parameters such as mass, reference temperature and

the nature of the nonequilibrium environment.

The physics thus enters in two ways, (1) how the friction parameter $\gamma(v)$ behaves for the detailed balance (undriven dynamics) and (2) what sort of $B(v)$ arises from the driving. Their effects add in the above set-up (72) where the evolution equation has the test particle exposed either to an equilibrium environment at temperature T or to (effectively infinite temperature) diffusive driving. We now discuss $\gamma(v)$ and $B(v)$.

We first determine the friction parameter $\gamma(v)$ for large v. A high-energetic particle experiences a friction force $\gamma(v)$ due to scattering events which cause it to lose energy. To estimate $\gamma(v)$ for large v we therefore need the large energy scattering cross-section $\sigma(v)$, with relation

$$\gamma(v) = v\,\sigma(v)$$

We ignore the angular dependencies; see e.g. [116] for a detailed analysis. For example, if we have elastic potential scattering for a central potential $V(r) \propto r^{-a}$ with exponent $a > 0$, then the cross-section scales as $\sigma(v) \propto v^{-4/a}$, and

$$\gamma(v) \propto v^{1-4/a} \tag{75}$$

Inelastic scattering may create other dependencies (see also in Section 5.5). To get a positive η in (73)–(74) when $B(v)$ is not growing with v, we need $\gamma(v)$ to decay with v. And η gets closer to one when $\gamma(v)$ is decaying faster with large v. That means that for high energy collisions the exchange of energy must be small. Such an effect is often observed and, for obvious reasons, we refer to it as localization, ensuring (relative) stability of high energy regions. Recent examples and demonstrations are presented in [120–123].

Let us now move to $B(v)$. One must first realize that the addition of the last term in (72) is (only and again) a diffusive approximation; see e.g. [124–126]. In particular one should not be forced to think that the true origin of the nonequilibrium condition is literally the connection (through the test particle) of the finite temperature dynamics (first two terms in (72)) with an infinite temperature reservoir (last term in (72)). On a more mesoscopic scale we must try to imagine the effect on a single particle of time- and space-dependent force fields arising in a turbulent plasma. To estimate $B(v)$ let us disconnect the last term in (72) from the other terms, and

only consider the diffusion with amplitude B. We need to know how spacetime force fields in the system accelerate the particle (and would have it run away if no sufficient friction is present). We will treat an example in the next section. Here it suffices to say that as always for Markov diffusions, here the last term in (72), we find the $B(v)$ from the small time ($= \epsilon$) variance

$$m^2 \langle |\mathbf{v}(\epsilon) - \mathbf{v}(0)|^2 \; |\mathbf{v}(0) = \mathbf{v}\rangle = B(v)\,\epsilon, \qquad \epsilon \downarrow 0 \tag{76}$$

In the left-hand side we condition on the initial velocity to be $\mathbf{v}$. If we take $B(v) \simeq v^{-k}$ for some k, then for large times t,

$$|\mathbf{v}(t)| \simeq t^{\frac{1}{2+k}}, \quad \text{or} \quad \frac{d}{dt}\langle v\rangle \propto \langle v^{-1-k}\rangle$$

Diffusion in velocity space is indeed a form of (stochastic) acceleration, where $B(v)$ gives the growth of kinetic energy in time. The idea therefore is that the extra diffusion term in (72) injects energy at rate $B(v)$. Shaking, vibrating or the presence of time-dependent interactions and fields can all contribute to that when treated in the underdamped case. There is in fact a large literature on the subject which originates from fundamental questions in the foundations of statistical mechanics; see e.g. [127] and the references to the Ulam model [128] and to Fermi acceleration [129]. Specific analyses have been carried out in a large number of cases; see e.g. [125, 130–132].

The conclusion is that, combined with $\gamma(v)$, the mechanism of energy injection and how it depends on large v determines the exponent η in (73)–(74).

5.4 Power-law tails in space plasmas

The formal set-up of Section 5.3 applies to space plasmas. There one observes suprathermal tails with $\eta = 0$, i.e., power law decay in the speed distribution. That class of heavy tailed distributions are called $\kappa-$distributions. Discussions on the $\kappa-$distribution in space plasmas have a long history, see e.g. [114, 115, 133] for theoretical discussions. A review of the various aspects in the detection, origin and consequences of $\kappa-$distributions is found in [134]. There we find more information also on measurement procedures and estimations of how the tails (and the kappa-distribution) depend on various parameters.

Confronting it with the Section 5.3 it is clear that because of the Coulomb scattering $a = 1$ in (75) (Rutherford scattering). On the other hand, various arguments have

been developed arguing that due to some form of electromagnetic driving $B(v) \propto 1/v$; see e.g. [135, 136]. Then, in (70), for large speeds $M(v) = 2(1+\kappa)\log(\frac{v}{\sqrt{\kappa}\, w})$ in terms of a parameter $\kappa > 0$. That leads to the κ-(non-thermal)-(nonMaxwellian)-(Lorentzian) velocity distribution which is indeed observed in space plasmas.

The plasma physics underlying the above scaling relations is complicated (and even today still somewhat controversial; see e.g. [137]) especially when dealing with anisotropies and the different types of plasma waves. Yet, that $B(v) \propto 1/v$ should not be too surprising for a force field when the effective force on the particle averages out to zero in the $v \uparrow \infty$ limit; the first correction around zero as governed by the central limit theorem naturally gives the $1/v$-behavior, see also below for more details. A quantitative analysis can be found in [131], when the kinetic energy grows like $t^{2/3}$ in time. We propose to see that as a generalization of Fermi-acceleration, which was first discussed in the context of cosmic rays [125, 127, 129], but is known also more broadly as turbulent or diffusive acceleration [125, 127, 131, 132]. Indeed, Fermi's motivation was to understand the abundance of high energy particles in the cosmos, which is very related of course to the subject of suprathermal tails.

Let us now sketch two concrete models from which the scaling $B(v) \sim 1/v$ emerges. We repeat that the discussion on the diffusive acceleration is disconnected here from the thermal part of the Fokker-Planck equation, i.e., from the first term in the right-hand side of (72). In fact the models that follow do not have an invariant probability for the velocity and may show run-away as was the case in the analysis of Fermi. The point of the analysis here is to estimate $B(v)$ as it originates from a separate mechanism that is additive in the evolution (72).

The first model simply has a random force field $\mathbf{F}(\mathbf{r})$ which for simplicity we take Gaussian and time-independent with mean zero and covariance

$$\langle F_i(\mathbf{r}) F_j(\mathbf{r}') \rangle = \delta_{i,j} f(\frac{\mathbf{r} - \mathbf{r}'}{\ell})$$

where f is a rapidly decaying function decay and ℓ is the correlation length. If we assume that the particle follows a straight trajectory (which is of course justified for short times), then the total momentum imparted by the force fields in time τ, i.e.

$\mathbf{P}_\tau = \int_0^\tau dt \mathbf{F}(\mathbf{r_0} + \mathbf{v}t)$ satisfies $\langle \mathbf{P}_\tau \rangle = 0$ and the variance scales as

$$\langle |\mathbf{P}_\tau|^2 \rangle \propto \frac{\tau v}{\ell} \times \left(\frac{\ell}{v}\right)^2 \sim \tau \frac{\ell}{v}$$

by a simple central limit argument, where $\frac{\tau v}{\ell}$ is roughly the number of independent values of the force field, seen in time τ. Comparing with (76) immediately gives $B(v) \sim 1/v$. That calculation promises to hold more generally when the force is continuous and random in an unbiased, translation-invariant way with short-ranged correlations as long as the central limit theorem applies to the integral (written along the $i-$direction in which the particle moves at great speed v)

$$mv_i(\epsilon) - mv_i(0) = \int_0^\epsilon ds\, F_i(vs) = \frac{1}{v} \int_0^{v\epsilon} dy\, F_i(y) = \sqrt{\frac{\epsilon}{v}}\, Z$$

where the last equality is in distribution for Z a Gaussian random variable with mean zero and finite variance. ($F_i(x)$ is the force at position x with the particle starting at time $s = 0$ from $x = 0$ and moving with speed $v \gg 1$ for a small time ϵ). Breaking of that central limit argument can occur when the force is conservative (gradient of a potential) and the randomness is on the level of the potential and not on the level of the force. We have no specific model in mind for space plasmas. A simple picture would take a dilute neutral plasma for charged particles, ions and electrons. We take such a test particle and it seems reasonable to suppose then that the first two terms in (72) describe the evolution of its velocity distribution before a nonequilibrium source is added. For that source (to be responsible for the last term in (72)) we assume an electromagnetic (EM) field which is stationary far-from-equilibrium. Here many details remain lacking, but it does not seem unreasonable to effectively think about a time-dependent Lorentz force acting on the test particle. Then, the electric field is not gradient by Faraday's law. Secondly we need that the EM-field is sufficiently mixing in the sense to allow sufficient spacetime decorrelation for the central limit argument above to apply. That requires of course also that the variance of the force remains bounded in that nonequilibrium EM-distribution. Various discussions in the literature are of course devoted to that point. It does remain a major problem in space plasma-physics to determine the nature of turbulent plasma that transfers energy from EM-fluctuations to the heating of plasma particles; see e.g. [138].

The above complications invite a second more simple model. Here we refer to his paper [113] which discusses the phenomenon of Taylor dispersion [112] in terms of

a telegraph process [40, 139]. It gives a clear analogy with active (velocity) diffusion that leads to $B(v) \propto 1/v$.
In one dimension, if the amplitude of the force F is constant but the sign flips between two values, we have an active diffusion in velocity space that mimics the run-and-tumble dynamics for active particles in one dimension, see e.g. [14],

$$\dot{v} = \eta\, F$$

where $\eta = \pm 1$, flipping at rate v/ℓ, where ℓ is a length scale related to the flipping of the force, be it a mean free path between collisions, a wave length or a distance like between magnetic mirrors. We think here of a particle for which the sign of the force changes randomly at a rate that is proportional to its speed v. Larger speeds brings the particle faster in a region (over distance ℓ) where the force points in the opposite direction. We get then a diffusion parameter $B(v) \simeq \ell\, F^2/v$, as enters the telegraph equation for the density function on speeds, [14, 113].
We believe that the two-dimensional model of active Brownian particles discussed in [140] provides even a further analogy (with the same conclusion) when the spatial coordinate there is replaced with the velocity, the harmonic trap is taken as Newtonian friction and a Lorentz force is added where the electric field undergoes rotational diffusion in the plane.
At any rate the behavior of $\gamma(v) \sim v^{-3}$ (from Coulomb scattering) and $B(v) \sim v^{-1}$ (from Taylor dispersion) are exactly what is needed to produce power-law decay ($\eta = 1$) in the tails of the speed distribution.

We make two additional remarks:
(1) We have restricted ourselves, as in the title, with the tail-behavior in the velocity distribution. For small speeds we expect close-to-equilibrium behavior where $B(v) = 0$ effectively (no diffusive acceleration). That supports the conclusion of Maxwellian behavior for small speeds.
(2) Statistical correlations between the velocity components or anisotropy may give rise to additional effects but here we focus on the simplest situation and show that the suprathermal tails can be explained without breaking spatial symmetries.

5.5 Injecting energy via negative friction

As mentioned at the end of Section 5.2 we can also change the friction (instead of the diffusion in Section 5.3). Mathematically, the scenario is very similar but the

physics for producing nonMaxwellians with heavy tails is now related to negative friction. As mentioned in [141] Lord Rayleigh was among the very first in his "The theory of sound" (1877) to study motion with energy supply via friction. energy producing high energy cosmic radiation. In the present section we discuss a specific example which is inspired by the physics of granular gases under vibration. The vibration is here taken as coming from the oscillatory motion of a macroscopic object (the boundary) giving energy to the grain particles.

Driven granular gases have been widely studied theoretically and experimentally. The kinetics poses a wide range of interesting questions; see e.g. [126, 142–144]. One of the main phenomena is the deviation from Maxwellian speed distributions. The literature is vast, and we only mention some references. For studies on establishing stretched exponentials, see e.g. [145] and [94]. For the influence of correlations on the velocity statistics of scalar granular gases, see [143, 146]. Many other people have generalized the result to $d > 1$; see [147]. A more recent review with many references and a treatment of inelastic Maxwell molecules is found in [117]. As far as we know there is no experimental evidence for power-law decay in the speed distribution.

One specific and simple dynamical mechanism to create fat tails in the velocity distribution of granular gases goes as follows. Consider "pseudo-Maxwell molecules" where the collision rate between the grains is governed by a restitution coefficient that depends on the relative speeds; see also [117] and the references there for similar and more detailed considerations. In other words, the elasticity of the energy exchanges depends on the speed. As a (one-dimensional) model we think of particles where in collision the velocity is rather drastically reset to close to zero during those (inelastic) collisions (events of resetting the speed to zero), happening after a random time as ticked by an exponential clock at rate $\lambda(v)$. That parameter is the escape rate in a Markov jump process, and is physically (in the diffusion approximation) related to the friction parameter $\gamma(v) = m\lambda(v)$ of (72); the bigger $\lambda(v)$ the easier energy is dissipated away. On the other hand, between the resettings, the particles are driven (e.g. via vibrations) to increase their speed so that in all we have a single particle driven stochastic dynamics for the speed $v_t \geq 0$ of the form (76),

$$\dot{v}_t = \frac{B(v_t)}{m^2 v_t} \qquad \text{and with resettting} \quad v_t \to 0 \ \text{ at rate } \ \gamma(v_t)/m > 0 \qquad (77)$$

To get an equilibrium Maxwellian density we would need to add thermal diffusion, but we ignore that here for simplicity. Obviously now, if $B \equiv 0$, then the grains

cool down and all speeds go to zero eventually. Instead, we take an energy injection of the scaling form

$$B(v) = k_B T\, \gamma(v)\, \left(\frac{v}{v_0}\right)^{2\eta}, \qquad v/v_0 \gg 1 \tag{78}$$

as in (73), where the temperature T and the speed v_0 are reference values, and

$$\gamma(v) = m\nu_0\, \exp\left(-\frac{c}{2\xi}\, \left(\frac{v}{v_0}\right)^{2\xi}\right), \qquad v \gg 1 \tag{79}$$

for parameters $\xi > 0, c \geq 0$, making a stronger high energy localization for $c > 0$, and with reference frequency $\nu_0 > 0$. (Below we require that $\xi \leq 1 - \eta$ and $\xi \downarrow 0$ is allowed. If $\xi + \eta = 1$ then $c < mv_0^2/(k_B T)$ must hold. For inelastic hard spheres, $c = 0$ and constant $\gamma(v) = m\nu_0$ are certainly a good option.)

On the other hand it is easy to see that a stationary density $\rho_s(v)$ for (77) satisfies

$$\begin{aligned} \frac{d}{dv}\left(\frac{B(v)}{m^2\, v}\, \rho_s(v)\right) + \frac{\gamma(v)}{m}\, \rho_s(v) &= 0 \\ \frac{d}{dv} \log \rho_s &= -\frac{m\gamma(v)\, v}{B(v)} - \frac{d}{dv} \log\left(\frac{B(v)}{m^2\, v\, v_0 \nu_0}\right) \\ \frac{d}{dv} \log \rho_s &= -\frac{m\, v_0^{2\eta}}{k_B T}\, v^{1-2\eta} + (1-2\eta)\, v^{-1} + \frac{c}{v_0^{2\xi}}\, v^{2\xi-1} \end{aligned} \tag{80}$$

which we want to solve for large v. Stretched exponential decay of the stationary speed density follows exactly like in (74) whenever $\xi + \eta < 1$ in which case

$$\rho_s \propto \exp\left[-\frac{m\, v_0^2}{2k_B T(1-\eta)}\, \left(\frac{v}{v_0}\right)^{2(1-\eta)}\right]$$

independent of $c \geq 0$. The main ingredient therefore is again to estimate the coefficient η in (78) for the energy injection (76). There is however no unique answer here, depending on the experimental conditions (vibration frequency, particle shape, material). We refer to e.g. [126, 144, 148, 149] for various studies and similar conclusions.

Note that exactly such a model as above was used by Fermi in [129]. Indeed again $\kappa-$distributions appear in the above from (80) for the choice $B(v) = bv^2$ (with some $b > 0$) in (77) (which is Eq. 3 in [129]) and $\eta = 1, c = 0$ in (78)–(79) (where the resetting to a small speed v_0 is discussed in Section IV of [129]). Indeed sections 5.3–5.4 and 5.5 are two sides of the same coin. Here the physics of space plasmas and granular gases meet. That is in particular true in the Fermi-Ulam model, [128]. Such models have been extended e.g. to two dimensions for chaotic billiards with

time-dependent boundaries, [124]. In the light of the previous sections, the scenario of combining localization with energy injection, be it from stochastic acceleration or from negative friction, will generically lead to nonMaxwellian velocity distributions with suprathermal tails.

5.6 A deterministic model for creating fast particles

Very much as an optional dessert, I want to devote a short Subsection to report briefly on an integrable Hamiltonian dynamics concerning a charged particle in interaction with an irradiated dielectric medium.

An EM wave propagates in the positive direction of the $\hat{\mathbf{z}}$-axis. Subjected to this wave is an ionized gas. The external EM wave contributes electric and magnetic fields in the xy-plane. The application of this field induces charge over- and underdensities that give rise to a secondary electric field along the $\hat{\mathbf{z}}$-axis. After all is said and done, one can verify that field-charge-current configuration $(\mathbf{E}(z-ct), \mathbf{B}(z-ct), \rho(z-ct), \mathbf{J}(z-ct))$ solving

$$B_y = \frac{E_x}{c}, \qquad B_x = -\frac{E_y}{c}$$
$$E_z' = \frac{\rho}{\varepsilon_0} = -\frac{J_z}{c\varepsilon_0}$$
$$J_x = J_y = 0$$

is a solution to the full Maxwell equations.
We will now study the motion of one charged test-particle which is subjected to this field-configuration and interacts with it via the Lorentz-force. Its equation of motion is

$$\begin{cases} \frac{dx}{dt}(t) = v_x(\mathbf{p}(t)) \\ \frac{dy}{dt}(t) = v_y(\mathbf{p}(t)) \\ \frac{dz}{\mathrm{d}t}(t) = v_z(\mathbf{p}(t)) \\ \frac{dp_x}{dt}(t) = qE_x(z(t)-ct)\left(1 - \frac{v_z(\mathbf{p}(t))}{c}\right) \\ \frac{dp_y}{dt}(t) = qE_y(z(t)-ct)\left(1 - \frac{v_z(\mathbf{p}(t))}{c}\right) \\ \frac{dp_z}{dt}(t) = q\left[E_z(z(t)-ct) + E_x(z(t)-ct)\frac{v_x(\mathbf{p}(t))}{c} + E_y(z(t)-ct)\frac{v_y(\mathbf{p}(t))}{c}\right] \end{cases}$$

Rewriting the last 3 equations in terms of the new independent variable $T(t) = ct - z(t)$,[3] we get

$$\begin{cases} \frac{dp_x}{dT}(T) = \frac{q}{c}E_x(T) \\ \frac{dp_y}{dT}(T) = \frac{q}{c}E_y(T) \\ (c - v_z(\mathbf{p}(T)))\frac{dp_z}{dT}(T) = \frac{q}{c}\left(E_z(T)c + E_x(T)v_x(\mathbf{p}(T)) + E_y(T)v_y(\mathbf{p}(T))\right) \end{cases} \tag{81}$$

5.6.1 The non-relativistic dynamic

(Optional reading)

In this case, $\mathbf{p} = m\mathbf{v}$ and (81) reduces to ($\kappa := \frac{q}{mc}$)

$$\begin{cases} \frac{dv_x}{dT}(T) = \kappa E_x(T) \\ \frac{dv_y}{dT}(T) = \kappa E_y(T) \\ (c - v_z(T))\frac{dv_z}{dT}(T) = \kappa\left(E_z(T)c + E_x(T)v_x(T) + E_y(T)v_y(T)\right) \end{cases}$$

$T \mapsto v_x(T)$ and $T \mapsto v_y(T)$ are readily obtained by integrating the two first equation w.r.t T (taking into account the initial conditions $v_x(0)$, $v_y(0)$). Note that the 3rd equation is equivalent to

$$\frac{d}{dT}\left(cv_z(T) - \frac{v^2(T)}{2}\right) = \kappa c E_z(T)$$

Integrating this equation yields in principle an explicit expression for v_z in terms of T. However, $cv_z(T) - \frac{v^2(T)}{2} = g(T)$ can not hold when $g(T) > c^2/2$. We will not explore these subtleties (related to the particle passing beyond the speed of light c) because Maxwell's laws and the Lorentz-force law have an awkward relationship with Galilean mechanics anyway.

5.6.2 The relativistic dynamic

In this case, $\mathbf{p} = \frac{m\mathbf{v}}{\sqrt{1-v^2/c^2}} \leftrightarrow \mathbf{v} = c\frac{\mathbf{p}}{\sqrt{(mc)^2+p^2}}$. Similarly as before, the 2 first equations of (81) can be integrated w.r.t. T so that we obtain the dependence of $p_{x,y}$ on T explicitly. The third equation of (81) then becomes

$$c\frac{dp_z}{dT}(T) - v_x(T)\frac{dp_x}{dT}(T) - v_y(T)\frac{dp_y}{dT}(T) - v_z(T)\frac{dp_z}{dT}(T) = qE_z(T) \tag{82}$$

[3] In the relativistic version of this dynamic, $t \mapsto T(t)$ is assured to be strictly increasing. In the non-relativistic version, t and T are perhaps only locally one-to-one.

The LHS of this equation equals $\frac{d}{dT}\left(cp_z(T) - c\sqrt{(mc)^2 + p^2(T)}\right)$. So integrating (82) w.r.t T yields an equation of the form $p_z(T) - \sqrt{(mc)^2 + p^2(T)} = -V_z(T)$ where V_z is an explicit function of T. Solving that equation for p_z yields

$$p_z(T) = \frac{(mc)^2 + p_x^2(T) + p_y^2(T) - V_z^2(T)}{2V_z(T)}$$

So the general picture is as follows:

- If $E_{x,y}$ are functions that oscillate around zero without any specific bias and within explicit amplitude-bounds, then $p_{x,y}$ will inherit a similar oscillatory and bounded character.

- The momentum p_z then remains bounded if the potential V_z remains uniformly removed from 0 and ∞. Note in this regard that the induced charge density ρ defines V_z only up to a constant and that constant is fixed by the particle's initial momentum. is defined up to a constant and that constant. If $\rho = 0$ (i.e. no polarization), then all components of the momenta and velocity are bounded.

- Let me show that when V_z is Lipschitz continuous[4] and it goes to zero at $T = T^*$, then the particle will reach T^* only after infinite real time t. Indeed, recall that $\frac{dT}{\mathrm{d}t} = c - v_z(T)$. Suppose that $\epsilon > 0$ is sufficiently small so that $v_z|_{(T^*-\epsilon,T^*)} > 0$ and $0 < V_z|_{(T^*-\epsilon,T^*)} < \frac{1}{2}mc$. Then $\forall T \in (T^* - \epsilon, T^*)$

$$\begin{aligned}
\frac{\mathrm{d}t}{dT}(T) = \frac{1}{c - v_z(T)} = \frac{c + v_z(T)}{c^2 - v_z^2(T)} &\geq \frac{c}{c^2 - v_z^2(T)} \\
&= \frac{(mc)^2 + p^2(T)}{c((mc)^2 + p_x^2(T) + p_y^2(T))} \\
&\geq \frac{p_z^2(T)}{c((mc)^2 + p_x^2(T) + p_y^2(T))} \\
&= \frac{((mc)^2 + p_x^2(T) + p_y^2(T) - V_z^2(T))^2}{4V_z^2(T)c((mc)^2 + p_x^2(T) + p_y^2(T))} \\
&\geq \frac{(mc/2)^2 + p_x^2(T) + p_y^2(T)}{4V_z^2(T)c} \underbrace{\frac{(mc/2)^2 + p_x^2(T) + p_y^2(T)}{(mc)^2 + p_x^2(T) + p_y^2(T)}}_{\geq 1/4} \\
&\geq \frac{(mc)^2}{64V_z^2(T)c}
\end{aligned} \tag{83}$$

[4]This means that the induced E_z-field is bounded which in turn is a consequence of the induced charge being bounded.

Finally, we use the Lipschitz continuity of V_z to obtain $V_z(T) = V_z(T) - V_z(T^*) \leq K(T^* - T)$ which together with (83) implies that $\frac{\mathrm{d}t}{dT}(T) \geq \frac{m^2 c}{64K^2(T^*-T)^2}$. Integrating this inequality shows that $t \to +\infty$ when $T \overset{<}{\to} T^*$.

- Important for our κ-purposes is however that apparently the induced electric field can catapult a fraction of particles (with approximately the right *resonant* initial conditions) to a relativistic velocity.

- One can imagine that this Hamiltonian dynamic, which models the interactions between a test particle and an environment where surrounding charges are adequately Debye-screened, should be supplemented with a stochastic protocol like occasional shot-noise (which reflects occasional close encounters between the test particle and other charges). If we consult the laws of Moller-Bhabha scattering, the collision cross-section $\sigma(E)$ (where E is the kinetic energy in the center of mass-frame) decays like E^{-2}.

5.6.3 Dynamics including interaction with the plasma bath

Let us integrate the following dynamic:

1. The particle moves according to the Hamiltonian dynamics already described in the previous Section with interruptions at discrete collision-times.

2. The collision times (or waiting time) are distributed in accordance with an inhomogeneous Poisson process.

3. The collision rate r by which such a collision is triggered is velocity-dependent, via the "luminosity $\times$ cross-section" formula

$$\begin{aligned} r(\mathbf{p}(\tau), \tau) &= \frac{\delta \,\#\text{ collisions before time } \tau}{\delta \tau} \\ &= \frac{\delta \,\#\text{ collisions before time } t(\tau)}{\mathrm{d}t} \frac{\mathrm{d}t}{\delta \tau}(\tau) \\ &= \frac{\delta \,\#\text{ collisions before time } t(\tau)}{\mathrm{d}t} \frac{1}{c - v_z(\tau)} \\ &= \underbrace{\sigma(v(\tau))}_{\text{scattering cross-section}} \underbrace{\rho(\tau) v(\tau)}_{\text{luminosity}} \frac{1}{c - v_z(\tau)} \end{aligned}$$

   (Recall again that the density of scatterers ρ may depend on $\tau = ct - z$ because of the induction effect of the passing EM-wave on the plasma)

4. When a collision occurs, say the j'th collision since the dynamics began, a stochastic update rule determines the outgoing momentum $\mathbf{p}_f$ of the particle in terms of the ingoing momentum $\mathbf{p}_i$ and a (i.i.d) random variable ω_j: $\mathbf{p}_f = \boldsymbol{\xi}(\mathbf{p}_i, \omega_j)$. The requirement that the unstimulated dynamics (i.e. the case with no applied external wave and a constant scatter-density ρ) is reversible and that its steady state is MBJ imposes certain restrictions on the protocol $\boldsymbol{\xi}(., \omega_j)$

We will show that for a physical functional ansatz for the cross-sectional dependence on velocity (or energy) there is a positive probability that our test-particle will have accelerated to speed c without a single intervening collision. Hence, the interaction with the bath does not resolve the runaway nature of the dynamic.

So how does σ typically depend on v or E? At high energies, the answer suggested by dimensional analysis is: proportional to $\lambda\frac{(\hbar c)^2}{E^2}\left(1 + o\left(\frac{mc^2}{E}\right)\right)$ (with λ a dimensionless number). More detailed scattering calculations (Mott, Moller scattering) confirm this picture [150].

Now, we've seen that in the Hamiltonian dynamics our test-particle momentum and energy can diverge to infinity at finite τ^*.
We will-show that the probability that such a take-off remains uninterrupted (say between time $\tau^* - \epsilon$ and τ^*) by collisions is non-zero. The demonstration is fairly easy: according to the rules of the inhomogeneous Poisson process, that probability P is given by

$$P = \exp\left(-\int_{\tau^*-\epsilon}^{\tau^*} r(\mathbf{p}(\tau), \tau)\delta\tau\right)$$
$$= \exp\left(-\int_{\tau^*-\epsilon}^{\tau^*} \frac{\lambda(\hbar c)^2}{E^2(\tau)}\rho(\tau)\frac{v(\tau)}{c - v_z(\tau)}\delta\tau\right)$$

So we have to show that the integral in the exponent is finite. We will grant ourselves a maximum $\rho_{\max}$ to the density $\rho(\tau)$. Next we have that $v(\tau) < c$ and $\frac{1}{c-v_z(\tau)} = \frac{c+v_z(\tau)}{c^2-v_z^2(\tau)} \leq \frac{c+v_z(\tau)}{c^2-v^2(\tau)} \leq (2c)\frac{E^2(\tau)}{m^2c^6}$. Hence

$$\int_{\tau^*-\epsilon}^{\tau^*} \frac{\lambda(\hbar c)^2}{E^2(\tau)}\rho(\tau)\frac{v(\tau)}{c - v_z(\tau)}\delta\tau \leq \int_{\tau^*-\epsilon}^{\tau^*} \lambda(\hbar c)^2\rho_{\max}\frac{2c^2}{m^2c^6}\delta\tau = \frac{2\lambda\rho_{\max}\hbar^2\epsilon}{(mc)^2} < \infty$$

Note finally that our dynamics is clearly sufficiently ergodic that every particle will repeatedly have the occasion to taxi to a state from where such a take-off is easy. Hence, regardless of the initial state, a test-particle will speed up to the speed of light with probability 1.

6 Stabilization of patterns by stirring

6.1 Introduction

The present chapter presents a mathematical study about the stabilization of a probe (the slow particle) which interacts with (fast) medium particles that are subject to a vortex-shaped force-field. The induced force on the probe is zero in the cyclone's eye explaining the title of the chapter, i.e., in the center of rotation which is a symmetry point for the medium dynamics. Simulations and heuristics have been given in the paper [35]; here we add new results combined with a mathematically rigorous treatment of previous questions. In words, we are dealing with a two-dimensional overdamped medium of diffusing particles in short range interaction with a probe. Each medium particle moves under a sufficiently confining self-potential and undergoes a rotational force. We consider the quasi-static regime in which the mechanical force on the probe is averaged over the (mostly unknown) stationary distribution of the medium. That mean force on the probe vanishes when the probe is placed at the center of rotation. We define the stiffness matrix to discuss the linear stability of that fixed point. It allows to discuss the stabilizing effect of the rotations, or how the effective spring constant between origin and probe changes as function of the rotation amplitude.

A more formal introduction to our results is to consider an overdamped dynamics of a medium particle with position $y(t) \in D(0,R) \subseteq \mathbb{R}^2$ on a disk of radius R centered at the origin (possibly $R = +\infty$),

$$\dot{y}_t = -\nabla_y U(x, y_t) - \epsilon\, F(y_t) + \sqrt{2\beta^{-1}}\, \xi_t \tag{84}$$

where (ξ_t) stands for standard white noise with prefactor β^{-1} equal to the temperature, representing the thermal environment of the medium. The $x \in \mathbb{R}^2$ is the position of a probe in interaction with the medium through a smooth potential $U(x,y)$. The latter contains also the self-potential on the medium particles. The nonequilibrium driving of strength ϵ is in the force $F(y) = \omega(|y|)\,(-y_2,\, y_1) = |y|\,\omega(|y|)\,\hat{\varphi}$ which is a divergence-less (possibly differential) rotation around the origin. The unit vector $\hat{\varphi}$ is in the azimuthal direction and the rotation profile $r \mapsto \omega(r)$ is assumed to be smooth in the radial coordinate $|y| = r$. For $\epsilon = 0$ the dynamics is reversible at inverse temperature β with equilibrium density $\rho_{\mathrm{eq}}(y) = \exp[-\beta U(x,y)]/Z_x$ with respect to dy. In the next section we give mathematical details and sufficient assumptions for the well-behavedness of the Markovian dynamics corresponding to

(84). There will be a unique smooth stationary probability measure $\rho_{x,\epsilon}(y)dy$ and we will discuss the 'smoothness' of the map $x \mapsto \rho_{x,\epsilon}(y)$, which is necessary to define the stiffness matrix $\mathcal{K}$ from the mean force $x \mapsto \mathscr{F}(x)$ exerted on the probe when $x \to 0$,

$$\mathcal{K}_{ij}(\epsilon) := -\frac{\partial \mathscr{F}_j}{\partial x^i}(0,\epsilon), \qquad \mathscr{F}_i(x,\,\epsilon) := -\left\langle \frac{\partial U}{\partial x^i}(x,y) \right\rangle_{x,\,\epsilon}, \quad i = 1,2$$

The expectation in $\langle\cdot\rangle_{x,\,\epsilon}$ is the average under $\rho_{x,\epsilon}(y)\,dy$. The force $\mathscr{F}(x)$ is zero for $x = 0$ so that the stiffness estimates the stability of the probe at the origin. The entry $\mathcal{K}_{ii}$ on the diagonal of the stiffness matrix can be called the spring constant $\kappa(\epsilon) = \kappa(-\epsilon)$ which starts as ϵ^2 around equilibrium (where $\epsilon = 0$).

After the preliminary material of Section 6.2 we start in Section 6.3 by proving a general expression for the stiffness matrix which distinguishes clearly the nonequilibrium effects. What we show is that

$$\mathcal{K}_{ij}(\epsilon) = \mathcal{K}_{ij}(0) + \beta\epsilon \int_0^{+\infty} dt \ \left\langle \frac{\partial U}{\partial x^i}(0,y_0) F^k(y_0) \frac{\partial}{\partial y^k} \frac{\partial U}{\partial x^j}(0,y_t) \right\rangle_0 \tag{85}$$

where the time-correlation is in the nonequilibrium medium dynamics with the probe at $x = 0$ and started at time zero with probability density $\rho_0(y) \propto \exp\left(-\beta U(0,y)\right)$. We also prove the universality of the stiffness in the limit $|\epsilon| \to \infty$ where the stiffness becomes independent of the imposed rotation profile, getting

$$\mathcal{K}_{ij}(\infty) := \lim_{\epsilon \uparrow \infty} \mathcal{K}_{ij}(\epsilon) = \int dy\, \rho_0(y)\ \frac{\partial^2 U}{\partial x^i \partial x^j}(0,y) = \left\langle \frac{\partial^2 U}{\partial x^i \partial x^j}(0) \right\rangle_0 \tag{86}$$

Clearly then the asymptotic spring constant depends only on the mechanical stiffness in that limit while the difference

$$\mathcal{K}_{ij}(\infty) - \mathcal{K}_{ij}(0) = \beta \left\langle \frac{\partial U}{\partial x^i}(0),\ \frac{\partial U}{\partial x^j}(0) \right\rangle_0$$
$$= \beta \left\{ \left\langle \frac{\partial U}{\partial x^i}(0)\, \frac{\partial U}{\partial x^j}(0) \right\rangle_0 - \left\langle \frac{\partial U}{\partial x^i}(0) \right\rangle_0 \left\langle \frac{\partial U}{\partial x^j}(0) \right\rangle_0 \right\} \geq 0$$

is non-negative and picks up the equilibrium fluctuation in terms of the force-force covariance.

In Section 6.5 we show that the stiffness matrix is a smooth function of the driving parameter ϵ so that we can carry out expansions around equilibrium, $\epsilon = 0$. That is used in Section 6.7 to prove that for either unequivocally attractive or for repulsive

probe-particle interaction U and non-negative rotation profile ω one has a relative stabilization, i.e.

$$\frac{d^2\mathcal{K}_{ij}}{d\epsilon^2}(\epsilon = 0)\xi^i\xi^j > 0, \qquad \xi \in \mathbb{R}^2$$

(Einstein summation is assumed throughout this chapter. Indices are always lowered or raised with respect to the standard metric δ_{ij}).

In Section 6.9 we show the monotonicity in ϵ of the symmetric part of $\mathcal{K}_{ij}(\epsilon)$ when the rotation is rigid ($\omega(r) = 1$), even when an interaction between the medium particles is added which only depends on the relative distance between the particles. That means that the spring constant $\kappa(\epsilon)$ is non-decreasing in ϵ. We expect (but do not prove) that that scenario of monotone stabilization of the probe at the center as function of the rotational amplitude holds true under much weaker conditions as well. Counterexamples exist however. While they are not explicitly discussed here, it is important for the type of mathematical arguments that can be made. One could indeed formulate the problem differently, whereby the probe itself is subjected to a certain dynamics. Stability would then allegedly be related to the speed of (exponential) relaxation to the stationary distribution $\rho(x, y)$. This relaxation speed is then a subject of entropy and (hypo)coercivity methods [151–154]. At any rate we here proceed quite differently — we apply a "force-method" which is physically very transparent. In fact our treatment in the linear case is almost trivial whereas the coercivity method proving exponential convergence is a lot of hard work, even for cases where we know the result is true.

6.2 Model and mathematical setup

The present section contains mathematical specifications concerning model (84). Some generalities from the theory of diffusion processes are repeated in the present context for self-consistency. We emphasize mostly the construction of the pseudo-inverse of the backward generator in Section 6.2.3.

We start with independent medium particles having positions y on the open disk $M = D(0, R) \subseteq \mathbb{R}^2$ (possibly $R = +\infty$) and a probe is placed statically at a position $x \in M$.

6.2.1 Forces

We give here assumptions on the potential $U(x, y) = V_{pp}(|x - y|) + V_{ext}(|y|)$ and forces $F(y) = \omega(|y|)\,(-y_2,\, y_1) = |y|\,\omega(|y|)\,\hat{\varphi}$ appearing in (84).

We assume $(x,y) \mapsto V_{pp}(|x-y|)$ and $y \mapsto V_{ext}(y)$ both are smooth maps. The same is then true for $(x,y) \mapsto U(x,y)$. We write $V(y) := U(x=0,\, y)$ and we suppose that $\int_M \exp(-\beta V(y))\, dy < \infty$. Moreover, the potential V is bounded below and diverges at the boundary of the disk M, i.e., for every closed interval $[a,b]$,

$$V^{-1}([a,b]) \subseteq M \text{ is compact} \tag{87}$$

We assume finally that the divergence at the boundary (when $R < \infty$) is sufficiently pronounced: there are $\delta, m, \gamma > 0$ so that for all $y \in M$ with $|y| > R - \delta$,

$$(1 - \frac{\gamma}{\beta})(\nabla V(y))^2 - \frac{1}{\beta}\nabla^2 V(y) \geq m \tag{88}$$

That condition assures that there is sufficient compactness, so that the Poincaré inequality (see (95)) holds true.
Additionally, we assume

$$\begin{aligned} \int_M dy\, \exp(-\beta V(y))(\nabla V(y))^2 < \infty \\ \int_M dy\, \exp(-\beta V)(\nabla_x U(x=0,y))^2 < \infty. \end{aligned} \tag{89}$$

We further assume there to be some $\epsilon > 0$ s.t. $\forall x \in B(0,\epsilon)$

$$\begin{aligned} k_1(x) := \sup_{z\in M:\, |z|<|x|} \left\|\nabla_y (U(z) - U(0))\right\|_\infty = \sup_{z\in M:\, |z|<|x|} \sup_{y\in M} |\nabla_x (U(z,y) - U(0,y))| < \infty \\ k_2(x) := \sup_{z\in M:\, |z|<|x|} \left\| \left(-(\nabla_y V)\cdot\nabla_y + \beta^{-1}\nabla_y^2\right)(U(z) - U(0)) \right\|_\infty < \infty \\ \limsup_{x\to 0} \frac{k_1(x)}{|x|},\ \limsup_{x\to 0} \frac{k_2(x)}{|x|} \ < \infty. \end{aligned} \tag{90}$$

For the rotational driving we suppose that the force $F = (F_1, F_2)$ is bounded: there is a finite C so that for all $y \in M$,

$$|F(y)| = \sqrt{F_1^2(y) + F_2^2(y)} = |\omega(|y|)\, |y| < C. \tag{91}$$

For e.g. rigid rotation, where $\omega(r) \equiv 1$, that implies we work on a finite disk: $R < \infty$.
Note that by the foregoing constructions the driving field leaves the potential invariant, i.e.,

$$F_i(y)\frac{\partial V}{\partial y^i}(y) = F_i(y)\frac{\partial U}{\partial y^i}(0,y) = 0 \tag{92}$$

Likewise, for a (weakly-)differentiable function u and for $\Omega := -F^i\partial_i$,

$$\int_M dy\, \rho_0 F^i \partial_i \left(\frac{u^2}{2}\right) = -\int_M dy\, \rho_0\, u\, \Omega u = 0 \tag{93}$$

6.2.2 Spaces

To define the generator and the diffusive dynamics, we first set the function-analytic stage. Consider the weight function given by the probability density

$$\rho_0(y) := \frac{1}{Z} \exp\left(-\beta V(y)\right), \quad Z = \int dy \, \exp\left(-\beta V(y)\right) < \infty$$

always with respect to the Lebesgue measure dy on $\mathbb{R}^2$. It is easy, by virtue of (92), to show that ρ_0 solves the stationary Kolmogorov forward equation associated to (84) provided $x = 0$ (but for ϵ arbitrary.)
We use the notation

$$\langle u \rangle_0 := \frac{1}{Z} \int dy \, \exp\left\{-\beta V(y)\right\} \, u(y) \, = \int dy \, \rho_0(y) \, u(y)$$

for the expectation of a function $u : \mathbb{R}^2 \to \mathbb{R}$. We define $\mathscr{L}^2$ as the real Hilbert space of functions $u : M \to \mathbb{R}$ whose norm associated to the inner product

$$(u, v)_{\mathscr{L}^2} := \int dy \, \rho_0 \, uv =: (u, v)$$

is finite. For example, (93) says that

$$(u, \Omega v) = -(\Omega u, v). \tag{94}$$

Next, we use the notation 1 for the constant function $y \in M \mapsto 1$ and $H := 1^\perp \subseteq \mathscr{L}^2$.
Consider the bilinear form

$$(u, v)_{H^0} := \int dy \, \rho_0 \nabla u \cdot \nabla v.$$

Note that (87), (88) imply that the smooth function $\eta : \mathbb{R} \to (1, +\infty) : y \mapsto \exp(\gamma(V(y) - \min(V))$ has the properties

1. $\lim_{|s| \to R} \eta(s) = +\infty$.

2. There exists an $m > 0$ and a compact subset $K \subseteq M$ so that:

$$\frac{1}{\eta} \left(\nabla V - \beta^{-1} \nabla^2\right) \eta \Big|_{M \setminus K} \geq \gamma m$$

It is shown in [155] that the existence of such a "Lyapunov function" implies a so-called Poincaré inequality: For all weakly differentiable functions $u : M \to \mathbb{R}$, we have the Poincaré inequality

$$c^2 \left(\|u\|^2_{\mathscr{L}^2} - (u, 1)(1, u) \right) = c^2 \left(\left\langle u^2 \right\rangle_0 - \langle u \rangle_0^2 \right) \leq \left\langle (\nabla u)^2 \right\rangle_0 = \|u\|^2_{H^0} \tag{95}$$

where the constant c depends only on the temperature β^{-1} and the potential V. As a consequence,

$$H^0 := \left\{ u \subseteq \mathscr{L}^2 \mid (u,u)_{H^0} < +\infty,\, (u,1)_{\mathscr{L}^2} = 0 \right\}$$

is a Hilbert space.

6.2.3 Operators

Definition 6.1. *$\ell_{x,\epsilon}$ is the formal backward operator acting on twice-weakly differentiable functions $u : M \mapsto \mathbb{R}$ as*

$$\ell_{x,\epsilon} u = -\left((\nabla_y U)(x,y) + \epsilon F\right) \cdot (\nabla u)(y) + \beta^{-1} (\nabla^2 u)(y)$$

(Its co-domain being locally integrable functions).

Proposition 6.1. *For all x in some open $\mathcal{W} \subseteq B(0,\epsilon)$ there exists a densely-defined unbounded operator $L_{x,\epsilon} : D \subseteq \mathscr{L}^2 \to \mathscr{L}^2$ with the following properties:*

1. *For $u \in H^0$ twice weakly-differentiable so that $\ell_{x,\epsilon} u \in \mathscr{L}^2$, one has*

$$L_{x,\epsilon} u = \ell_{x,\epsilon} u \tag{96}$$

2. *$L_{x,\epsilon}$ is the generator of a positive strongly-$\mathscr{L}^2$-continuous contraction semigroup $\{S(t) : \mathscr{L}^2 \to \mathscr{L}^2\}_{t \geq 0}$ which is probability-conserving: $S(t)1 \equiv 1$.*

3. *For $x = 0$ and all $u, v \in D$, abbreviating $L_{0,\epsilon} =: L_\epsilon$, one has*

$$(u, L_\epsilon v) = (L_{-\epsilon} u, v) \tag{97}$$

   and

$$(u, L_\epsilon u) = -\beta^{-1} (u,u)_{H^0}$$

   so that L_ϵ is negative–definite.

4. *Further abbreviating $L_0 =: L$, one has $L_\epsilon = L + \epsilon\Omega$ with $\Omega : H^0 \to \mathscr{L}^2 : u \mapsto -F^i \partial_i u$ and for all $u, v \in H^0$,*

$$(u, Lv) = -\beta^{-1} (u,v)_{H^0}$$

Proofs of these statements can be found Appendices F and G.

We now define the pseudo-inverse, as appearing in the following

Proposition 6.2. *There exists an operator $L_\epsilon^{-1} : \mathscr{L}^2 \to H^0 \subseteq \mathscr{L}^2$ with the following properties:*

1. *One has*

$$\forall u \in D:\ L_\epsilon^{-1} L_\epsilon u = P_H u := u - 1(u,1), \qquad \forall u \in \mathscr{L}^2 : L_\epsilon^{-1} u \in D \text{ and } L_\epsilon L_\epsilon^{-1} u = P_H u$$

2. *There are $k_3(x), k_4(x) > 0$ so that $\forall x \in B(0,\epsilon)$*

$$\sup_{u \in \mathscr{L}^2} \frac{\left\| L_{x,\epsilon}^{-1} u \right\|_{\mathscr{L}^2}}{\|u\|_{\mathscr{L}^2}} \leq k_3(x) \tag{98}$$
$$\sup_{u \in \mathscr{L}^2} \frac{\left\| L_{x,\epsilon}^{-1} u \right\|_{H^0}}{\|u\|_{\mathscr{L}^2}} \leq k_4(x)$$

3. *For all $u, v \in \mathscr{L}^2$,*

$$(u, L_\epsilon^{-1} v) = (L_{-\epsilon}^{-1} u, v) \text{ and } (u, L_\epsilon^{-1} u) \leq 0 \tag{99}$$

Proofs of these statements are in the Appendix, subsection F, where the notation $R_\epsilon := L_\epsilon^{-1}$ is used.

6.2.4 Stationary density: construction and uniqueness

In this section, we construct the stationary density $\rho_{x,\epsilon}$ corresponding to probe position $x(\neq 0)$ and driving parameter ϵ.

Definition 6.2. *Let $x \in B(0,\epsilon)$, and let $\langle 1 \rangle$ denote the vector space generated by the constant functions.*
Define the map (suppressing the y-dependence) $F_x : H^0 \oplus \langle 1 \rangle \to \mathscr{L}^2$

$$\begin{aligned} F_x u &= -\exp(\beta V) \nabla \left[\exp(-\beta V) \cdot \nabla \left(U(x) - U(0) \right) u \right] \\ &= \beta \ell_{0,0}(U(0) - U(x)) u - \nabla \left(U(x) - U(0) \right) \cdot \nabla u \\ &= \beta L(U(0) - U(x)) u - \nabla \left(U(x) - U(0) \right) \cdot \nabla u \end{aligned}$$

A few remarks:

1. Replacing $\ell_{0,0}$ by L, in the last step, is justified by (96) and assumption (90).

2. F_x is well-defined with the stated (co-)domain since

$$\begin{aligned} \|F_x u\|_{\mathscr{L}^2} &\leq \beta \|L(U(0) - U(x))\|_\infty \|u\|_{\mathscr{L}^2} + \|\nabla [U(x) - U(0)]\|_\infty \|u\|_{H^0} \\ &\leq \beta k_2(x) \|u\|_{\mathscr{L}^2} + k_1(x) \|u\|_{H^0} \end{aligned}$$

   If $u \in H^0$, the Poincaré inequality (95) implies that the RHS is smaller than $(\beta c^{-1} k_2(x) + k_1(x)) \|u\|_{H^0} =: k_F(x) \|u\|_{H^0}$ and $k_F(x) = O(x)$ by (90).

Proposition 6.3. *In some open neighborhood of $x = 0$, the function*

$$\nu_{x,\epsilon} = \sum_{n=0}^{+\infty} (L_{-\epsilon}^{-1} F_x)^n 1 \tag{100}$$

is well-defined and $\nu_{x,\epsilon} - 1 \in \mathscr{L}^2 \cap H^0$. Moreover, $\nu_{x,\epsilon}$ is the unique element in $\mathscr{L}^2$ solving ($\forall u \in D$)

$$(\nu_{x,\epsilon}, L_{x,\epsilon} u) = 0. \tag{101}$$

One also has

$$\nu_{x,\epsilon} = 1 + L_{-\epsilon}^{-1} F_x 1 + O(x^2) \tag{102}$$

Therefore $\rho_{x,\epsilon} := \rho_0 \nu_{x,\epsilon}$ is the unique stationary density.
A proof of these statements can be found in the Appendix, subsection (G).

6.3 The stiffness matrix

The statistical force $\mathscr{F}$ exerted on the probe when at position x (in a neighborhood of the origin) and at driving ϵ is given by

$$\mathscr{F}_i(x,\, \epsilon) := -\left\langle \frac{\partial U}{\partial x^i}(x) \right\rangle_{x,\,\epsilon}$$

That force is zero for $x = 0$, due to the rotational symmetry of the system. To estimate the stability of the origin we introduce the stiffness matrix (at the origin), defined as

$$\mathcal{K}_{ij}(\epsilon) := -\frac{\partial \mathscr{F}_j}{\partial x^i}(0, \epsilon)$$

It is not hard to show that rotational and reflection symmetry[5] imply that the stiffness matrix takes the form

$$\mathcal{K}(\epsilon) = \begin{pmatrix} m(\epsilon) & a(\epsilon) \\ -a(\epsilon) & m(\epsilon) \end{pmatrix} \tag{103}$$

where moreover $\forall \epsilon \in \mathbb{R}$

$$m(\epsilon) = m(-\epsilon), \qquad a(\epsilon) = -a(-\epsilon). \tag{104}$$

Theorem 6.1. *The statistical force $x \mapsto \mathscr{F}(x, \epsilon)$ is differentiable at $x = 0$ and the stiffness matrix equals*

$$\mathcal{K}_{ij}(\epsilon) = \left\langle \frac{\partial^2 U}{\partial x^i \partial x^j}(0) \right\rangle_0 - \beta \left(\frac{\partial U}{\partial x^i}(0),\, \frac{\partial U}{\partial x^j}(0) \right) + \beta \left(\frac{\partial U}{\partial x^i}(0),\, \epsilon \Omega L_\epsilon^{-1} \frac{\partial U}{\partial x^j}(0) \right) \tag{105}$$

[5]Note that plane reflection switches the direction of the nonequilibrium force $\epsilon F \to -\epsilon F$. So formally, such a reflection switches the sign of the driving parameter ϵ.

or equivalently

$$\mathcal{K}_{ij}(\epsilon) = \left\langle \frac{\partial^2 U}{\partial x^i \partial x^j}(0) \right\rangle_0 - \beta \left(\frac{\partial U}{\partial x^i}(0),\, L L_\epsilon^{-1} \frac{\partial U}{\partial x^j}(0) \right) \tag{106}$$

That expression distinguishes between the "equilibrium" and the "nonequilibrium" contributions to the stiffness matrix as announced in (85). The relation of the expression (105) to the expression (86) (involving the time-integral) stems from the semigroup-identity $L_\epsilon^{-1} v = \int_0^{+\infty} e^{L_\epsilon t} v \, dt$ which holds for all $v \in H$.

Proof. One has

$$\begin{aligned} \left\langle \frac{\partial U}{\partial x^i}(x) \right\rangle_x - \left\langle \frac{\partial U}{\partial x^i}(0) \right\rangle_0 &= \left\langle \left(\frac{\rho_{x,\epsilon}}{\rho_0} - 1 \right) \frac{\partial U}{\partial x^i}(x) \right\rangle_0 + \left\langle \frac{\partial U}{\partial x^i}(x) - \frac{\partial U}{\partial x^i}(0) \right\rangle_0 \\ &= \left(\frac{\rho_{x,\epsilon}}{\rho_0} - 1, \frac{\partial U}{\partial x^i}(x) \right) + \left(\frac{\partial U}{\partial x^i}(x) - \frac{\partial U}{\partial x^i}(0), 1 \right) \end{aligned} \tag{107}$$

For the first term (107), (102) and (90) imply that

$$\begin{aligned} \left(\frac{\rho_{x,-\epsilon}}{\rho_0} - 1, \frac{\partial U}{\partial x^i}(x) \right) &= \left(L_{-\epsilon}^{-1} F_x 1, \frac{\partial U}{\partial x^i}(0) \right) + O(x^2) \\ &= \beta \left(L_{-\epsilon}^{-1} L(U(0) - U(x)),\, \frac{\partial U}{\partial x^i}(0) \right) + O(x^2) \\ &= \beta \left(L(U(0) - U(x)),\, L_\epsilon^{-1} \frac{\partial U}{\partial x^i}(0) \right) + O(x^2) \qquad (108) \\ &= \beta \left(U(0) - U(x),\, L L_\epsilon^{-1} \frac{\partial U}{\partial x^i}(0) \right) + O(x^2) \qquad (109) \\ &= -\beta \left(\frac{\partial U}{\partial x^j}(0),\, L L_\epsilon^{-1} \frac{\partial U}{\partial x^i}(0) \right) x^j + O(x^2) \qquad (110) \\ = -\beta \left(\frac{\partial U}{\partial x^j}(0),\, \frac{\partial U}{\partial x^i}(0) \right) x^j &+ \beta \left(\frac{\partial U}{\partial x^j}(0),\, \epsilon \Omega L_\epsilon^{-1} \frac{\partial U}{\partial x^i}(0) \right) x^j + O(x^2) \end{aligned}$$

where in (108) we use that, by the RHS of (89), $\frac{\partial U}{\partial x}(x=0)$ is in $\mathscr{L}^2$ so that we can apply (99). In (109) we use that L_ϵ^{-1} maps to D and (97). In (110) we use that by Lagrange's theorem

$$\left| U(0,y) - U(x,y) - \frac{\partial U}{\partial x^j}(0,y) x^j \right| = \left| \frac{\partial U}{\partial x^j}(x_y, y) - \frac{\partial U}{\partial x^j}(0,y) \right| |x| \leq k_1(x_y)|x| \leq k_1(x)|x|$$

so that $\left\| U(0) - U(x) - \frac{\partial U}{\partial x^j}(0) \right\|_{\mathscr{L}^2} \leq \left\| U(0) - U(x) - \frac{\partial U}{\partial x^j}(0) \right\|_\infty = O(x^2)$.
Regarding the second term in (107), by (90) we see that the map

$$\varphi : (0,1) \times M \to \mathbb{R} : (t,y) \mapsto \frac{1}{|x|t} \left(\frac{\partial U}{\partial x^i}(xt, y) - \frac{\partial U}{\partial x^i}(0,y) \right)$$

is bounded above by $q1$ for some $q > 0$. Since this upper bound is integrable, the dominated convergence theorem implies that

$$\lim_{t\to 0+} \frac{1}{t}\left\langle \frac{\partial U}{\partial x^i}(xt) - \frac{\partial U}{\partial x^i}(0)\right\rangle_0 = \left\langle \frac{\partial^2 U}{\partial x^k \partial x^i}(0)\right\rangle_0 (x^k) + o(|x|).$$

Now one arrives at the desired expression by combining the two terms again. □

6.4 Example: linear forces

As interludium consider the example (introduced in [35]) where

1. The reservoir is $\mathbb{R}^2$, i.e., $R = \infty$.
2. The potentials are harmonic: $V_{ext}(y) = \frac{1}{2}k_1|y|^2$, $V_{pp}(|x-y|) = \frac{1}{2}k_2|x-y|^2$.
3. The driving is rigid: $F = (-y_2, y_1) \leftrightarrow \omega \equiv 1$.

Note that while 1 and 3 are incompatible within the framework of this chapter due to the constraint (91), this example can be worked out in full details and it provides useful insight in what can be expected.
Under those circumstances, one can compute that the density

$$\rho_{x,\epsilon}(y) = \left(\frac{\beta(k_1+k_2)}{2\pi}\right) \exp\left(-\beta\frac{k_1+k_2}{2}(y-c_x)^2\right)$$

is stationary for

$$c_x = \frac{k_2}{(k_1+k_2)^2+\epsilon^2}\begin{bmatrix} k_1+k_2-\epsilon \\ \epsilon k_1 + k_2 \end{bmatrix}\begin{bmatrix} x_1 \\ x_2 \end{bmatrix}.$$

Taking $x = (x_1, 0)$, we can compute the components of the statistical force:

$$\mathscr{F}_1(x) = -\left\langle \frac{\partial}{\partial x_1} V_{pp}(|x-y|)\right\rangle_{x,\epsilon} = k_2 \int_{\mathbb{R}^2} (y_1 - x_1)\rho_{x,\epsilon}(y)dy = k_2((c_x)_1 - x_1)\int_{\mathbb{R}^2}\rho_{x,\epsilon}(y)dy$$
$$= k_2((c_x)_1 - x_1) = k_2\left[\frac{k_2(k_1+k_2)}{(k_1+k_2)^2+\epsilon^2} - 1\right]x_1$$
$$\mathscr{F}_2(x) = -\left\langle \frac{\partial}{\partial x_2} V_{pp}(|x-y|)\right\rangle_{x,\epsilon} = k_2(c_x)_2 = \left[\frac{k_2^2\epsilon}{(k_1+k_2)^2+\epsilon^2}\right]x_1$$

So we see that the radial force $f_1(x,\epsilon)$ becomes more center-directed as $|\epsilon|$ increases, saturating at a finite value $-k_2x_1$ as $|\epsilon| \to \infty$. A tangential component $f_2(x,\epsilon)$ is picked up due to the rotational force, yet this component vanishes again in the limit $\epsilon \to \infty$.

At the level of the stiffness matrix (103), these calculations yield the following results for the on- and off-diagonal elements:

$$m(\epsilon) = -k_2 \left[\frac{k_2(k_1+k_2)}{(k_1+k_2)^2+\epsilon^2} - 1 \right], \qquad a(\epsilon) = \left[\frac{k_2^2 \epsilon}{(k_1+k_2)^2+\epsilon^2} \right].$$

We recognize the following qualitative properties:

1. $\epsilon \mapsto m(\epsilon)$ is a smooth increasing map and $\lim_{\epsilon\to\infty} m(\epsilon) = k_2$ exists.

2. $\epsilon \mapsto a(t)$ is smooth, zero at $\epsilon = 0$ and zero as $\epsilon \to \infty$.

3. (86) in this system (since $\frac{\partial^2}{\partial x^i \partial x^j} V_{pp} = k_2 \delta_{ij}$).

The smoothness of these maps is a property which will be confirmed at the general level in Section 6.5. The limiting behavior for large $|\epsilon|$ is again confirmed in appreciable generality as discussed in Section 6.8. The positivity and monotonicity of m does not hold in general. Positivity however holds for small $|\epsilon|$ when the probe exerts an unequivocally attractive or repulsive force on the medium and the profile $\omega \geq 0$, as proven in Section 6.7. Monotonicity is shown to hold for $\omega \equiv 1$, as shown in Section 6.9.

6.5 Smooth dependence on the driving strength

Lemma 6.1. *$\forall u \in D$, $\forall m \in \mathbb{N}_0$ and $\forall \epsilon_0 \in \mathbb{R}$ we have*

$$(L+\epsilon\Omega)^{-1}u = \sum_{k=0}^{m-1} (\epsilon_0-\epsilon)^k ((L+\epsilon_0\Omega)^{-1}\Omega)^k (L+\epsilon_0\Omega)^{-1}u + \underbrace{(L+\epsilon\Omega)^{-1}((\epsilon_0-\epsilon)\Omega(L+\epsilon_0\Omega)^{-1})^m u}_{=:I_m(\epsilon)} \tag{111}$$

and the $\mathscr{L}^2$-norm of $I_m(\epsilon)$ is $O(|\epsilon_0-\epsilon|^m)$.

Remark: recall that $(L+\epsilon\Omega)^{-1}$ maps to H^0 which is in the domain of Ω. Therefore the domain of the composition $\Omega(L+\epsilon\Omega)^{-1}$ is the entire $\mathscr{L}^2$-space and the expressions in the lemma above make sense without limitation.

Proof. We prove (111) by induction. The basis step is verified by

$$\begin{aligned}\left\{(L+\epsilon\Omega)^{-1} - (L+\epsilon_0\Omega)^{-1}\right\} u &= (L+\epsilon\Omega)^{-1}\left\{(L+\epsilon_0\Omega) - (L+\epsilon\Omega)\right\}(L+\epsilon_0\Omega)^{-1}u \\ &= (\epsilon_0-\epsilon)(L+\epsilon\Omega)^{-1}\Omega(L+\epsilon_0\Omega)^{-1}u.\end{aligned}$$

For the induction-step we have

$$\begin{aligned} &I_m(\epsilon) - (\epsilon_0-\epsilon)^m(L+\epsilon_0\Omega)^{-1}(\Omega(L+\epsilon_0\Omega)^{-1})^{m+1}u \\ &= (\epsilon_0-\epsilon)^m\left\{(L+\epsilon\Omega)^{-1} - (L+\epsilon_0\Omega)^{-1}\right\}(\Omega(L+\epsilon_0\Omega)^{-1})^m u \\ &= (\epsilon_0-\epsilon)^m(L+\epsilon\Omega)^{-1}\left\{(L+\epsilon_0\Omega) - (L+\epsilon\Omega)\right\}(L+\epsilon_0\Omega)^{-1}(\Omega(L+\epsilon_0\Omega)^{-1})^m u \\ &= (\epsilon_0-\epsilon)^{m+1}(L+\epsilon\Omega)^{-1}(\Omega(L+\epsilon_0\Omega)^{-1})^{m+1}u = I_{m+1}(\epsilon). \end{aligned}$$

The $\mathscr{L}^2$-norm of $I_m(\epsilon)$ can be bounded as

$$\|I_m(\epsilon)\| \leq |\epsilon_0-\epsilon|^m \underbrace{\left\|(L+\epsilon\Omega)^{-1}\right\|}_{\leq k_3(0) \text{ by (98)}} \left\|\Omega((L+\epsilon_0\Omega)^{-1}\Omega)^m u\right\| \leq \text{ constant } |\epsilon_0-\epsilon|^m$$

□

Recall the expression (106) for the stiffness matrix. writing $f_i := \frac{\partial U}{\partial x^i}(0)$ and applying the expansion (111), we then get

Proposition 6.4. *(smoothness of the stiffness matrix)*

$$\mathcal{K}_{ij}(\epsilon) = \mathcal{K}_{ij}(\epsilon_0) - \beta\sum_{k=1}^{m-1}(\epsilon_0-\epsilon)^k\left(f_i,\, L[L_{\epsilon_0}^{-1}\Omega]^k L_{\epsilon_0}^{-1}f_j\right) - \beta\left(f_i,\, LL_\epsilon^{-1}((\epsilon_0-\epsilon)\Omega L_{\epsilon_0}^{-1})^m f_j\right) \tag{112}$$

implying that $\mathcal{K}_{ij}$ is a smooth function of ϵ.

In particular, when we set $\epsilon_0 = 0$. We get

$$\mathcal{K}_{ij}(\epsilon) = \mathcal{K}_{ij}(0) - \beta\sum_{k=1}^{m-1}(-\epsilon)^k\left(f_i,\, [\Omega L^{-1}]^k f_j\right) - \beta\left(f_i,\, LL_\epsilon^{-1}((-\epsilon)\Omega L^{-1})^m f_j\right) \tag{113}$$

6.6 Vector fields and rotation invariance

Definition 6.3. *A radial function $\varphi : M \to \mathbb{R}$ is of the form $y \mapsto u(|y|)$ for some map $u : (0,+\infty) \to \mathbb{R}$. A vectorfield $V : M \to \mathbb{R}^2 : y \mapsto (V_1(y), V_2(y))$ is called rotation invariant if a.e.*

$$\begin{cases} V_1(y) = \frac{1}{|y|}\left(V_r(y)y_1 - V_\varphi(y)y_2\right) = V_r(y)\hat{y}_1 - V_\varphi(y)\hat{y}_2 \\ V_2(y) = \frac{1}{|y|}\left(V_r(y)y_2 + V_\varphi(y)y_1\right) = V_r(y)\hat{y}_2 + V_\varphi(y)\hat{y}_1. \end{cases} \tag{114}$$

where V_r and V_φ are radial functions. When V_φ vanishes in that expression, V is a radial vectorfield.

When we write e.g. $V \in \mathscr{L}^2$ or $V_i \in \mathscr{L}^2$ it is understood that all components of V are in $\mathscr{L}^2$. The same agreement holds for $V \in H^0$, $V \in D$.
Let V, W be rotation invariant vector fields, then $\Omega V_i = \omega I_i^j V_j$, where

$$I_i^j = \begin{pmatrix} I_1^1 I_1^2 \\ I_2^1 I_2^2 \end{pmatrix} = \begin{pmatrix} 0 & -1 \\ 1 & 0 \end{pmatrix}$$

Note that when $V \in D$, then $\Omega V \in D$. When $V \in \mathscr{L}^2$ is rotation invariant and of the form (114), Proposition F.2 (in the Appendix) implies that

$$\begin{cases} (L^{-1}V_1)(y) = (\tilde{R}V_r)(y)\hat{y}_1 - (\tilde{R}V_\varphi)(y)\hat{y}_2 \\ (L^{-1}V_2)(y) = (\tilde{R}V_r)(y)\hat{y}_2 + (\tilde{R}V_\varphi)(y)\hat{y}_1. \end{cases}$$

where $\tilde{L}_\epsilon = L_\epsilon - \frac{1}{\beta r^2}$ maps radial functions to radial functions. So $L_\epsilon^{-1}V := (L_\epsilon^{-1}V_1,\, L_\epsilon^{-1}V_2)$ is rotation invariant as well. Likewise, when $V \in D$, $L_\epsilon V := (L_\epsilon V_1,\, L_\epsilon V_2)$ is rotational invariant.
When $V \in \mathscr{L}^2$ and the rotation profile $r \mapsto \omega(r) \equiv \omega$ is constant, we have $(\forall \epsilon \in \mathbb{R})$

$$[\Omega, L_\epsilon^{-1}]V := \Omega L_\epsilon^{-1}V - L_\epsilon^{-1}\Omega V = 0$$

Moreover, when $V \in D$

$$[\Omega, L]V := \Omega L V - L\Omega V = 0.$$

6.7 Stabilization close to equilibrium

In this section, we prove a result detailing that when the probe-particle force is unequivocally attractive or repulsive and the rotation-profile $\omega \geq 0$, then close to equilibrium one has a relative stabilization of the stiffness matrix.

Theorem 6.2. *Suppose $y \mapsto f_i(y)y^i$ is either non-negative or non-positive. Suppose in addition that $y \mapsto \omega(|y|)$ is non-negative and $\omega f \neq 0$ in the sense of $\mathscr{L}^2$, then*

$$\frac{d^2\mathcal{K}_{ij}}{d\epsilon^2}(\epsilon = 0)\xi^i\xi^j > 0$$

for all $\xi \in \mathbb{R}^2$.

Proof. Due to the rotational symmetry (104), it suffices to check the positivity of the trace

$$\frac{d^2\mathcal{K}_i^i}{d\epsilon^2}(0).$$

Using expression (113), we see that

$$\mathcal{K}_i^i(\epsilon) = \mathcal{K}_i^i(0) + \epsilon \underbrace{(f_i,\, \Omega L^{-1} f^i)}_{=0} - \epsilon^2 (f_i,\, (\Omega L^{-1})^2 f^i) + o(\epsilon^2).$$

Now

$$\begin{aligned}(f_i,\, (\Omega L^{-1})^2 f^i) = \delta^{ij}(f_i,\, (\Omega L^{-1})^2 f_j) = \delta^{ij}(f_i,\, \omega I_j^k L^{-1} \omega I_k^l L^{-1} f_l) \\ = -(f_i,\, \omega L^{-1} \omega L^{-1} f^i) = -(f,\, \omega \hat{y}_i L^{-1} \omega L^{-1} f^i) = -(f,\, \omega \tilde{R}(\omega \hat{y}_i L^{-1} f^i)) \\ = -(f,\, \omega \tilde{R} \omega \tilde{R}(f^i \hat{y}_i)) = -(f,\, \omega \tilde{R} \omega \tilde{R} f)\end{aligned}$$

where we write $f := f^i \hat{y}_i$ and we use Proposition F.2 in the Appendix (recall that $L^{-1} = R_0$). But by item 4 of Proposition F.1, $-\tilde{R}$ maps non-zero, non-negative functions to positive functions. So $\tilde{R} f > 0$. But then $\omega \tilde{R} f \geq 0$ and non-zero. But then $\tilde{R} \omega \tilde{R} f > 0$. Finally then, $\omega \tilde{R} \omega \tilde{R} f \geq 0$ is positive in the support of ω. Therefore, since $\omega f \neq 0$ in the sense of $\mathscr{L}^2$, $y \mapsto \omega(y) f(y) [\tilde{R} \omega \tilde{R} f](y)$ is a non-negative measurable function whose support has non-zero $\mathscr{L}^2$-measure. Therefore

$$\frac{d^2}{d\epsilon^2} \mathcal{K}_i^i(\epsilon) = -2(f_i,\, (\Omega L^{-1})^2 f^i) = 2(f,\, \omega \tilde{R} \omega \tilde{R} f) > 0$$

□

6.8 Infinite driving limit

Throughout this section, the bound (98) plays an important role.

Lemma 6.2. *For every radial vectorfield V for which both V, $\frac{V}{\omega} \in \mathscr{L}^2$, one has*

$$\|L_\epsilon^{-1} V\|_{\mathscr{L}^2} \leq \frac{1}{\epsilon} \left\| \frac{1}{\omega} V \right\|_{\mathscr{L}^2}.$$

Proof. Notice that for every radial vectorfield $W \in D$, one has

$$\begin{aligned}\left\| \frac{1}{\omega} L_\epsilon W \right\|_{\mathscr{L}^2} \geq \left(I_i^j \hat{y}_j,\, \frac{1}{\omega} L_\epsilon W^i \right) = \left(I_i^j \hat{y}_j,\, \frac{1}{\omega} L(w \hat{y}^i) \right) + \epsilon \delta^{il} \left(I_i^j \hat{y}_j,\, I_l^k w \hat{y}_k \right) \\ = \underbrace{(I_i^j \hat{y}_j \hat{y}^i}_{=0},\, \frac{1}{\omega} \tilde{L}(w)) + \epsilon \left(\hat{y}_i,\, w \hat{y}^i \right) = \epsilon \|W\|_{\mathscr{L}^2}\end{aligned}$$

Plugging in $W = L_\epsilon^{-1} V$, which is indeed in D, we get $\left\| \frac{1}{\omega} V \right\|_{\mathscr{L}^2} \geq \epsilon \|L_\epsilon^{-1} V\|_{\mathscr{L}^2}$. □

Recall that the force $f(y) := -(\nabla_x U)(x = 0, y)$ is a smooth and compactly supported vector-field. Therefore $f \in D$. So in the expression (106) for the stiffness-matrix, (97) implies that

$$\left(f_i,\, L L_\epsilon^{-1} f_j \right) = \left(L f_i,\, L_\epsilon^{-1} f_j \right).$$

We can thus establish (86) by virtue of the following corollary

Corollary 6.1. *Suppose the force on the probe* $f = -(\nabla_x U)(x = 0)$ *and the rotation profile* ω *share the property that* $f/\omega \in \mathscr{L}^2$*, then*

$$\lim_{\epsilon \to \infty} \left(L f_i,\, L_\epsilon^{-1} f_j \right) = 0.$$

6.9 Monotonicity of the stabilization for rigid driving

We say that the driving is rigid when ω is constant, say $\omega(r) \equiv 1$. The rotational driving is now $\Omega = \frac{\partial}{\partial \varphi}$. The arguments that follow are based on the property that $[\Omega, L]V_i := \Omega L V_i - L\Omega V_i = 0$ for a radial vectorfield $V_i \in D$ (for which ΩV_i is still in D, so that the second term of the commutator makes sense). That remains so when we add interaction between the medium particles which is rotation invariant, i.e. a two-body potential function of the distance between the medium particles.

Lemma 6.3. *On all relevant operator domains,* $[\Omega, L] = 0$ *implies that for all* $\epsilon_1, \epsilon_2 \in \mathbb{R}$

1. $L_{\epsilon_1} L_{\epsilon_2} = L_{\epsilon_2} L_{\epsilon_1}$
2. $L_{\epsilon_1} L_{\epsilon_2}^{-1} = L_{\epsilon_2}^{-1} L_{\epsilon_1}$
3. $L_{\epsilon_1}^{-1} L_{\epsilon_2}^{-1} = L_{\epsilon_2}^{-1} L_{\epsilon_1}^{-1}$

Proof. The first identity is trivial. For the second identity, consider that for all $V \in D$,

$$L_{\epsilon_2}^{-1} L_{\epsilon_1} V = L_{\epsilon_2}^{-1} L_{\epsilon_1} L_{\epsilon_2} L_{\epsilon_2}^{-1} V = L_{\epsilon_2}^{-1} L_{\epsilon_2} L_{\epsilon_1} L_{\epsilon_2}^{-1} V = L_{\epsilon_1} L_{\epsilon_2}^{-1} V$$

where we used the first identity in the middle. For the third identity, note that for all $V \in H$,

$$\begin{aligned} L_{\epsilon_1}^{-1} L_{\epsilon_2}^{-1} V &= L_{\epsilon_1}^{-1} L_{\epsilon_2}^{-1} L_{\epsilon_1} L_{\epsilon_1}^{-1} V \\ &= L_{\epsilon_1}^{-1} L_{\epsilon_1} L_{\epsilon_2}^{-1} L_{\epsilon_1}^{-1} V = L_{\epsilon_2}^{-1} L_{\epsilon_1}^{-1} V \end{aligned}$$

where we used the second identity in the middle. □

Theorem 6.3. *When* Ω *corresponds to rigid rotation, then the nonequilibrium contribution to the stiffness matrix is negative semi-definite and it is monotone in* $|\epsilon|$*.*

Proof. $f_i := \frac{\partial U}{\partial x^i}(x = 0)$ is a rotation–invariant vector field, so all the identities of Lemma (6.3) apply.

When $\epsilon = 0$, the nonequilibrium contribution is zero, so it suffices to check the monotonicity in $|\epsilon|$.

According to the expansion (112), that monotonicity amounts to verifying that for all $\xi \in \mathbb{R}^d$ and $\epsilon > 0$ we have

$$\begin{aligned} 0 \geq \left(L_{-\epsilon}^{-1} L L_{-\epsilon}^{-1} \Omega f_i,\, f_j\right) \xi^i \xi^j = \left(L_{-\epsilon}^{-1} L L_{-\epsilon}^{-1} \Omega f_i \xi^i,\, f_j \xi^j\right) \\ = \frac{1}{2} \left(\left(L_{-\epsilon}^{-1} L L_{-\epsilon}^{-1} \Omega v,\, v\right) + \left(v,\, L_{-\epsilon}^{-1} L L_{-\epsilon}^{-1} \Omega v\right) \right) = I(\epsilon) \end{aligned}$$

where $v = f^j \xi_j$ has the same domain and symmetry properties as f^j.

Now,

$$\begin{aligned} 2I(\epsilon) = \left(L \Omega L_{-\epsilon}^{-1} L_{-\epsilon}^{-1} v,\, v\right) + \left(v,\, L \Omega L_{-\epsilon}^{-1} L_{-\epsilon}^{-1} v\right) \\ = \left(L_{-\epsilon}^{-1} L_{-\epsilon}^{-1} v,\, \left\{ -\Omega L L_{-\epsilon} L_{-\epsilon} + L_\epsilon L_\epsilon L \Omega \right\} L_{-\epsilon}^{-1} L_{-\epsilon}^{-1} v\right) \end{aligned}$$

and it suffices to check that the operator $-\Omega L L_{-\epsilon} L_{-\epsilon} + L_\epsilon L_\epsilon L \Omega$ is negative–definite. After a calculation, one gets $4 \Omega L L \Omega = -(2L\Omega)^\dagger (2L\Omega)$. □

7 The dark energy problem through a statistical mechanical lens

7.1 Introduction

Within the classical Friedmann-Lemaître-Robertson-Walker model of the universe the cosmological constant Λ has traditionally been thought to provide an effective way to account for cosmological data showing acceleration in the cosmic expansion. That model assumes a homogeneous and isotropic universe with metric

$$\mathrm{d}s^2 = \mathrm{d}t^2 - a^2(t)\,\mathrm{d}\Omega_k^2 \tag{115}$$

with a the scale factor and $\mathrm{d}\Omega_k^2$ the spatial line element with spatial curvature $k = 0, \pm 1$, for which the Einstein equation gives rise to the Friedmann equations. If matter is a perfect fluid with mass density ρ and pressure p, then the scale factor enters the Hubble parameter $H = \dot{a}/a$ to satisfy

$$H^2 = 2\kappa^2\rho - k\,\frac{c^2}{a^2R^2} + \frac{\Lambda c^2}{3} \tag{116}$$

where $\kappa^2 = 4\pi G/3$, G is Newton's constant, and R refers to the size of the universe. The second Friedmann equation is

$$\frac{\ddot{a}}{a} = -\kappa^2\left(\rho + 3\frac{p}{c^2}\right) + \frac{\Lambda\, c^2}{3} \tag{117}$$

The presence of Λ in the right-hand side thus indeed makes all the difference for cosmic acceleration, so it seems. There remain controversies on the exact nature or physical origin of that Λ. In particular, it is not settled whether the cosmological constant is strictly of quantum mechanical origin and/or whether it represents a systematic (dynamical) *versus* a fluctuation effect. One suggestion is that in a UV-complete theory it corresponds to the quantum vacuum energy. Another suggestion is to attribute Λ to the back-reaction of cosmic fluctuations onto the background evolution or even to a violation of the Copernican principle by assigning a special place for the earth in the universe [156, 157]. There have also been explorations to derive it as a quantum gravity effect [158–160].

The contribution in the present chapter is much more modest: it only concerns a change of physics at an effective, more macroscopic level, with white noise or quantum forces being added to the energy-stress tensor, while local properties of the cosmos are not to be altered. We assume e.g. that photons still move on null

geodesics and redshift according to the laws of geometric optics in general relativity. More specifically, we discuss the modifications of the corresponding Friedmann equations (116)–(117) in the context of a mini-superspace description of quantum gravity following ideas of Squires [161] and of Pinto-Neto and Santini [162]. The set-up thus arises from applying the usual quantization techniques to a symmetry-reduced classical theory but, in contrast with [162] where stiff matter is considered, in the present chapter matter is given by dust as described by Brown and Kuchař [163]. We believe that is more adequate to describe the universe shortly after recombination. Similarly as in [162] we find that the evolution may display accelerated expansion, without any need for an explicit cosmological constant.

In the case of a dust universe, the pressure term in (117) is negligible, $p/c^2 = 0$, and we think of a perfect classical fluid which has very small kinetic energy compared to its rest mass. In the next Section, we present the quantum description of gravity coupled to dust in the case of mini-superspace. The wave equation has the simple form of the free Schrödinger equation with the matter field playing the role of a clock variable. The quantum Friedmann equations follow from that equation by identifying the rate of change of the scale factor with the flux in the corresponding continuity equation. We discuss the main constraints on the dynamics in Section 7.5. The time-evolution of the scale factor is investigated in Section 7.8 for describing a scenario with cosmic acceleration. We give examples of wave functions for which there is a period of accelerated expansion of the universe, without introducing a cosmological constant, yielding an excellent fit to the concordance model.

7.2 Noise-induced force: the example of thermophoresis

Let us consider a colloid dissolved in a vessel filled with an overdamping fluid with a place-dependent time-independent temperature-profile $T(x)$. Suppose moreover that...

- The colloid-fluid interactions are sufficiently short-ranged (compared to the length-scale defined by the temperature-gradient), translation-invariant and isotropic. Collectively, they allow for a local-equilibrium state where the colloid-position x is uniformly distributed over the vessel.

- Ignoring the solvent, the colloid is amenable to a reduced Markovian description.

- In that reduced description, if x_0 is the colloid's initial position at time $t = 0$, then

$$\langle (x_t^\alpha - x_0^\alpha)(x_t^\beta - x_0^\beta) \rangle = \gamma T(x_0) \delta^{\alpha\beta} t + o(t)$$
$$\langle (x_t^\alpha - x_0^\alpha) \rangle = v^\alpha(x_0) t + o(t)$$
$$\langle |x_t - x_0|^{2+\delta} \rangle = o(t)$$

Under these conditions, the Fokker-Planck equation governing the colloid position's probability density acquires the form

$$\partial_t \rho = \nabla_x \cdot \left(\gamma T(x) \nabla_x \rho + \underbrace{(\gamma \nabla T - v)}_{=\tilde{v}} \rho \right). \tag{118}$$

and $\rho(x,t) \equiv 1$ being a solution requires that $\nabla_x \cdot \tilde{v} = 0$, i.e. $\tilde{v}$ must be divergence-free. On the other hand, one can imagine the type of system with isotropic short-range interactions we have in mind $\tilde{v}(x)$ will have to be a function depending on the value of the fluid pressure, temperature at x and the gradients of those quantities at x. One can imagine that such a pointwise local dependence plus the divergence-free property forces $\tilde{v}$ to be zero. So in the end the Fokker-Planck equation is simply

$$\partial_t \rho = \nabla_x \cdot (\gamma T(x) \nabla_x \rho)$$

which corresponds to a stochastic differential equation

$$dx_t = \sqrt{2\gamma(x) T(x)} \circ d\mathbf{B}_t$$

where the coupling $\circ$ is neither Itô nor Stratonovich but, in integral form, corresponds to $x_t - x_0 = \lim_{n\to\infty} \frac{1}{n} \sum_{j=1}^n \sqrt{2T(\frac{j}{n}t)}\, (B(\frac{j}{n}t) - B(\frac{j-1}{n}t))$.
Multiplying (118) by x and integrating over x, we find:

$$\langle x_t \rangle = x_0 - \gamma(\nabla T)(x_0) t + o(t)$$

The drift in the second term of the rhs is the result of a so-called *thermophoretic force*. Physically, it is a consequence of microreversibility but at a superficial mathematical level that force is simply a consequence of addition of non-Itô noise to the equation of motion.
In the next Subsection, this observation will inspire us to add non-Itô noise to the Einstein equations of general relativity, e.g. to reflect the backreaction of small-scale structure or reflecting small-scale quantum fluctuations.

7.3 Adding noise to the Friedmann equations

We can solve the Einstein-equations

$$G_{\mu\nu} = \frac{8\pi G}{c^4} T_{\mu\nu} \tag{119}$$

for a flat FLRW-metric $g_{\mu\nu}\mathrm{d}x^\mu \mathrm{d}x^\nu = \mathrm{d}t^2 - a^2(t)\left((\mathrm{d}x^1)^2 + (\mathrm{d}x^2)^2 + (\mathrm{d}x^3)^2\right)$, with the energy-stress tensor of the form ([164] 1.5.14)

$$T_{00}(x) = \rho(t), \qquad T_{ij}(x) = a^2(t)p(t)\delta_{ij}, \qquad T_{i0} = T_{0i} = 0$$

where the energy density ρ and the pressure p are usually regarded as sufficiently smoothly depending on t. In our treatment, these functions will be replaced by stochastic processes. The functions ρ and p will be of a stochastic nature, but that is not relevant at this point. Relevant is however that the Einstein equation (119) in this FLRW-context is equivalent to the following two equations ([164], 1.5.19 and 1.5.20):

$$\begin{cases} \left(\frac{\dot{a}}{a}\right)^2 = \frac{8\pi G}{3}\rho \\ \dot{\rho} = -3\frac{\dot{a}}{a}\left(\rho + p\right) \end{cases}$$

Writing $\kappa^2 = \frac{8\pi G}{3}$ and eliminating $\frac{\dot{a}}{a}$ from the second equation, we get the equivalent set of ODE's (assuming $\dot{a}(t_0) > 0$ and $t \mapsto \rho(t)$ never vanishes)

$$\begin{cases} \dot{a} = \kappa\sqrt{\rho}\, a \\ \dot{\rho} = -3\kappa\sqrt{\rho}\,(\rho + p) \end{cases} \tag{120}$$

It is now natural to introduce stochasticity into this dynamics via the pressure $p(t)$. We can imagine that averaging over spatial and microscopic fluctuations may give a noisy contribution to the pressure. The most straightforward hypothesis is that this noise is approximately white with an amplitude depending on the instantaneous scale factor $a(t)$:

$$p = \overline{p_{\mathrm{matter}}}(t) + \sqrt{2C(a(t))}\,\xi(t)$$

This equation raises the question how the amplitude $\sqrt{2C(a(t))}$ is precisely coupled to the white noise. In the previous discussion, we had a special invariant probability density as a guide. Requiring time-reversibility can be another guide, but these are both uncompelling guides in the present context. Purely concerning dynamical considerations, if we think of the pressure-fluctuations to be a smooth approximation to white noise, the Wong-Zakai theorem [165, 166] hints towards a Stratonovich coupling as the 'correct' choice.

Next, note that we have the white noise depend on the time-variable t. That seems natural because t is the proper time along a worldline $t \mapsto (t, x^1, x^2, x^3)$ of any co-moving observers. So it is natural that fast microscopic dynamical fluctuations must evolve at a rate set by this time-variable and that we choose to have the white noise depend on t.

Let consider a dust universe and put $\overline{p_{\text{matter}}} = 0$ from now on.
As for the dependence of the amplitude C on a, we are particularly interested in the following three possibilities:

1. $C(a) = a^{-3}$ or $C(a) = a^3$: If we imagine that noise results from $N \propto \text{Vol}(t) \propto a^3(t)$ ($\text{Vol}(t)$ is the relative volume of the spatial Cauchy-surface at FLRW time t) independent processes or variables $P_1^t, ..., P_N^t$ (which are active at FLRW-time t) and the average cosmological pressure is

$$p(t) = \sum_{j=1}^{N} P_j^t, \qquad \text{or} \qquad p(t) = \frac{1}{N} \sum_{j=1}^{N} P_j^t,$$

   then by the CLT, $p(t)$ is going to be a Gaussian random variable with rms $\propto \sqrt{N} \propto a^{3/2}$ in the first case or rms $\propto \sqrt{1/N} \propto a^{-3/2}$ in the second case.

2. $C = 1$.

Before proceeding to the solving of (120), let me mention that that system of equations does not tolerate that ρ becomes negative. With p the white noise sketched above we unfortunately lack a confinement or other safeguard to protect that requirement. The most conservative way to proceed then is to consider white-noise realizations where ρ does not become negative.

Now, the Fokker-Planck equation (governing the probabiliy density $\mathcal{P}(a, \rho, t)$ associated to (120)) is of the form

$$\partial_t \mathcal{P} = -\partial_a \left(\kappa \sqrt{\rho}\, a\, \mathcal{P}\right) - \partial_\rho \left(3\kappa \sqrt{\rho^3}\, \mathcal{P}\right) + 3\kappa C(a) \partial_\rho \left(f(\rho)\, \partial_\rho \left(g(\rho)\, \mathcal{P}\right)\right)$$
$$f(\rho) g(\rho) = \rho$$

If the dynamics is released at a point (a_0, ρ_0) at time t_0, the ensuing solution will drift at small times like

$$\begin{pmatrix} \langle a(t) \rangle \\ \langle a(t) \rangle \end{pmatrix} = \begin{pmatrix} a_0 + v_a(a_0, \rho_0) t \\ \rho_0 + v_\rho(a_0, \rho_0) t \end{pmatrix} + o(t)$$

where expressions for the vector-field v can be obtained from the Fokker-Planck equation. To get an idea of the typical behaviour of solutions of this diffusion, one can study the integral-curves of the vector-field v. That is depicted in figures 13, 14 and 15 and shows that in the case $C(a) \sim a^3$ we can expect the noise to significantly boost the cosmic expansion rate. We will not pursue this line of investigation further at this point. The next subsection will delve into the main line of research of this chapter, which concerns a toy model in quantum gravity.

Figure 13: This graph displays integral curves of the vector-field $v = (v_a, v_\rho)$ for $\kappa = 1$, $C(a) = \frac{2}{300}a^{-3}$. The graphs show the results for $\rho(t = 0) = 5$ and (from top to bottom) $a(t = 0) = 2, 1.5, 1, 0.5$. On short time-scales the behaviour is very much agreement with that of a standard dusty FLRW-universe ($a(t) \propto t^{2/3}$), while the lower graph shows that the deceleration comes to a standstill on a longer time-scale (due to the fluctuating pressure) and $t \mapsto \langle a(t) \rangle$ approaches a linear curve.

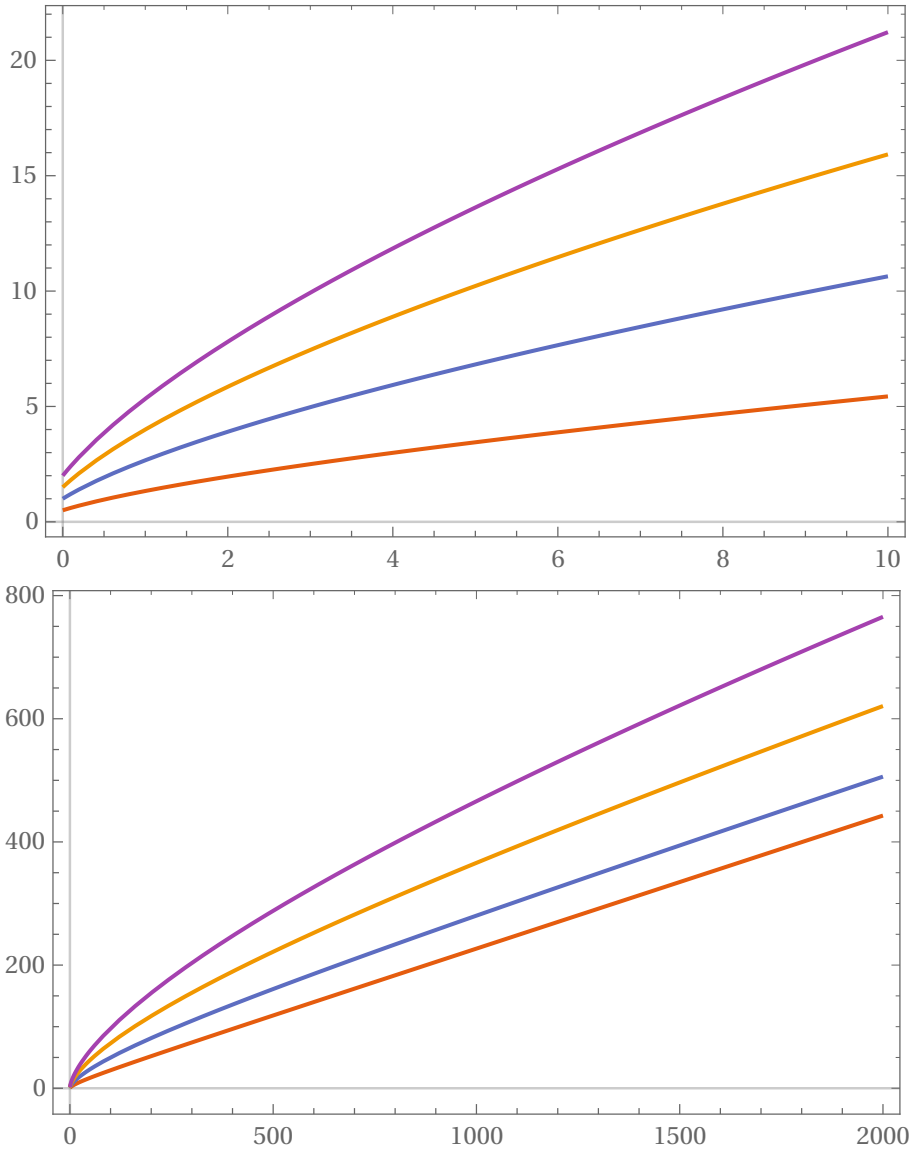

Figure 14: This graph displays integral curves of the vector-field $v = (v_a, v_\rho)$ for $\kappa = 1$, $C(a) = \frac{2}{300}a^3$ and $a(t = 0) = 0.5$, $\rho(t = 0) = 5$. In this case, the initial deceleration is overtaken by an abrupt acceleration.

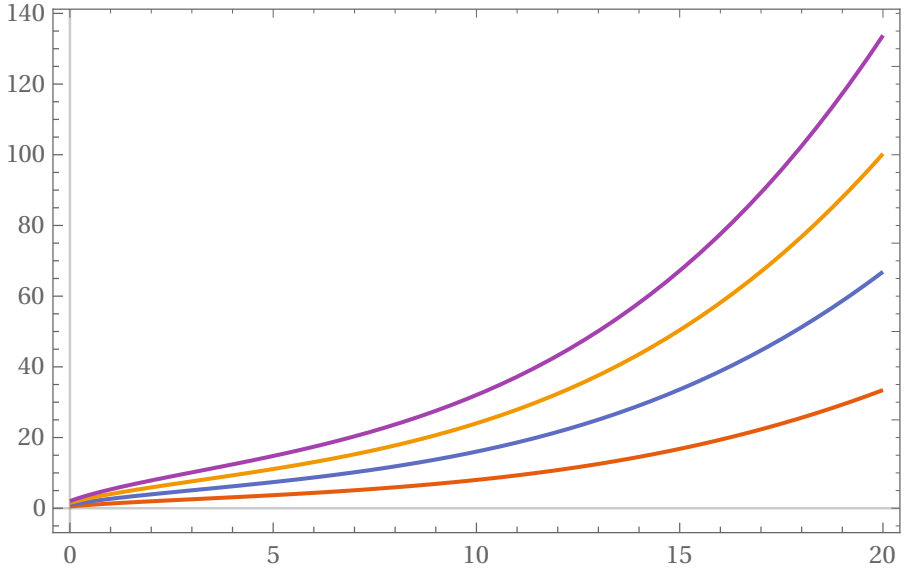

Figure 15: This graph displays integral curves of the vector-field $v = (v_a, v_\rho)$ for $\kappa = 1$, $C(a) = \frac{2}{300}$ and $a(t = 0) = 0.5$, $\rho(t = 0) = 5$. In this case, the initial deceleration is still overtaken by an abrupt acceleration.

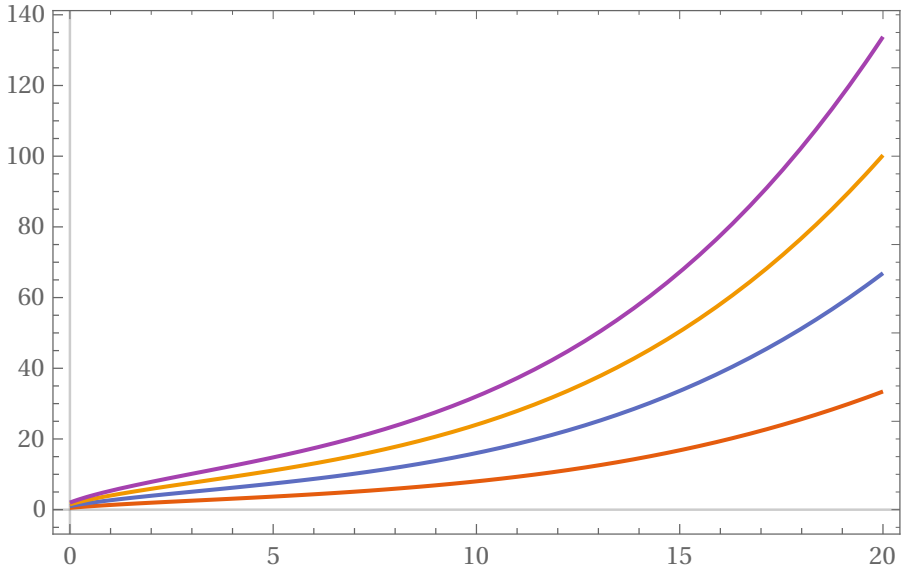

7.4 Mini-superspace with dust

A possible quantum description of the coupling between gravity and matter proceeds via the Wheeler–DeWitt equation [167]. We make two simplifications. First of all, we limit ourselves to an analysis in mini-superspace by assuming homogeneity and isotropy where the wave function (of the universe) becomes a function of the scale factor and the matter field, that matter being a comoving dust (ideal pressure-less fluid). That modeling follows as a special case of the Brown-Kuchař description of dust [163, 168].

In the case of zero curvature $k = 0$ and zero cosmological constant $\Lambda = 0$, the classical description of a homogeneous Brown-Kuchař dust is determined by the Lagrangian

$$L = V\left[\frac{1}{2}Na^3\rho\left(\frac{\dot{T}^2}{N^2}-1\right)-\frac{1}{2N\kappa^2}a\dot{a}^2\right],$$

where V is the comoving volume, which must be such that the volume today Va^3 exceeds the Hubble volume [168], the field $T = T(t)$ (with dimensions of time) parametrizes the four-velocity U^μ of the dust field as $U_\mu = \partial_\mu T$. $N(t)$ is the lapse function, which remains an arbitrary function that we will set to 1 in the following. The other equations of motion then yield the equations (116) and (117), together with

$$\frac{\mathrm{d}}{\mathrm{d}t}\left(a^3\rho\right) = 0, \quad \left(\frac{\mathrm{d}T}{\mathrm{d}t}\right)^2 = 1$$

So we get the classical dust equations together with a matter scalar T that can be treated a clock variable.

The canonical quantization of this theory is straightforward and is detailed in e.g. [168]. It leads to the Wheeler–DeWitt equation[6]

$$\mathrm{i}\hbar\,\partial_T\,\psi(a,T) = \frac{\hbar^2\kappa^2}{2Vc^2}\left(\frac{1}{\sqrt{a}}\partial_a\right)^2\psi(a,T) \tag{121}$$

where ψ represents the wave function of the universe in the reduced description. It is a function of the scale factor and the scalar T. A common way to extract predictions from this wave equation is to define the scale factor through an expectation value, i.e., $\langle a(T)\rangle = \int|\psi(a,T)|^2 a\,da$. However, we suggest to adopt a more fine-grained

[6] There are operator ordering ambiguities in the canonical quantization procedure. Here, we adopt the ordering based on the Laplace-Beltrami operator corresponding to the DeWitt metric on mini-superspace [168]. For a discussion of other operator orderings in the context of cosmological singularities, see [169].

approach which consists in defining the evolution of $a(t)$ and hence of the metric (115) through the streamlines of the continuity equation associated to (121). That is, we consider the conserved current

$$J = (J_a, J_T) = (\frac{\kappa^2}{Vc^2}\frac{1}{\sqrt{a}}\partial_a S|\psi|^2, -\sqrt{a}|\psi|^2)$$

in terms of the polar decomposition $\psi = |\psi|\mathrm{e}^{\mathrm{i}S/\hbar}$ and we put

$$\frac{d}{dt}\begin{pmatrix} a(t) \\ T(t) \end{pmatrix} = \frac{1}{\sqrt{a}\,|\psi|^2}\begin{pmatrix} J_a \\ J_T \end{pmatrix}$$

or, explicitly,[7]

$$\frac{da}{dt} = \frac{J_a}{\sqrt{a}|\psi|^2} \equiv \frac{\kappa^2}{Vc^2}\frac{1}{a}\partial_a S, \qquad \frac{dT}{dt} \equiv \frac{J_T}{\sqrt{a}|\psi|^2} = -1 \tag{122}$$

The last equation implies that $T = -t$ (up to a constant), like in the classical case.[8] Introducing the constant $m = \frac{Vc^2}{\kappa^2}$ (with dimensions of mass $\times$ length^2), we obtain the "quantum Friedmann equations,"

$$\left(\frac{\dot{a}}{a}\right)^2 = \frac{1}{m^2}\frac{(\partial_a S)^2}{a^4} =: 2\kappa^2\rho_{\mathrm{eff}} \tag{123}$$

$$\frac{\ddot{a}}{a} = -\frac{1}{2m^2}\frac{(\partial_a S)^2}{a^4} + \frac{F_\psi}{a} = -\kappa^2\rho_{\mathrm{eff}} + \frac{F_\psi}{a} \tag{124}$$

where,

$$F_\psi := -a^{-1}\partial_a\left[\frac{\hbar^2}{4m^2|\psi|}\left(\frac{1}{\sqrt{a}}\partial_a\right)^2|\psi|\right]$$

may be called a quantum force. The equation (124) is obtained by taking the time-derivative of (123) and using the Wheeler–DeWitt equation (121). While classical dust always decelerates the expansion, $\ddot{a} = -\kappa^2\rho a < 0$ in (117), that is not necessarily so in the quantum case where F_ψ may be non-zero and we may have eras of accelerated expansion as we will discover in Section 7.8.

The second equality in (123), i.e., the definition of an effective density ρ_{eff}, is inspired by (116). Note that for a classical dust universe, we have in addition to the equations (116)-(117) (with $p = k = \Lambda = 0$) that $d(\rho a^3)/dt = 0$, so that $\rho = \rho_0/a^3$

[7] Those equations follow the Bohmian approach to quantum dynamics [170]. Note that in (121) a and T enter as arguments of the wave function, whereas in (122) they are functions. The meaning will always be clear from the context.

[8] It is possible to flip the sign of J (as was done e.g. in [169]), which yields the opposite velocities in (122). Yet the set of solutions is the same, because they are connected by the usual time-reversal operation $\psi(a, T) \to \psi^*(a, -T)$.

with ρ_0 a constant. The quantum dynamics (122) reduces to the classical one iff $(\partial_a S)^2/a$ is constant along the trajectory. But typical solutions of (121)-(122) do not fulfill that condition.

We continue in the next section with a general discussion on further constraints before we analyze in Section 7.8 the nature of the accelerated expansion that follows from **using** (121) **in** (122).

7.5 Constraints: boundary conditions and scale

We first simplify the dynamics and express it in terms of dimensionless variables by introducing $x := \frac{2}{3}a^{3/2} \geq 0$ and the dimensionless time-variable $\tau := t/t_0$ with $t_0 = 13.4$ Gyear, which is a common estimate of the age of our universe, and the dimensionless parameter $M := \frac{Vc^2}{\kappa^2 t_0 \hbar} = \frac{m}{t_0 \hbar}$. The dynamics (121) and (122) then reduces to the simple form

$$\mathrm{i}\,\partial_\tau \psi = -\frac{1}{2M}\,\partial_x^2 \psi \tag{125}$$

$$\frac{dx}{d\tau} = \frac{1}{M}\,\partial_x s, \qquad \psi = |\psi| \mathrm{e}^{\mathrm{i}s} \tag{126}$$

which are the familiar equations for a non-relativistic free particle on the half-line with mass M.

In terms of these variables, the quantum Friedmann equation (124) reads

$$M\frac{d^2x}{d\tau^2} = \tilde{F}_\psi, \qquad \tilde{F}_\psi = -\partial_x \frac{\partial_x^2 |\psi|}{|\psi|}$$

Classical evolution is obtained when $\tilde{F}_\psi$ is zero. This will be the case for plane wave solutions to the Schrödinger equation (125). For a generic wave function, there will be a deviation from classicality and hence a potential effective cosmological constant. For square integrable wave functions (over $x \in \mathbb{R}$, with (125) then viewed as the restriction to the positive half-line — more on this in the next section), classicality will be obained for large x and t [171], due to the dispersive character of the free Schrödinger evolution. So in the case of these wave functions, the appearance of an effective cosmological constant can merely be a transient feature.

7.6 Boundary conditions

As usual, the dynamics (125) may be taken as unitary on the Hilbert space $\mathrm{L}^2(0, +\infty)$ with flux-prohibiting boundary conditions: $\psi|_{x=0} = \ell\, \partial_x \psi|_{x=0}$ with $\ell \in \mathbb{R} \cup \{\infty\}$, see

e.g. [168]. These boundary conditions imply that the density $|\psi(x,t)|^2$ is preserved by the dynamics (126) and can be taken as a probability distribution. Moreover, since $(|\psi|^2\partial_x S)|_{x=0} = 0$, trajectories never visit $x = a = 0$ (after a finite cosmic proper time). In other words, there is never a big bang or big crunch. Trajectories can also not reach $+\infty$ in finite time, which means that there is no big rip.

Despite appearances however, the dynamics (125) is not quite the usual Schrödinger equation; it remains a Wheeler-deWitt equation in which the variable τ started out to represent the dust content. It is then less clear what is the Hilbert space or why the wave function would satisfy such a boundary condition as above. Rather we may consider and allow a flux through $x = 0$ which leads to the possibility of a big bang or big crunch. For example, the Vilenkin-type wave functions are of such a kind [172].

In the following section, we consider wave functions for which there is flux through $x = 0$ as well as a wave function for which there is no flux. The former will give big bang trajectories while the latter will give bouncing trajectories (where a minimal spatial volume is reached). In any case, we must remember that we merely consider a dust model of our universe, and near the big bang the trajectories should not be taken too seriously as that concerns a radiation dominated era.

7.7 Scale

The parameter M in the equations (125)–(126) depends on V. To model our universe, the spatial volume should at least be our current Hubble volume, which is of the order $(10^{10}\text{lightyear})^3$. Fixing the value of the scale factor a today to be one, we take $V = (10^{10}\text{lightyear})^3$. As such, M is roughly of the order of 10^{120}.

Because of our choice of coordinates x and τ, we will aim to fit the evolution of the universe roughly between (x,τ) equal to $(0,0)$ and $(2/3,1)$. Therefore the expansion rate must be of order one. Looking at (126), since the "mass" M is exceedingly large we must have $\partial_x S$ large as well. That can be obtained in various ways but it does constrain the possible wave functions or initial conditions. As an example, consider a Gaussian wave function,

$$\psi_{\bar{x},v,\sigma}(x,\tau) = \sqrt{\frac{\sigma}{\sqrt{\pi}(\sigma^2 + \mathrm{i}\tau/M)}}\mathrm{e}^{\mathrm{i}M(vx+v^2\tau/2)}\mathrm{e}^{-\frac{(x-\bar{x}-v\tau)^2}{2(\sigma^2+\mathrm{i}\tau/M)}} \tag{127}$$

$$x(\tau) = \bar{x} + v\tau + [x(0) - \bar{x}]\sqrt{1 + \frac{\tau^2}{\sigma^4 M^2}}$$

To have the desired expansion rate, we take v of order 1 and σ such that $\sigma^2 M \gg 1$. Then, the wave packet has a high $\mathcal{O}(M)$ momentum. (Alternatively, we could take σ appropriately small, but then $x(0)$ would have to be far away from the bulk of the packet.)

A second problem related to the large value of M is numerical. To solve (125)–(126) with parameter $M = 10^{120}$ requires the time-steps to have a size of order 10^{-120}. As shown in Appendix E, that problem can be overcome by instead solving directly the limiting case $M \to \infty$. By taking this limit a simplified integration method is available.

7.8 Acceleration as a quantum effect

As is apparent from the second quantum Friedmann equation (124), it is the quantum force F_ψ that enables acceleration of the expansion. Of course, not all (initial) wave functions ψ lead to universes compatible with cosmological observations. Here we investigate how easy it is to get full qualitative and even quantitative compatibility for some class of wave functions.

We first consider three different wave functions: two different superpositions of Gaussian wave packets for which the evolution of the scale factor is obtained numerically and one for an Airy wave where the solution is exact. For each case we aim to fit a ΛCDM universe with parameters $H_0 = 70$ km/s/Mpc (the Hubble parameter today), $\Omega_M = 1 - \Omega_\Lambda = 0.3$ (the matter and dark energy density parameter): hereafter this model is referred to as the "standard ΛCDM model". More precisely, the present day scale factor and Hubble rate are fitted exactly, while the evolution of the modeled universe may deviate from the one corresponding to the ΛCDM universe near the big bang era (in particular the big bang might be replaced by a bounce), since the experimental data are less restrictive there. We end the section by a discussion on the *genericity* of wave functions leading to the observed cosmic acceleration.

7.8.1 Gaussian superposition with big bang trajectories

Using the notation (127), we consider first a superposition of two Gaussian wave functions,

$$\psi(x,\tau) = \alpha_1\, \psi_{\bar{x}_1,v_1,\sigma_1}(x,\tau) + \alpha_2\, \psi_{\bar{x}_2,v_2,\sigma_2}(x,\tau)$$

with parameters

$$\bar{x}_1 = 0, \quad \bar{x}_2 = -1, \quad v_1 = 0.3, \quad v_2 = 2, \quad \sigma_1 = 0.35, \quad \sigma_2 = 1, \quad \alpha_1^2 = 1 - \alpha_2^2 = 0.59 \tag{128}$$

This wave function carries incoming flux at the origin $x = 0$: all trajectories $x(\tau)$ move from the negative reals at early times to the positive reals later on. When passing through $x = 0$ a big bang occurs whereby the universe is newly created. The two packets move at high but comparable momentum towards larger x with the second one overtaking the first one, at which moment the acceleration sets in. We refer to Appendix E for the numerical recipe that produces the trajectories.

In all, we get a very good fit to our ΛCDM universe up to a redshift $z = \frac{1}{a} - 1$ of about 4 (corresponding to the time interval $\tau \in [0.2, 1]$); see Fig. 16. This model predicts that, in the far future, the cosmic expansion will decelerate again and converge onto a trajectory of the form $a(\tau) \sim (3(\tau - \tau_0))^{2/3}$, as exhibited in the lower part of Fig. 16. Moreover the acceleration remains relatively mild without excessive choices of the parameters (128) (the velocities and widths are of the same order in the two packets). Therefore, that those trajectories in bounded time-intervals resemble "coincident" ΛCDM models (i.e., those with $\frac{\Omega_\Lambda}{\Omega_{\text{dust}}} = \frac{\rho_\Lambda}{\rho_{\text{dust}}} = \mathcal{O}(1)$, [173]) seems to appear here "naturally."

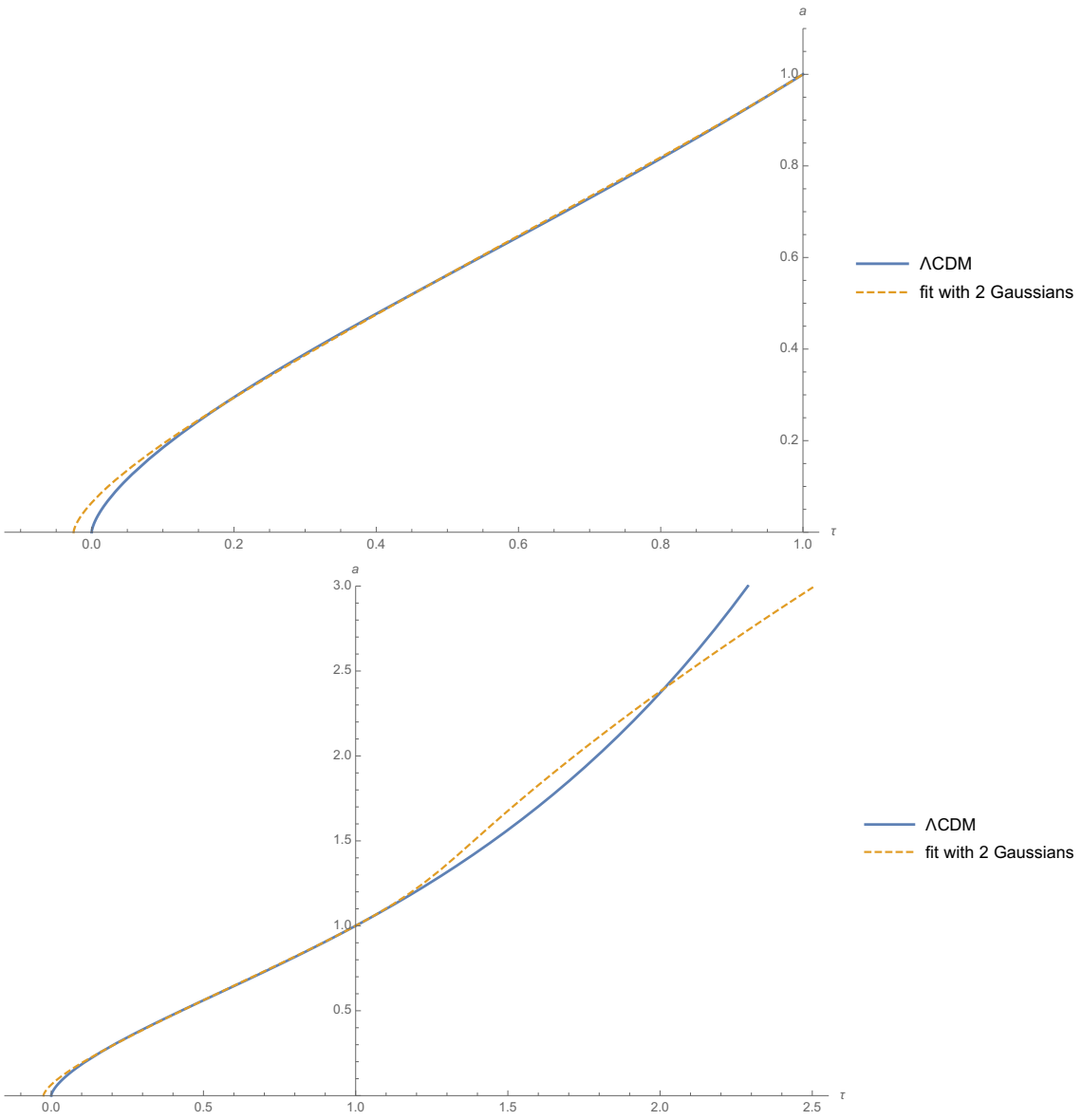

Figure 16: The evolution of the scale factor $a(\tau)$ in the case of the Gaussian superposition (128). Upper plot: the current history of the standard ΛCDM model and a fitting trajectory (which agrees very well). We also compare with an Einstein-de Sitter universe, i.e., with a dust-dominated universe, $a(\tau) \propto (\tau - \tau_B)^{2/3}$ fitting the observed expansion H_0 of today. Lower plot: a longer-time comparison of the evolution of the standard ΛCDM model with the same trajectory, showing a deviation in our future.

7.8.2 Gaussian superposition with bouncing trajectories

In this Section we consider a unitary evolution for the following superposition of four Gaussians:

$$\psi(x,\tau) = \frac{5}{\sqrt{74}}[\psi_{0,v_1,\sigma_1}(x,\tau-\tau_0)+\psi_{0,-v_1,\sigma_1}(x,\tau-\tau_0)]+\frac{7}{\sqrt{74}}[\psi_{0,v_2,\sigma_2}(x,\tau-\tau_0)+\psi_{0,-v_2,\sigma_2}(x,\tau-\tau_0)] \tag{129}$$

where $v_1 = 0.733$, $v_2 = 0.975$, $\sigma_1 = 5.64 \times 10^{-6}$, $\sigma_2 = 0.705$, $\tau_0 = 3.84 \times 10^{-2}$. This wave function satisfies the Neumann boundary condition towards $x = 0+$ and hence its L^2-norm is preserved on the half-line $(0, +\infty)$. As said before, that implies that trajectories never start with a big bang or end up in a big crunch. The value of σ_1 is chosen such that there is a bounce with a minimal scale factor within 10^{-4} for the range of initial conditions we are interested in: in our universe that scale-factor lies beyond the surface of last-scattering and well in the radiation-dominated epoch.

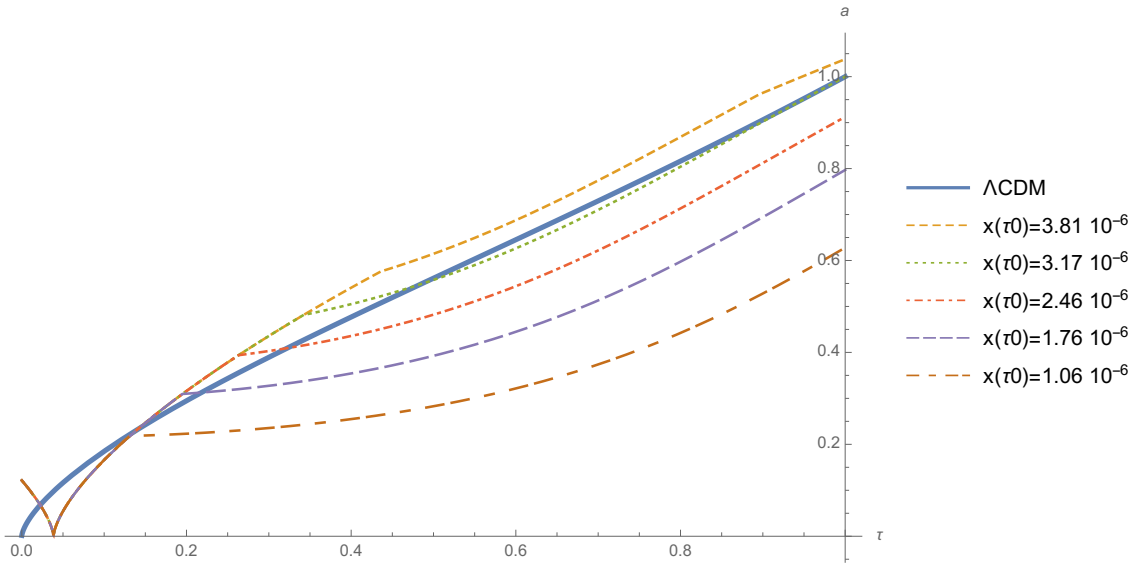

Figure 17: The scale factor $a(\tau)$ for the Gaussian superposition (129). The bold blue curve corresponds to the standard ΛCDM model while the other curves are ordered top-down in the same order as in the legend. The best fit to the ΛCDM model is given by the trajectory with initial $x(0) = 3.6 \times 10^{-6}$. Other initial scales lead to trajectories with overall the same qualitative features. Note that the big bang that is implied by the ΛCDM model is replaced by a bounce (which despite appearances is smooth).

To numerically calculate the trajectories, we again use the limit $M \to \infty$ as explained in Appendix E. In Fig. 17, we consider 5 different initial values $x(0) \in I :=$

$[1.2 \times 10^{-6}, 4.4 \times 10^{-6}]$. For each of those values, the scale factor $a(t)$ decelerates (the abrupt change in speed stems from the fact that $\sigma_1 \ll 1$) and then accelerates before finally (in our future) to decelerate again onto a classical $a(\tau) \propto \tau^{2/3}$ trajectory. The first epochs are in qualitative agreement with our ΛCDM model. The $|\psi|^2$-probability of the range I is about 15%, so that these initial conditions are not particularly special.

7.8.3 Airy wave train

Finally, we consider the Airy packet solution, [174],

$$\psi(x,\tau) = \mathrm{Ai}\left(M^{2/3}B\left[x - B^3(\tau-\tau_0)^2/4\right]\right)\exp\left\{\mathrm{i}M\frac{B^3(\tau-\tau_0)[x - B^3(\tau-\tau_0)^2/6]}{2}\right\} \tag{130}$$

parameterized by B and τ_0. Here, [175],

$$x(\tau) = \frac{2}{3}a^{\frac{3}{2}}(\tau) = \frac{B^3(\tau-\tau_0)^2}{4} + x(\tau_0)$$

For late times, $a(\tau) \sim \tau^{4/3}$, which is the classical motion corresponding to a perfect fluid with equation of state $p = -\rho/2$. That illustrates that quantum solutions may behave very differently from the classical ones.

If $B > 0$ and $x(\tau_0) \geq 0$ (which implies that $x(0) > 0$), then the trajectory corresponds to a bouncing universe. (So even though there is a non-zero flux through $x = 0$, a particular trajectory may never reach $x = 0$). Moreover, such trajectories are always accelerating, very much unlike classical trajectories which are constantly decelerating. Unlike the examples in the preceding section, there is no classical evolution for large x and t, because the Airy wave train is a non-dispersive (and non-normalizable) packet when viewed over the whole line $x \in \mathbb{R}$.

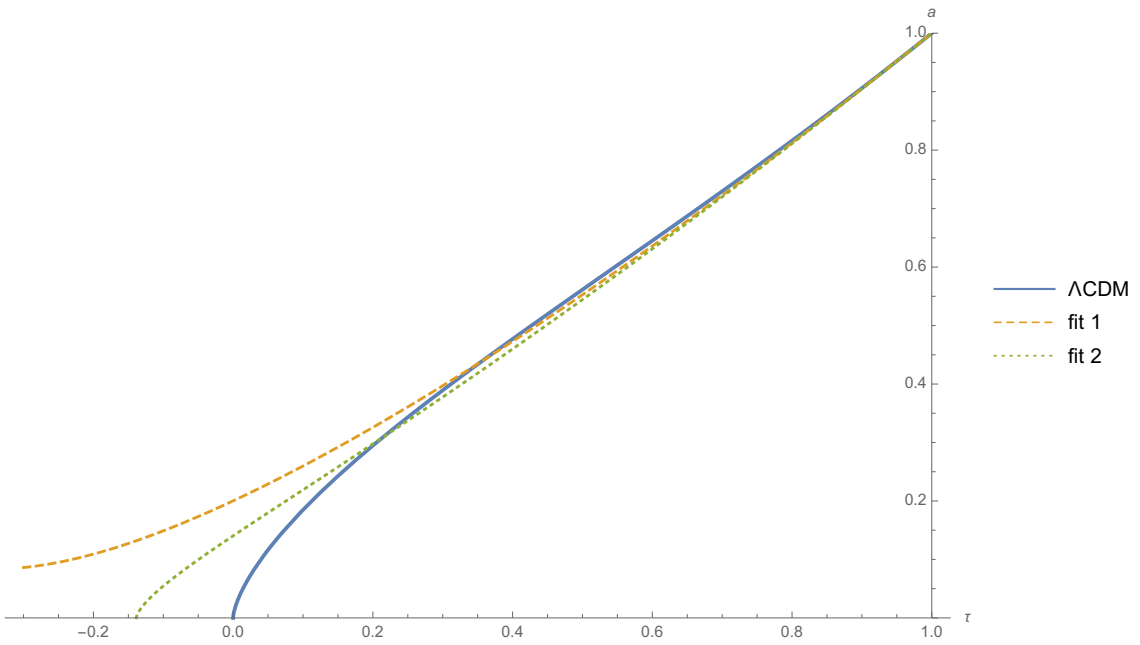

Figure 18: The scale factor $a(\tau)$ fitting the standard ΛCDM model for the Airy wave train (130).

On the other hand, when $B > 0$ and $x(\tau_0) < 0$ (for which $x(0) = 0$ is possible), there is a big bang with an initial period of deceleration. Fits of trajectories of the latter type to the standard ΛCDM model are displayed in Figs. 18 and 19. It is clear that $x(\tau_0)$, τ_0 and B can be tuned so that e.g. the present-day Hubble parameter H_0 is fitted. All considered fits do just that. The remaining free parameter, τ_0, equals -0.35 for fit 1 and -0.45 for fit 2.

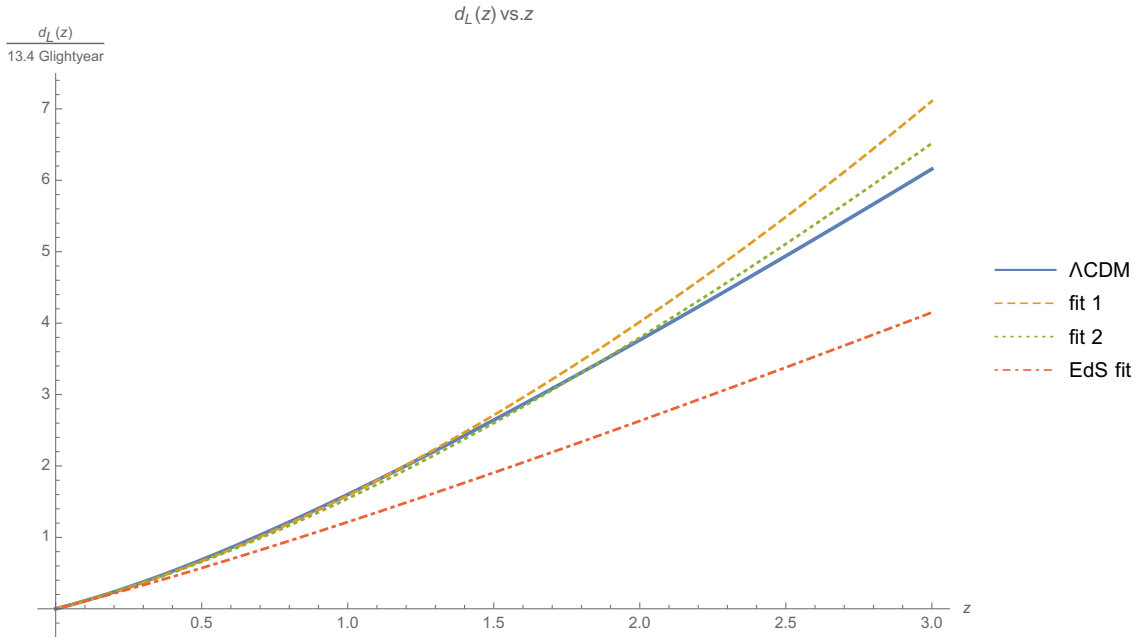

Figure 19: The luminosity distance $d_L(z)$ *versus* redshift $z = \frac{1}{a} - 1$, fitting the standard ΛCDM model for the Airy wave train (130). The lower curve corresponds to an Einstein-de Sitter universe, i.e., dust-dominated, $a(t) \propto t^{2/3}$, and fitting the expansion H_0 of today.

7.8.4 Genericity, decoherence and optics

One may wonder how generic and under what conditions a period of accelerated expansion arises. The evolution of the scale factor is determined by the initial wave function and initial value of the scale factor. We have seen that with a rather simple wave function (i.e., a superposition of two Gaussians), we have the desired period of accelerated expansion. And for those wave functions, such a period is rather generic. Of course, there are also other wave functions, which don't give the desired behaviour. As already noted, the plane waves give classical motion. Other wave functions will give consecutive periods of acceleration (e.g., superpositions of a higher number of Gaussians). While it may be interesting to quantify that in great detail, one should remember that as a matter of fact, we only need "one good wave function," in the same sense as we only have "one universe."

A second point of discussion concerns the classical versus quantum nature of the description. Does quantum physics not only matter for early universe considerations? The majority position is probably 'yes.' Our work does give quantum corrections to the motion of the scale factor in recent times, and that is clearly questionable.

Therefore further work is required to show that the result still holds when we go beyond the mini-superspace approximation. It will then be relevant to consider possible decoherence effects that might arise from the coupling between homogeneous and inhomogeneous degrees of freedom. This decoherence in the quantum evolution of the universe is not exactly a well-understood phenomenon. Estimates of decoherence times for the scale factor are difficult, also in the many other approaches to the dark energy problem. At least, in the present work, we see precisely that the very long-time solutions of our quantum Friedmann equations become indeed classical: the geometry of the late future Universe is described by a classical solution of Einstein's equations.

Finally, we stress that our study did not concern local properties of the cosmos. We gave predictions for specific trajectories of the scale factor. That 'only' gives a motivated correction to the evolution of the scale factor (i.e., a quantum modification in the FLWR-metric for a dust universe); the laws of free-fall motion in the resulting curved space are the same as always.

8 Summary and conclusions

In this dissertation, we have presented a diverse array of innovations in non-equilibrium statistical mechanics. One unifying theme is that of "active" matter: As discussed in chapters 2 and 3, active particles can be modelled usefully as diffusions or random walkers coupled to internal *spin* degrees of freedom. For run-and-tumble processes a form of generalized reversibility holds for the total system. Yet, the Sutherland–Einstein relation between diffusion constant and mobility is broken. In the case of run-and-tumble processes with multiple spin values and corresponding driving velocities we obtained a generalized telegraph equation for the evolution of the spatial density. Subsequently, we studied the modification of the Arrhenius formula where activity is in general seen to enhance the escape from a potential well. We pointed out the importance of the (local) slope of the potential as a typical nonequilibrium effect. Finally, we studied models where the coupling between spin and position becomes kinetically constrained as in molecular motors. There the asymmetry in activity parameters in the spin dynamics may govern the direction of the spatial current.

In chapter 3, we explored classes of reaction-diffusion equations which typically come about in systems of branching or replicating active particles. To be less cryptic: we calculated the expected position (as a function of time) of the outermost particles of such a process. The cumulative probability distribution $p(r,t) = \mathrm{Prob}[dist(\text{ Outermost particle at time } t, \text{ original particle at time } 0)]$ is expected to relax to a traveling wave $p(r - v_\infty t)$ and our main goal was to extract the asymptotic speed v_∞. Our method rests on the assumption that the relevant speed is always equal to the minimal speed that can be attained in a traveling wave solution to the linearized dynamics. Using this assumption and method, we found evidence that the front slows down with respect to a corresponding passive case in one-dimensional run-and-tumble processes while the opposite is true for active Brownian particles in dimension $d > 1$. We have found explicit expressions detailing the speed's dependence on the various relevant parameters such as persistence, driving speeds, dimension and temperature.

Research in active matter can be *and is being* extended in various directions. Going from one-dimensional active to several dimensions allows more freedom for steady-state currents and opens questions about recurrence vs. transience [176, 177]. Next,

there are questions to be solved regarding activity-induced pattern-formation [178] and interacting active-particle systems [57] (e.g. understanding motility-induced phase-transition or lane-formation-transitions). Regarding research on active branching, there is an outstanding question of understanding corrections to the asymptotic speed such as via logarithmic and other corrections in time, [66, 67]. Secondly there is the wider study of surface growth, interface motion and other growth processes in the presence of active components. To the best of our knowledge the case of active Eden growth or active DLA has not been studied yet. Such active interface models would be relevant, so it seems, within biological contexts of growth. Fluctuations around the speed could then be compared with those for other front motions such as studied e.g. in the Kardar-Parisi-Zhang universality class.

Another major chapter in this dissertation concerned the occurrence and explanation of stable patterns and fixed points for probes in contact with a driven medium, a long-standing challenge within nonequilibrium statistical mechanics. We provided rigorous results regarding the stabilization of a probe approaching the rotation center of an overdamped medium. We have shown that the associated stiffness increases for small nonequilibrium driving and is positive for large rotational driving. It could prove worthwhile to extend such results to systems where probes are in contact with active matter.

Thus far, applications of active matter are thought to be restricted to biological systems or artificial nanotechnology. However, as we highlighted in our investigation of the kappa velocity distributions occurring in outer space, it may turn out that models and paradigms of active matter may also carry explanatory power in that realm.

The observation of suprathermal tails in velocity distributions indicate that high energy levels get an unusual large weight compared to the equilibrium case, i.e., a case of population inversion in velocity space. We combined two classical effects, localization and diffusive acceleration, to set up a scenario for space plasmas and their power law tails in the speed distribution. The diffusive acceleration is related to Taylor dispersion for which we discussed a relation with the telegraph process. For granular gases we attempted a model combining localization with energy injection (negative friction). It would be interesting to add other examples, such as the dynamical generation of nonPlanckian laws [179] or, even outside physics, for

the understanding of the Pareto distribution of wealth in a society; see e.g. [180]. For the last example and depending on the economy it may well be that the wealth runs away towards the rich via a phenomenon similar to diffusive acceleration, and cannot quite redistribute itself due to localization effects.
The subject of nonMaxwellian velocity distributions touches on a number of fundamental issues in physics, which more recently have been named localization and active diffusion and that relate to older subjects introduced by Rayleigh (in the theory of sound), Kelvin and Kac (for the telegraph process), Fermi (for the origin of cosmic radiation), Taylor (for the subject of turbulent diffusion) and Ulam (on statistical properties of dynamical systems).

Another theme of this manuscript, explored at length in chapter 4, is the current-force characteristic $J(E)$ in random environments and arbitrarily far from equilibrium. We have presented mathematically fully treatable models of phase transitions in the current. For independent particles we gave two models where the current vanishes discontinuously beyond a certain field strength, either due to disorder along the backbone or due to trapping in dead-ends. A special example was discussed where the current vanishes identically, prompting an apparent violation of the Sutherland-Einstein relation. When particle interactions are included, we confirm the expected result that repulsive interactions boost the current while attractive interactions tend to quench it. Finally, we have also demonstrated how an arbitrary weak shaking in terms of a time-modulation can make the current nonzero in regimes where it would otherwise vanish.

The final theme of this dissertation is somewhat of an outlier: we discussed humble modifications to general relativity informed by statistical mechanics, with the goal of explaining a part of the dark energy conundrum in modern cosmology. In layman's terms, we can summarize by saying that we added a noise term to the Friedmann equations. If the amplitude of that noise-term depends on the cosmic scale-factor, then the noise may push for a faster cosmic expansion: an effect similar to the phenomenon of thermophoresis in condensed matter. Pausing there, we quickly ventured to a toy model of quantum gravity where the quantum correction to the classical equation of motion ought to be one and the same as the noise we added previously to the equation of motion.
More specifically: by quantizing a symmetry-reduced classical theory with an effective description of a dust fluid in terms of a non-canonical scalar field, we have ob-

tained the quantum analogue of a Friedmann-Lemaître-Robertson-Walker universe with dust as matter. The quantum treatment of such a mini-superspace model readily allows for deviations compared to the classical motion. These deviations can be understood in terms of a "quantum force" appearing in the second quantum Friedmann equation. We have identified solutions for which there is a period of accelerated expansion which matches the classical evolution of the standard ΛCDM model very well for the period of the age of the universe. There are also differences. Namely, the effective cosmological constant is usually transient. Other solutions could also lead to, say, consecutive eras of accelerated expansion. This fact is interesting in the light of the recent puzzle concerning the discrepancy in the measured values of the Hubble rate, measured on the one hand by the Hubble Space Telescope and by the Planck satellite [39]. This discrepancy, which does not appear to be resulting from a systematic error, could for example be explained by the appearance of an effective cosmological constant at early times [181]. While this was modelled by a scalar field in [181], it could also appear naturally in our model without having to introduce a scalar field.

9 References

References

[1] J. Ingen-housz, "Bemerkungen über den Gebrauch des Vergrösserungsglases", *Verm. Schriften physisch-medicinischen Inhalts* (1784).

[2] E. Nelson, *Dynamical theories of Brownian motion*, Princeton University Press, 2nd edition (1967).

[3] R.A. Fisher, "The wave of advance of advantageous genes", *Ann. Eugenics* **7**, 353–369 (1937).

[4] A. Kolmogorov, I. Petrovsky and N. Piscounov, "Étude de l'équation de diffusion avec croissance de la quantité de matière", *Moscou Universitet. Bull. Math.* **1**, 1-25 (1937).

[5] J. L. Lebowitz, *Physics Today* **46**, 9-32 (1993).

[6] J. C. Maxwell, "Molecules", *Nature* **8**, 437–441 (1873).

[7] A. Einstein, *Naturwissenschaften* **14**, 223–224 (1926).

[8] C. Mouhot and C. Villani, "On Landau damping", *Acta Math.* **207** (1), 29-201 (2007).

[9] L. Bertini, A. De Sole, D. Gabrielli, G. Jona-Lasinio and C. Landim, *Rev. Mod. Phys.* **87**, 593- (2015).

[10] C. Kipnis and C. Landim, "Scaling Limits of Interacting Particle Systems", *Grundl. der math. Wiss.* , 593- (1999).

[11] B. Derrida, "Random-energy model: An exactly solvable model of disordered systems", *Phys. Rev. B* **24**, 2613- (1981).

[12] C. Kipnis, C. Marchioro and E. Presutti, "Heat flow in an exactly solvable model", *Phys. Rev. B* **24**, 2613- (1981).

[13] F. Bonetto, J.Ł. Lebowitz and L. Rey-Bellet, "Fourier's law: a challange for theorists", *Math. Phys.* **2000**, 128-150 (2000).

[14] T. Demaerel, C. Maes *Phys. Rev. E* **97**, 032604 (2018). .

[15] T. Demaerel, C. Maes *J Phys A*, (2019) 54: 24. .

[16] É. Fodor, M.C. Marchetti, "The statistical physics of active matter: from self-catalytic colloids to living cells", Lecture notes for the international summer school "Fundamental Problems in Statistical Physics" 2017 in Bruneck. arXiv:1708.08652v3 [cond-mat.soft].

[17] C. Bechinger, R. Di Leonardo, H. Löwen, C. Reichhardt, G. Volpe and G. Volpe, "Active particles in complex and crowded environments", *Rev. Mod. Phys.* **88**, 045006 (2016).

[18] P. de Buyl, A.S. Mikhailov and R. Kapral, "Self-propulsion through symmetry breaking", *EPL (Europhysics Letters)* **103**, 60009 (2013).

[19] T. Demaerel and C. Maes, *J Stat Phys* (2018) 173: 99.

[20] J. Krug, "Boundary-induced phase transitions in driven diffusive systems", *Phys. Rev. Lett.* **67**, 1882 (1991).

[21] A. Lazarescu, "Generic Dynamical Phase Transition in One-Dimensional Bulk-Driven Lattice Gases with Exclusion", *J. Phys. A: Math. Theor.* **50**, 254004 (2017).

[22] Y. Baek, A.P. Solon, X. Xu, N. Nikola, and Y. Kafri, "Generic long-range interactions between passive bodies in an active fluid", arXiv:1709.02281 [cond-mat.stat-mech].

[23] J.P. Garrahan, R.L. Jack, V. Lecomte, E. Pitard, K. van Duijvendijk, and F. van Wijland, "First-order dynamical phase transition in models of glasses: an approach based on ensembles of histories", *J. Phys. A: Math. Gen.* **42**, 075007 (2009).

[24] J.P. Garrahan, P. Sollich, C. Toninelli, "Kinetically Constrained Models", arXiv:1009.6113. In: L. Berthier, G. Biroli, J-P. Bouchaud, L. Cipelletti and W. van Saarloos, editors, pages 341-369, Oxford University Press, 2011.

[25] R. Jack, J.P. Garrahan, D. Chandler, "Space-time thermodynamics and subsystem observables in kinetically constrained models of glassy materials", *J. Chem. Phys.* **125**, 184509 (2006).

[26] T. Demaerel, W. De Roeck, C. Maes *Physica A* (2019), 122179, ISSN 0378-4371. .

[27] T. Demaerel, C. Maes and K. Netočný *Ann. Henri Poincaré* **19**, 2673-2699 (2018).

[28] S. A. Mallory, C. Valeriani, and A. Cacciuto, "Curvature-induced activation of a passive tracer in an active bath", *Phys. Rev. E* **90**, 032309 (2014).

[29] W. Yan and J. F. Brady, "The force on a boundary in active matter", *J. Fluid Mech.* **785**, R1 (2015).

[30] N. Nikola, A. P. Solon, Y. Kafri, M. Kardar, J. Tailleur, and R. Voituriez, "Active Particles with Soft and Curved Walls: Equation of State, Ratchets, and Instabilities", *Phys. Rev. Lett.* **117**, 098001 (2016).

[31] C. Maes and T. Thiery, "The induced motion of a probe coupled to a bath with random resettings", *J. Phys. A: Math. Theor.* **50**, 415001 (2017).

[32] U. Basu, P. de Buyl, C. Maes and K. Netočný, "Driving-induced stability with long-range effects", *EPL* **115**, 30007 (2016).

[33] U. Basu, C. Maes, and K. Netočný, "How Statistical Forces Depend on the Thermodynamics and Kinetics of Driven Media", *Phys. Rev. Lett.* **114**, 250601 (2015).

[34] R. Sheshka, P. Recho, and L. Truskinovsky, "Rigidity generation by nonthermal fluctuations", *Phys. Rev. E* **93**, 052604 (2016).

[35] U. Basu, C. Maes and K. Netočný, "Statistical forces from close-to-equilibrium media", *New J. of Phys.* **17**, 115006 (2015).

[36] T. Demaerel, C. Maes and W. Struyve , "Cosmic acceleration from quantum Friedmann equations", arXiv:1901.09767 [gr-qc].

[37] M. Li, X.-D. Li, S. Wang and Y. Wang, "Dark Energy", *Commun. Theor. Phys.* **56**, 525-604, (2011) and arXiv:1103.5870 [astro-ph.CO].

[38] J. Martin, "Everything you always wanted to know about the cosmological constant problem (but were afraid to ask)", *C. R. Phys.* **13**, 566-665 (2012) and arXiv:1205.3365 [astro-ph.CO].

[39] L. Verde, T. Treu and A.G. Riess, "Tensions between the Early and the Late Universe", arXiv:1907.10625 [astro-ph.CO].

[40] M. Kac, "A stochastic model related to the telegrapher's equation", *Rocky Mountain J. Math.* **4**, 497–509 (1974).

[41] I. Bena, C. Van den Broeck, R. Kawai and K. Lindenberg, "Drift by Dichotomous Markov Noise", *Phys. Rev. E* **68**, 041111 (2003).

[42] I. Bena, C. Van den Broeck, R. Kawai and K. Lindenberg, "Nonlinear Response With Dichotomous Noise", *Phys. Rev. E* **66**, 045603(R) (2002).

[43] S. Goldstein, "On diffusion by discontinuous movements, and on the telegraph equation", Q. J. Mech. Appl. Math. bf 4, 129–156 (1951).

[44] G. H. Weiss, "Some applications of persistent random walks and the Telegrapher's equation", *Physica A* **311**, 381–410 (2002).

[45] K. Malakar, V. Jemseena, A. Kundu, K. Vijay Kumar, S. Sabhapandit, S. N. Majumdar, S. Redner and A. Dhar, "Steady state, relaxation and first-passage properties of a run-and-tumble particle in one-dimension", `arXiv:1711.08474 [cond-mat.stat-mech]`.

[46] P. Castro–Villarreal and F. J. Sevilla, "Active motion on curved surfaces", arXiv:1712.04619 [cond-mat.stat-mech] .

[47] R.F. Fox, "Uniform convergence to an effective Fokker-Planck equation for weakly colored noise", *Phys. Rev. A* **34**, 4525 (1986).

[48] P. Hänggi and P. Jung, "Colored Noise in Dynamical Systems", *Advances in chemical physics* **89**, 239–326 (1995).

[49] É. Fodor, C. Nardini, M.E. Cates, J. Tailleur, P. Visco and F. van Wijland, "How far from equilibrium is active matter?" *Phys. Rev. Lett.* **117**, 038103 (2016).

[50] S. Schott, E.R. McNellis, C.B. Nielsen, H.-Y. Chen, S. Watanabe, H. Tanaka, I. McCulloch, K. Takimiya, J. Sinova and H. Sirringhaus, "Tuning the effective spin-orbit coupling in molecular semiconductors", *Nature Communications* **8**, 15200 (2017).

[51] N.J. Harmon and M.E. Flattè, "Spin relaxation in materials lacking coherent charge transport", *Phys. Rev. B* **90**, 115203 (2014).

[52] D. Sun ali Sun, Kipp J. van Schooten, M. Kavand, H. Malissa, Chuang Zhang, M. Groesbeck, C. Boehme and Z. Valy Vardenyet, "Inverse spin Hall effect from pulsed spin current in organic semiconductors with tunable spin–orbit coupling", *Nat. Mater.* **15**, 863–869 (2016).

[53] C. Nardini, É. Fodor, E. Tjhung, F. van Wijland, J. Tailleur, M.E. Cates, "Entropy production in field theories without time reversal symmetry: Quantifying the non-equilibrium character of active matter", *Phys. Rev. X* **7**, 021007 (2017).

[54] P. Romanczuk, M. Bär, W. Ebeling, B. Lindner and L. Schimansky-Geier, "Active brownian particles", *The European Physical Journal Special Topics* **202**, 1–162 (2012).

[55] M.E. Cates and J. Tailleur, "When are active Brownian particles and run-and-tumble particles equivalent? Consequences for motility-induced phase separation", *Europhysics Letters* **101**, 20010 (2013).

[56] G.N. Ord, "The Schrödinger and Dirac Free Particle Equations without Quantum Mechanics", *Ann. of Physi.* **250**, 51–62 (1996).

[57] D. Levis and L. Berthier, "From single-particle to collective effective temperatures in an active fluid of self-propelled particles", `arXiv:1506.08553 [cond-mat.stat-mech]` .

[58] M. Baiesi, C. Maes and B. Wynants, "The modified Sutherland-Einstein relation for diffusive non-equilibria", *Proc. Roy. Soc. A* **467**, 2792–2809 (2011).

[59] P. Garrett, *Abstract algebra*, NY: Chapman and Hall/CRC, 2007.

[60] U. Basu, C. Maes and K. Netočný, "How Statistical Forces Depend on the Thermodynamics and Kinetics of Driven Media", *Phys. Rev. Lett.* **114**, 250601 (2015).

[61] C. Maes, *Non-Dissipative Effects in Nonequilibrium Systems*, SpringerBriefs in Complexity, ISBN 978-3-319-67780-4 (2018).

[62] M. Stichelbaut, *Steady currents in necklaces and ratchet systems,* Master thesis KU Leuven 2016-2017.

[63] C. Maes, "What decides the direction of a current?" *Mathematics and Mechanics of Complex Systems* **3-4**, 275–295 (2016).

[64] D.G. Aronson and H.F. Weinberger, "Nonlinear diffusion in population genetics, combustion, and nerve propagation", in Partial Differential Equations and Related Topics, ed. J. A. Goldstein; Lecture Notes in Mathematics No. 446, pp. 5-49, Springer, New York, (1975).

[65] H. P. McKean, "Application of brownian motion to the equation of Kolmogorov-Petrovsky-Piskunov", *Commun. Pure Appl. Math.* **27**, 323-331 (1975).

[66] M. Bramson, "Maximal displacement in branching Brownian motion", *Commun. Pure Appl. Math.* **31**, 531–581 (1978).

[67] E. Brunet, B. Derrida, "An Exactly Solvable Travelling Wave Equation in the Fisher KPP Class", *J. Stat. Phys.* **161**, 801–820 (2015).

[68] J. Berestycki, E. Brunet, B. Derrida, "Exact solution and precise asymptotics of a Fisher-KPP type front", arXiv:1705.08416.

[69] U. Basu, S.N. Majumdar, A. Rosso and G. Schehr, "Active Brownian Motion in Two Dimensions", *Phys. Rev. E* **98**, 062121 (2018).

[70] T. Michelot and P. G. Blackwell, "State-switching continuous-time correlated random walks", arXiv:1808.01755v1 [q-bio.QM].

[71] T.S. Lim and A. Zlatoš, "Transition fronts for inhomogeneous Fisher-KPP reactions and non-local diffusion", *Trans. Am. Math. Soc.* **368**, no. 12 (December 22, 2015): 8615-8631.

[72] T.S. Lim, "Traveling fronts for reaction-diffusion equations with ignition reactions and Lévy diffusion operators", preprint.

[73] B.H. Gilding and R. Kersner, "Wavefront solutions of a nonlinear telegraph equation", *J. Diff. Eq.* **254**, 599–636 (2013).

[74] D. Vergni, S. Berti, A. Vulpiani and M. Cencini, "Reaction fronts in persistent random walks with demographic stochasticity", arXiv:1809.06137v1 [physics.bio-ph].

[75] R. D. Benguria, M. C. Depassier and V. Mendez, "Minimal speed of fronts of reaction-convection-diffusion equations", *Phys. Rev. E* **69**, 031106(7) (2004).

[76] Rita Maria Zorzenon dos Santos, "Dynamics of Infection and Spread of Diseases", AIP Conference Proceedings **658**, 259 (2003).

[77] V. Mèndez, S. Fedotov and W. Horsthemke, *Reaction-Transport Systems Mesoscopic Foundations, Fronts, and Spatial Instabilities.* Springer-Verlag Berlin Heidelberg (2010).

[78] D. G. Aronson and H.F. Weinberger, "Multidimensional nonlinear diffusion arising in population genetics", *Adv. in Math.* , 30, **1**, 33-76 (1978).

[79] S. Goldstein, "On diffusion by discontinuous movements and on the telegraph equation", *Q. J. Mech. Appl. Mech.* **4**, 129–55 (1950).

[80] V. Mèndez, D. Campos and W. Horsthemke, "Growth and dispersal with inertia: Hyperbolic reaction-transport systems", *Phys. Rev. E* **90**, 042114 (2014).

[81] B. Everest, I. Lesanovsky, J.P. Garrahan and E. Levi, "Role of interactions in a dissipative many-body localized system", *Phys. Rev. B* **95**, 024310 (2017).

[82] R. Ramaswamy and M. Barma, "Transport in random networks in a field: interacting particles", *J. Phys. A: Math. Gen.* **20**, 2973–2987 (1987). .

[83] O. Zeitouni, "Random walks in random environments", Proceedings of the ICM, Beijing 2002, vol. 3, 117–130 (2003).

[84] A.-S. Sznitman, *Brownian Motion, Obstacles and Random Media*. Springer-Verlag — Berlin, 1998.

[85] B.D. Hughes, *Random Walks and Random Environments*, Volume 2: Random Environments. Oxford University Press, Oxford, UK (1995).

[86] M. Barma and D. Dhar, "Directed diffusion in a percolation network", *J. Phys. C: Solid State Phys.* **16**, 1451–1458 (1983).

[87] S.R. White and M. Barma, "Field-induced drift and trapping in percolation networks", *J. Phys. A: Math. Gen.* **17**, 2995–3008 (1984).

[88] D. Chowdhury, "Random walk on self-avoiding walk in external bias: diffusion, drift and trapping", *J. Phys. A: Math. Gen.* **18**, L761–L766 (1985).

[89] A. Bunde, S. Havlin, H. E. Stanley, B. Trus, and G.H. Weiss, "Diffusion in random structures with a topological bias", *Phys. Rev. B* **34**, 8129–8132 (1986).

[90] V. Balakrishnan and C. Van den Broeck, "Transport properties on a random comb", *Physica A* **217**, 1–21 (1995).

[91] R.B. Pandey, "Classical diffusion, drift, and trapping in random percolating systems", *Phys. Rev. B* **30**, 489–491 (1984).

[92] S. Leitmann and T. Franosch, "Nonlinear response in the driven lattice Lorentz gas", *Phys. Rev. Lett.* **111**, 190603 (2013).

[93] A. Slapik, J. Luczka and J. Spiechowicz, "Negative mobility of a Brownian particle: Strong damping regime", *Commun. Nonlinear Sci. Numer. Simulat.* **5**, 316–325 (2018).

[94] O. Bénichou, P. Illien, G. Oshanin, A. Sarracino and R. Voituriez, "Microscopic theory for negative differential mobility in crowded environments", *Phys. Rev. Lett.* **113**, 268002 (2014).

[95] P. Baerts, U. Basu, C. Maes and S. Safaverdi, "The frenetic origin of negative differential response", *Phys. Rev. E* **88**, 052109 (2013).

[96] U. Basu and C. Maes, "Nonequilibrium Response and Frenesy", *J. Phys.: Conf. Ser.* **638**, 012001 (2015).

[97] R.K.P. Zia, E. L. Præstgaard, and O.G. Mouritsen, "Getting more from pushing less: Negative specific heat and conductivity in nonequilibrium steady states", *Am. J. Phys.* **70**, 384 (2002).

[98] F. Solomon, "Random walks in a random environment", *Ann. Prob.* **3**, 1–31 (1975).

[99] A. Larkin, *Sov. Phys. JETP* **31**, 784 (1970).

[100] H. Leschhorn et L.-H. Tang, "Avalanches and correlations in driven interface depinning", *Phys. Rev. E* **49**, 1238–1245 (1994).

[101] T. Thiery, "Analytical Methods and Field Theory for Disordered Systems", Ph.D. Thesis at the Laboratoire de Physique Thèorique de l'Ecole Normale Supèrieure, 2016.

[102] W. Sutherland, "The Measurement of Large Molecular Masses", Report of the 10th Meeting of the Australasian Association for the Advancement of Science, Dunedin, 117–121 (1904). —, "A Dynamical Theory for Non-Electrolytes and the Molecular Mass of Albumin", *Phil. Mag. S.* **6**, 781–785 (1905).

[103] E. Ben-Naim and P.L. Krapivsky, "Strong Mobility in Weakly Disordered Systems", *Phys. Rev. Lett.* **102**, 190602 (2009).

[104] M. Campanino and M. Gianfelice, "On the Ornstein-Zernike Behaviour for the Bernoulli Bond Percolation on $\mathbb{Z}^d$,$d \geq 3$, in the Supercritical Regime", *J. Stat. Phys.* **145**, 1407 – 1422 (2011).

[105] B.K. Oksendal, *Stochastic Differential Equations: An Introduction with Applications*. Berlin: Springer, 2003.

[106] S. Redner, *A Guide to First-Passage Processes*. Cambridge University Press, 2001.

[107] C. Maes, *Non-Dissipative Effects in Nonequilibrium Systems*. SpringerBriefs in Complexity (2018).

[108] T. Demaerel and C. Maes, "Activity induced first order transition for the current in a disordered medium", *Condensed Matter Physics* **20**, 33002 (2017).

[109] J.-P. Bouchaud, "Weak ergodicity breaking and aging in disordered systems", *J. Phys. I (France)* **2** , 1705–1713 (1992).

[110] C. Ness, R. Mari, M. E. Cates, "Shaken and stirred: Random organization reduces viscosity and dissipation in granular suspensions", *Sci. Adv.* **4** (3), eaar3296 (2018).

[111] M. R. Evans and T. Hanney, "Nonequilibrium Statistical Mechanics of the Zero-Range Process and Related Models", *J. Phys. A: Math. Gen.* **38**, R195–R239 (2005).

[112] G.I. Taylor, "Diffusion by continuous movements", *Proc. Lond. Math. Soc.* (2) **20**, 196–212.

[113] C. Van den Broeck, "Taylor dispersion revisited", *Physica A* **168**, 677–696 (1990).

[114] Chun-yu Ma and D. Summers, "Formation of Power-law Energy Spectra in Space Plasmas by Stochastic Acceleration due to Whistler-Mode Waves", *Geophysical research letters* **25**, 4099–4102 (1998).

[115] N.H. Bian, A.G. Emslie, D.J. Stackhouse and E.P. Kontar, "The formation of kappa-distribution accelerated electron populations in solar flares", *The Astrophysical Journal* **796**, 142 (2014).

[116] S.A. Trigger, G.J.F. van Heijst and P.P.J.M. Schram, "Velocity-Dependent Friction and Diffusion for Grains in Neutral Gases, Dusty Plasmas and Active Systems", *Physica A* **347**, 77-98 (2005).

[117] V.V. Prasad and R. Rajesh, "Asymptotic behavior of the velocity distribution of driven inelastic one-component granular gases: analytical results", arXiv:1803.11031v2 [cond-mat.stat-mech].

[118] C. Maes, "On the Second Fluctuation-Dissipation Theorem for Nonequilibrium Baths", *J. Stat. Phys.* **154**, 705–722 (2014).

[119] C. Maes and S. Steffenoni, "Friction and noise for a probe in a nonequilibrium fluid", *Phys. Rev. E* **91**, 022128-7 (2015).

[120] W. De Roeck and F. Huveneers, "Asymptotic localization of energy in nondisordered oscillator chains", *Comm. on Pure and Appl. Math.* **68**, 1532–68 (2015).

[121] N. Cuneo, J.P. Eckmann and C.E. Wayne, "Energy dissipation in Hamiltonian chains of rotators", *Nonlinearity* **30**, R81 (2017).

[122] T. Mithun, C. Danieli, Y. Kati and S. Flach, "Dynamical Glass and Ergodization Times in Classical Josephson Junction Chains", *Phys. Rev. Lett.* **122**, 054102 (2019).

[123] S. Iubini, L. Chirondojan, G.L. Oppo, A. Politi and P. Polito, "Dynamical freezing of relaxation to equilibrium", arXiv:1811.05798v2 [cond-mat.stat-mech].

[124] A.K. Karlis, F.K. Diakonos and V. Constantoudis, "A consistent approach for the treatment of Fermi acceleration in time-dependent billiards," *Chaos* **22**, 026120 (2012).

[125] D. Dolgopyat, "Fermi acceleration", In: *Geometric and Probabilistic Structures in Dynamics* (Workshop on Dynamical Systems and Related Topics in Honor of Michael Brin on the Occasion of his 60th Birthday, March 15-18, 2008, University of Maryland), p 149, 2008.

[126] V.V. Prasad, S. Sabhapandit and A. Dhar, "Driven inelastic Maxwell gases", *Phys. Rev. E* **90**, 062130 (2014).

[127] L.D. Pustyl'nikov, "Poincaré models, rigorous justification of the second element of thermodynamics on the basis of mechanics, and the Fermi acceleration mechanism", *Russian Mathematical Surveys* **50**, 145 (1995).

[128] S.M. Ulam, "On some statistical properties of dynamical systems", In: Proc. 4th Berkeley Sympos. on Math. Statist. and Prob., Vol. III, UnivĊalifornia Press, Berkeley, CA 1961, pp. 315-320.

[129] E. Fermi, "On the Origin of the Cosmic Radiation", *Phys. Rev.* **75**, 1169–1174 (1949).

[130] P. A. Sturrock, "Stochastic Acceleration", *Phys. Rev.* **41**, 186 (1966).

[131] B. Aguer, S. De Bièvre. P. Lafitte, P.E Parris, "Classical Motion in Force Fields with Short Range Correlations", *J. Stat. Phys.* **138**, 780–814 (2010).

[132] E. Soret and S. De Bièvre, "Stochastic acceleration in a random time-dependent potential", *Stochastic Processes and their Applications* **125**, 2752–2785 (2015).

[133] A. Hasegawa, K. Mima, M. Duong-van, "Plasma distribution function in a superthermal radiation field", *Phys. Rev. Lett.* **54**, 2608–2610 (1985).

[134] V. Pierrard and M. Lazar, "Kappa Distributions: Theory and Applications in Space", *Plasmas. Solar Phys.* **267**, 153–174 (2010).

[135] O.G. Bakunin, *Turbulence and Diffusion: Scaling Versus Equations*. Springer Science & Business Media, 2008.

[136] T.H. Stix, *Waves in Plasmas*. Springer Science & Business Media, 1992.

[137] B.D. Shizgal, "Suprathermal particle distributions in space physics: Kappa distributions and entropy", *Astrophys Space Sci.* **312**, 227–237 (2007).

[138] G.G. Howes, "Laboratory space physics: Investigating the physics of space plasmas in the laboratory", *Physics of Plasmas* **25**, 055501 (2018).

[139] W. Thomson, "On the theory of the electric telegraph", *Proc. R. Soc. London* **7**, 382–399 (1854).

[140] K. Malakar, A. Das, A. Kundu, K.V. Kumar and A. Dhar, "Exact Steady State of Active Brownian Particles in a 2D Harmonic Trap", arXiv:1902.04171v1 [cond-mat.stat-mech].

[141] U. Erdmanna, W. Ebeling, L. Schimansky-Geier and F. Schweitzer, "Brownian particles far from equilibrium?" *Eur. Phys. J.* B **15**, 105–113 (2000).

[142] N.V. Brilliantov and T. Pöschel, *Kinetic Theory of Granular Gases*. Oxford University Press, Oxford (2004).

[143] A. Baldassarri, A. Puglisi and U. Marini Bettolo Marconi, "Kinetic models of inelastic gases", *Mathematical Models and Methods in Applied Sciences* **12**, No. 7 (2002) 1–19.

[144] A. Megías and A. Santos, "Driven and undriven states of multicomponent granular gases of inelastic and rough hard disks or spheres", arXiv:1901.11307v1 [cond-mat.soft].

[145] A.V. Bobylev, I.M. Gamba and V.A. Panferov, "Moment Inequalities and High-Energy Tails for Boltzmann Equations with Inelastic Interactions", *J. Stat. Phys.* **116**, (2004).

[146] A. Baldassarri, U. Marini Bettolo Marconi and A. Puglisi, "Influence of correlations on the velocity statistics of scalar granular gases", *Europhys. Lett.* (1) **58**, 14–20 (2002).

[147] M.H. Ernst and R. Brito, "Scaling Solutions of Inelastic Boltzmann Equations with Over-Populated High Energy Tails", *J. Stat. Phys.* **109** (2002).

[148] V. V. Prasad, D. Das, S. Sabhapandit and R. Rajesh, "Velocity distribution of a driven inelastic one-component Maxwell gas" *Phys. Rev. E* **95**, 032909 (2017).

[149] P. Evesque, "New corner stones in dissipative granular gases", *Poudres & Grains* **14**, 8–53 (2004).

[150] M. E. Peskin, D. V. Schroeder, *An introduction to Quantum Field Theory*, ABP Westview Press, 1995.

[151] D. Bakry and M. Emery, "Hypercontractivité de semi-groupes des diffusion", *C. R. Acad. Sci. Paris, Sér. I* **299**, 775-777 (1984).

[152] A. Arnold, P. Markowich, G. Toscani and A. Unterreiter, "On convex Sobolev inequalities and the rate of convergence to equilibrium for Fokker-Planck type equations", *Communications in Partial Differential Equations* **26**, 43-100 (2001).

[153] C. Villani, *Hypocoercivity*. American Mathematical Soc., 8. October 2009.

[154] J. Dolbeault, C. Mouhot, C. Schmeiser, "Hypocoercivity for linear kinetic equations conserving mass", *Transactions of the American Mathematical Society* **367**, 3807–3828 (2015).

[155] B. Bakry, and G. Cattiaux, "A simple proof of the Poincaré inequality for a large class of probability measures including the log-concave case", *Elect. comm. in Probab.* **13**, 60–66 (2008).

[156] T. Buchert *et al.*, "Is there proof that backreaction of inhomogeneities is irrelevant in cosmology?", *Class. Quantum Grav.* **32**, 215021 (2015) and arXiv:1505.07800 [gr-qc].

[157] K. Enqvist, "Lemaitre-Tolman-Bondi model and accelerating expansion", *Gen. Rel. Grav.* **40**, 451-466 (2008) and arXiv:0709.2044 [astro-ph].

[158] T. Josset, A. Perez and D. Sudarsky, "Dark energy as the weight of violating energy conservation", *Phys. Rev. Lett.* **118**, 021102 (2017) and arXiv:1604.04183 [gr-qc].

[159] A. Perez, D. Sudarsky and J.D. Bjorken, "A microscopic model for an emergent cosmological constant", *Int. J. Mod. Phys. D* **27**, 1846002 (2018) and arXiv:1804.07162 [gr-qc].

[160] A. Perez and D. Sudarsky, "Dark energy from quantum gravity discreteness", *Phys. Rev. Lett.* **122**, 221302 (2019) and arXiv:1711.05183 [gr-qc].

[161] E.J. Squires, "A quantum solution to a cosmological mystery", *Phys. Lett. A* **162**, 35-36 (1992).

[162] N. Pinto-Neto and E. Sergio Santini, "The accelerated expansion of the Universe as a quantum cosmological effect", *Phys. Lett. A* **315**, 36-50 (2003) and arXiv:gr-qc/0302112.

[163] J.D. Brown and K.V. Kuchař, "Dust as a standard of space and time in canonical quantum gravity", *Phys. Rev. D* **51**, 5600 (1995) and arXiv:gr-qc/9409001.

[164] S. Weinberg, *Cosmology*, Oxford university press, 2008.

[165] E. Wong and M. Zakai, *Ann. Math. Statist.* **36** (5), 1560-1564 (1965).

[166] M. Hairer and E. Pardoux , *J. Math. Soc. Japan* **67** (4), 1551-1604 (2015).

[167] C. Kiefer, *Quantum Gravity*, International Series of Monographs on Physics **124**, Clarendon Press, Oxford (2004).

[168] H. Maeda, "Unitary evolution of the quantum Universe with a Brown-–Kushar dust", *Class. Quantum Grav.* **32**, 235023 (2015) and arXiv:1502.06954.

[169] T. Demaerel and W. Struyve, "Elimination of cosmological singularities in quantum cosmology by suitable operator orderings", *Phys. Rev. D* **100**, 046008 (2019) and arXiv:1904.09244 [gr-qc].

[170] N. Pinto-Neto and W. Struyve, "Bohmian quantum gravity and cosmology", in *Applied Bohmian Mechanics: From Nanoscale Systems to Cosmology*, 2nd edition, eds. Xavier Oriols Pladevall and Jordi Mompart, 607-656 (2019).

[171] D. Dürr and S. Teufel, *Bohmian Mechanics*, Springer-Verlag, Berlin (2009).

[172] A. Vilenkin, "Creation of universes from nothing", *Phys. Lett. B* **117**, 25-28 (1982).

[173] H.E.S. Velten, R.F. vom Marttens and W. Zimdahl, "Aspects of the cosmological "coincidence problem"", *W. Eur. Phys.* **74**, 3160 (2014) and arXiv:1410.2509 [astro-ph.CO].

[174] M.V. Berry and N.L. Balazs, "Nonspreading wave packets", *Am. J. Phys.* **47**, 264-267 (1979).

[175] P.R. Holland, *The Quantum Theory of Motion*, Cambridge University Press, Cambridge (1993).

[176] S. Das , G. Gompper, R. G. Winkler, "Confined active Brownian particles: theoretical description of propulsion-induced accumulation", *New J. Phys.* **20** (2018) 015001.

[177] G. Szamel, "Self-propelled particle in an external potential: Existence of an effective temperature", *Phys. Rev. E* **90**, 012111 (2014).

[178] C. Maes, K. Netočný, "Non-reactive forces and pattern formation induced by a nonequilibrium medium", `arXiv:1711.05168 [cond-mat.stat-mech]`.

[179] K. Fang and T. Linde, "Cluster Mergers and the Origin of the ARCADE-2 Excess", *Journal of Cosmology and Astroparticle Physics* **10**, (2016).

[180] B.C. Arnold, *Pareto Distributions*. Chapman and Hall/CRC; 2nd edition (March 10, 2015).

[181] V. Poulin, T.L. Smith, T. Karwal and M. Kamionkowski, "Early Dark Energy can Resolve the Hubble Tension", *Phys. Rev. D* **122**, 221301 (2019).

[182] S. Goldstein, "Absence of chaos in Bohmian dynamics", *Phys. Rev. E* **60**, 7578-7579 (1999) and arXiv:quant-ph/9901005.

[183] L.C. Evans, *Partial differential equations*. Graduate Studies in Mathematics — American Mathematical Society; 2nd edition (March 3, 2010).

[184] D.-Q. Jiang, M. Qian, M.-P. Qian, *Mathematical theory of nonequilibrium steady states*, Lecture Notes in Mathematics 1833, Springer (2002).

A Arrhenius formula for run-and-tumble particles

We collect here details about the derivation of (29).

When we have a run-and-tumble process on the state space $\mathbb{R}\times\{1,-1\}$ with driving velocity $c(x,\sigma)$ and spin-transition rates $a(x,\sigma)$ the backward generator L is of the form

$$\begin{aligned}(Lf)(x,\sigma) = T(\partial_x^2 f)(x,\sigma) + c(x,\sigma)(\partial_x f)(x,\sigma) \\ +a(x,\sigma)[f(x,-\sigma)-f(x,\sigma)]\end{aligned} \tag{131}$$

The expectation value $\tau(x,\sigma)$ of the time-span required to hit $(-\infty,-h]\cup[h,+\infty)$ if the process (131) is initialized at (x,σ) ($x\in(-h,h)$) must obey the boundary value problem

$$\begin{cases} L\tau = -1 \\ \lim_{x\to h}\tau(x,\pm 1) = 0 = \lim_{x\to -h}\tau(x,\pm 1)\end{cases} \tag{132}$$

If c transforms anti-symmetrically around $x=0$ the solution to (132) is symmetric under the same reflection. That implies that (132) yields the same solution on $(0,h)$ as

$$\begin{cases} L\tau = -1 \\ \lim_{x\to 0+}(\partial_x\tau)(x,\pm 1) = 0 = \lim_{x\to h-}\tau(x,\pm 1)\end{cases} \tag{133}$$

This is precisely what we do in the derivation of (29). The hard-wall condition is simply implemented by defining the process (x_t,σ_t) considered there as $(|y_t|,\sigma_t)$ where

$$\dot{y}_t - c\sigma_t\theta(y_t) = -\mathcal{E}\theta(y_t) + \sqrt{2T}\xi_t$$

where θ is the standard Heaviside-function. The latter process has the necessary antisymmetry to have (132) reduce to (133). Abbreviating $\tau(.,\pm 1) =: \tau_\pm$, $a(.,\pm 1) =: a_\pm$, our problem now consists of solving the following system of ODE's (to be solved on the interval $(0,h)$):

$$\begin{cases} T\tau_+'' + (c-\mathcal{E})\tau_+' + a_+[\tau_- - \tau_+] = -1 \\ T\tau_-'' + (-c-\mathcal{E})\tau_-' + a_-[\tau_+ - \tau_-] = -1 \\ \tau_+'(0) = \tau_-'(0) = \tau_+(h) = \tau_-(h) = 0\end{cases} \tag{134}$$

The solution is in general of the form

$$\begin{cases} \tau_+(x) = \tau_{+,\mathrm{part}}(x) + \mu_0 + \sum_{j=1}^3 \mu_j e^{\lambda_j x} \\ \tau_-(x) = \tau_{-,\mathrm{part}}(x) + \mu_0 + \sum_{j=1}^3 \mu_j z_j e^{\lambda_j x} \end{cases} \tag{135}$$

wherein

1. The complex numbers $\{\lambda_j\}_{1\leq j\leq 3}$ are the roots of the polynomial

$$\begin{aligned} p(\lambda) &:= \frac{1}{\lambda}\begin{vmatrix} T\lambda^2 + [c-\mathcal{E}]\lambda - a_+a_+ \\ a_-T\lambda^2 - [c+\mathcal{E}]\lambda - a_- \end{vmatrix} \\ &= T^2 \,.\, \text{polynomial (2.2.7)} \end{aligned}$$

   The pairs $\{(1,z_j)\}_j = \{(1, \frac{a-(c-\mathcal{E})\lambda_j - T\lambda_j^2}{a})\}_j$ are the associated generalized eigenvectors.

2. $(\mu_j)_{0\leq j\leq 4}$ are real parameters which are determined by the boundary conditions (note: 4 boundary conditions and 4 parameters)

3. $\tau_{\sigma,\mathrm{part}}$ are a certain "particular" solution that absorb the -1's in the right-hand side of the system (134). Let us agree on the following choice:

$$\begin{cases} \tau_{+,\mathrm{part}}(x) = A + Dx \\ = \frac{-2c}{-a_+(c+\mathcal{E})+a_-(c-\mathcal{E})} - \frac{a_++a_-}{-a_+(c+\mathcal{E})+a_-(c-\mathcal{E})}x \\ = A + \frac{a_++a_-}{a_+(\mathcal{E}+c)+a_-(\mathcal{E}-c)}x \\ \tau_{-,\mathrm{part}}(x) = Dx \end{cases} \tag{136}$$

To proceed, it is worthwhile to observe that the characteristic polynomial (1) must have three different real roots

$$\lambda_1 > (\mathcal{E}+c)/T \geq \lambda_2 \geq (\mathcal{E}-c)/T > \lambda_3,$$

Indeed, for $a_\pm\, c > 0$ (active diffusion),

$$\begin{cases} p(\frac{\mathcal{E}-c}{T}) = 2\, a_+\, c > 0 \\ p(\frac{\mathcal{E}+c}{T}) = -2\, a_-\, c < 0 \end{cases}$$

so that the intermediate value and the large-λ asymptotics of a cubic function yield the statement. In the marginal case $c = 0$ (passive diffusion), the roots are given by $\{\xi, \frac{\xi}{2} \pm \sqrt{\left(\frac{\xi}{2}\right)^2 + a_+/T + a_-/T}\}$ with $\xi = \mathcal{E}/T$, which are three different real

numbers, the middle one again being $\lambda_2 = \mathcal{E}/T$.

The boundary conditions of (134), written in terms of the expressions (135) (136), take the form

$$\begin{cases} 0 = D + \sum_{j=1}^{3} \lambda_j \mu_j \\ 0 = D + \sum_{j=1}^{3} \lambda_j z_j \mu_j \\ 0 = A + Dh + \mu_0 + \sum_{j=1}^{3} e^{\lambda_j h} \mu_j \\ 0 = Dh + \mu_0 + \sum_{j=1}^{3} e^{\lambda_j h} z_j \mu_j \end{cases}$$

By Cramer's rule, the solution for μ_0 is given by

$$\begin{aligned} \mu_0 &= \frac{\begin{vmatrix} -D\lambda_1\lambda_2\lambda_3 \\ -D\lambda_1 z_1 \lambda_2 z_2 \lambda_3 z_3 \\ -A - Dhe^{\lambda_1 h} e^{\lambda_2 h} e^{\lambda_3 h} \\ -Dhe^{\lambda_1 h} z_1 e^{\lambda_2 h} z_2 e^{\lambda_3 h} z_3 \end{vmatrix}}{\begin{vmatrix} 0\lambda_1\lambda_2\lambda_3 \\ 0\lambda_1 z_1 \lambda_2 z_2 \lambda_3 z_3 \\ 1e^{\lambda_1 h} e^{\lambda_2 h} e^{\lambda_3 h} \\ 1e^{\lambda_1 h} z_1 e^{\lambda_2 h} z_2 e^{\lambda_3 h} z_3 \end{vmatrix}} \\ &\approx -D \frac{(z_3 - 1)\lambda_3 (z_2 - z_1) e^{\lambda_1 h} e^{\lambda_2 h}}{(z_3 - z_2)\lambda_2 \lambda_3 (z_1 - 1) e^{\lambda_1 h}} \\ &= \frac{D(1 - z_3)(z_2 - z_1) e^{\lambda_2 h}}{(z_3 - z_2)(z_1 - 1)\lambda_2} \end{aligned} \tag{137}$$

where the approximation becomes better provided $\lambda_2 > 0$ (In the special case where $\lambda_2 \leq 0$ one can calculate that $\tau \propto h$, i.e. the escape acquires a "ballistic" speed) and with increasing h, in the sense that the inequality $\lambda_1 > \lambda_2 > \lambda_3$ becomes amplified to

$$(\lambda_1 - \lambda_2)h \gg 1 \qquad (\lambda_2 - \lambda_3)h \gg 1. \tag{138}$$

A similar computation reveals that $\mu_{1,2,3}$ are only of order $\max\{e^{\lambda_3 h}, e^{(\lambda_2 + \lambda_3 - \lambda_1)h}\}$ and due to (138), in the large-h limit this is much smaller than (137). So in this large-h limit $\tau_{\pm}(x = 0) \approx \mu_0$. The careful reader will want to ensure that the prefactor in (137) has a nonzero numerator $(1 - z_3)(z_2 - z_1)$: $1 - z_3 = -a^{-1}(\lambda_3^2 + (c - \mathcal{E})\lambda_3) > 0$ since $\lambda_3 < 0$. Likewise, one can verify that in general $z_2 - z_1 > 0$. Wrapping

everything together,

$$\begin{cases} \tau_{\pm} \approx \frac{D(1-z(\lambda_3))(z(\lambda_2)-z(\lambda_1))e^{\lambda_2 h}}{(z(\lambda_3)-z(\lambda_2))(z(\lambda_1)-1)\lambda_2} \\ z(\lambda) := -\frac{T\lambda^2+(c-\mathcal{E})\lambda-a_+}{a_+} = -\frac{\lambda^2 T-(\mathcal{E}-c)\lambda-a_+}{a_+} \\ D = -\frac{a_++a_-}{\alpha_+ c_- + a_- c_+} = \frac{a_++a_-}{a_+(\mathcal{E}+c)+a_-(\mathcal{E}-c)} \\ \lambda_1 > \lambda_2 > \lambda_3 \text{ roots of the polynomial (1)} \end{cases}$$

B Derivation of the first-hitting time formula

In this section we derive the expression (174) for the expected time for a diffusion $X(t)$ with $X(0) = x_j \in \mathbb{R}$ and evolving according to

$$\dot{X}_t = -V'(X_t) + \sqrt{2}\,\xi_t \tag{139}$$

to first hit a given point $x_{j+1} > x_j$. Here, we replace the notation x_j by $x \in \mathbb{R}$ and x_{j+1} by $y \in \mathbb{R}$.

One proceeds by using Dynkin's formula; for a smooth function f,

$$\mathbb{E}^x[f(X_\tau)] = f(x) + \mathbb{E}^x\left[\int_0^\tau (Lf)(X_s)\mathrm{d}s\right] \tag{140}$$

wherein

- $\mathbb{E}^x$ is the expectation value conditioned on the initial condition $X(0) = x$;
- τ is the (random) first exit time from some open bounded interval surrounding x. We denote it $I_a = (a, y) \subseteq \mathbb{R}$ and keep in mind to let $a \to -\infty$ when we are ready;
- L is the backward generator associated to the Markov process (139):

$$(Lg)(.) = -V'(.)g'(.) + g''(.) = e^{V(.)}\left(e^{-V(.)}g'(.)\right)'$$

The first way we want to use Dynkin's formula is by defining the function f as the solution to the following Dirichlet boundary value problem:

$$\begin{cases} (Lf)(x) \equiv -1 \\ f(a) = f(y) = 0 \end{cases}$$

Note that for such function f the Dynkin formula (140) reduces to

$$0 = f(x) + \mathbb{E}^x\left[\int_0^\tau (-1)\mathrm{d}s\right] = f(x) - \mathbb{E}^x[\tau]$$

So $f(x) = \mathbb{E}^x[\tau]$ is the expected escape time required to leave the interval $[a, y]$. The (unique) solution to this problem is given by

$$f_{(a)}(x) = \left(-C_a \int_x^b dy\, e^{V(y)-V(b)} + \int_x^b dy \int_a^y dz\, e^{V(y)-V(z)}\right), \tag{141}$$

$$C_a = \frac{\int_a^b dy \int_a^y dz\, e^{V(y)-V(z)}}{\int_a^b dy\, e^{V(y)-V(b)}}$$

The escape time increases if we lower a as can be verified from the expression (141). In any case, once the probability that the diffusion diverges to $-\infty$ before hitting y is proven to be zero, we then know that the true average escape time $\langle t_{x\to y}\rangle$ from the interval $(-\infty, y)$ is given by

$$\langle t_{x\to y}\rangle = \lim_{a\to-\infty} f_{(a)}(x) = \inf_{a<x} f_{(a)}(x)$$

Letting $a \to -\infty$ in the expression (141) yields $C_a \to 0$ provided

$$\exists C_1 > 0,\, C_2 \in \mathbb{R} :\, \forall z \le y \le b :\, V(y) - V(z) \le -C_1(y-z) + C_2. \tag{142}$$

which is the case with probability 1 in our setup, by the strong law of large numbers. Hence (141) reduces to (174).

To finally show that the scenario of a divergence of the diffusion to $-\infty$ before hitting y has zero probability, we want to apply the Dynkin formula to the function $\tilde{f}$ defined through the boundary value problem

$$\begin{cases} (L\tilde{f})(x) \equiv 0 \\ \tilde{f}(a) = 1,\, \tilde{f}(y) = 0 \end{cases} \tag{143}$$

Inserting this into the Dynkin formula (140) yields

$$\mathbb{E}^x(\tilde{f}(X_\tau)) = \tilde{f}(x)$$

wherein the left-hand side expresses the probability that the diffusion will hit $x = a$ before hitting $x = y$. The (unique) solution to (143) is given by

$$\tilde{f}_{(a)}(x) = \frac{\int_x^b dy\, e^{V(y)-V(b)}}{\int_a^b dz\, e^{V(z)-V(b)}} \underset{(142)}{\le} \frac{\int_x^b dy\, e^{V(y)-V(b)}}{C_1^{-1}(1+e^{C_1(b-a)})e^{C_2}} \to 0$$

as $a \to -\infty$. This implies the requested result.

C Waiting times on a random comb

Here we give details for better understanding of the equalities (61):

$$\begin{aligned} v = \frac{1}{\mathbb{E}[\Delta t_0]} &= \frac{\tanh(E_1/2)}{\mathbb{E}[t_0^r]} \\ = \frac{\tanh(E_1/2)}{\sum_{j=0}^{\infty} \mathrm{Prob}[L_0 = j] \frac{e^{(j+1)E_2}-1}{e^{E_2}-1}} &2\cosh(E_1/2) \\ = 2\sinh(E_1/2) &\frac{e^{E_2}-1}{e^{E_2}\langle e^{L_0 E_2}\rangle - 1} \end{aligned} \tag{144}$$

where $\mathbb{E}[\Delta t_0]$ is the average time required for the walker to reach the site $(1,0)$ for the first time when he starts at the site $(0,0)$. Likewise, $\mathbb{E}[t_0^r]$ is the average time required for the walker to reach either $(-1,0)$ or $(1,0)$ given that he started at $(0,0)$. A derivation of the first two equalities was already given in the body of the text. For the third equality, consider that

$$\mathbb{E}[t_0^r \mid L_0 = 0] = \frac{1}{e^{E_1/2} + e^{-E_1/2}}$$

and for $n \in \mathbb{N}_0$,

$$\mathbb{E}[t_0^r \mid L_0 = n] =$$

$$\sum_{j=0}^{\infty} ((j+1)t_0 + j\tau_n)\, \mathrm{Prob}[\text{ The walker makes } j \text{ successive sorties from site } (0,0)$$

$$\text{into the dead-end } \{(0,j)\}_{1\le j\le n} \text{ before finally jumping to } (\pm 1, 0)\ ]$$

$$= \sum_{j=0}^{\infty} ((j+1)t_0 + j\tau_n)\,(1-p)^j p = \frac{1}{p}t_0 + \frac{1-p}{p}\tau_n$$

wherein

- $p = \mathrm{Prob}[\text{A random walk initialized at } (0,0) \text{ hits } (\pm 1, 0) \text{ before hitting } (0,1)]$;
- $t_0 = \mathbb{E}[\text{Amount of time a walker initialized at } (0,0) \text{ remains on site } (0,0)]$;
- $\tau_n = \mathbb{E}[\text{time required for a random walk initialized at site } (0,1) \text{ to hit } (0,0)]$.

One easily sees that $p = \frac{e^{E_1/2}+e^{-E_1/2}}{e^{E_1/2}+e^{-E_1/2}+e^{E_2/2}}$ and $t_0 = \frac{1}{e^{E_1/2}+e^{-E_1/2}+e^{E_2/2}}$.

$$\begin{aligned} &= \frac{e^{E_1/2}+e^{-E_1/2}+e^{E_2/2}}{e^{E_1/2}+e^{-E_1/2}} \frac{1}{e^{E_1/2}+e^{-E_1/2}+e^{E_2/2}} + \frac{e^{E_2/2}}{e^{E_1/2}+e^{-E_1/2}}\tau_n \\ &= \frac{1}{2\cosh(E_1/2)}\left(1 + e^{E_2/2}\tau_n\right) \end{aligned} \tag{145}$$

The τ_n can be computed by induction: clearly, $\tau_1 = e^{E_2/2}$ (that is simply the Poisson waiting time to jump back from $(0,1)$ to $(0,0)$). We can compute τ_{n+1} from τ_n via the following consideration. In a dead-end with length $n+1>2$ a walker initialized at $(0,1)$ (i.e., the neck of the dead-end) will remain stuck on that site with an average waiting time $\frac{1}{e^{E_2/2}+e^{-E_2/2}}$. After waiting till the first jump, the probability to jump to $(0,0)$ is $\frac{e^{-E_2/2}}{e^{E_2/2}+e^{-E_2/2}}$ while the probability to jump deeper into the dead-end (i.e., into $\{(0,j)\}_{2\leq j\leq n+1}$) is $\frac{e^{E_2/2}}{e^{E_2/2}+e^{-E_2/2}}$. In the latter case, the time required to return from $\{(0,j)\}_{2\leq j\leq n+1}$ to $(0,1)$ is τ_n. Hence,

$$\tau_{n+1} =$$

$$\sum_{j=0}^{\infty}\left((j+1)t_0' + j\tau_n\right)\text{Prob}[\text{ The walker makes } j \text{ successive sorties from site } (0,1)$$

$$\text{into the dead-end } \{(0,j)\}_{2\leq j\leq n+1} \text{ before finally jumping to } (0,0)\ ]$$

$$= \sum_{j=0}^{\infty}\left((j+1)t_0' + j\tau_n\right)(1-q)^j q = \frac{1}{q}t_0' + \frac{1-q}{q}\tau_n$$

wherein

- $q = \text{Prob}[\text{A random walk initialized at } (0,1) \text{ hits } (0,0) \text{ before hitting } (0,2)]$;
- $t_0' = \mathbb{E}[\text{Amount of time a walker initialized at } (0,1) \text{ remains on site } (0,1)]$.

Since $q = \frac{e^{-E_2/2}}{e^{E_2/2}+e^{-E_2/2}}$ and $t_0' = \frac{1}{e^{E_2/2}+e^{-E_2/2}}$, we can solve the recursion for τ_n. The result is $\tau_n = e^{E_2/2}\frac{e^{nE_2}-1}{e^{E_2}-1}$. Plugging this into (145) yields that

$$\mathbb{E}[t_0^r \mid L_0 = n] = \frac{1}{2\cosh(E_1/2)}\frac{e^{(n+1)E_2}-1}{e^{E_2}-1}$$

Also for $n=0$, that formula turns out to be accurate. That in turn explains the third equality of (144). The fourth equality of (144) is a simple rewriting involving no calculations.

D Asymptotic speed for thermal active Brownians

We give the derivation of (55). If we write $f = e^g$ (f was already required to be a positive function) in (54), we have

$$c\lambda\cos(\theta)f(\theta) + D_\theta \sin^{2-d}(\theta)\left(\sin^{d-2}(\theta)f'(\theta)\right)' \equiv Cf(\theta) \text{ and } f'(0) = f'(\pi) = 0$$
$$\Leftrightarrow c\lambda\cos(\theta) + D_\theta\left(\sin^{2-d}(\theta)\left(\sin^{d-2}(\theta)g'(\theta)\right)' + g'(\theta)^2\right) \equiv C \text{ and } g'(0) = g'(\pi) = 0$$

We solve (146) by iteration until we are close enough to the actual solution. For this, write $h = g'$, decompose into $h = h_0 + h_1 + h_2$ and let $h_{0,1,2}$ solve

$$\begin{cases} \sin^{2-d}(\theta)\left(\sin^{d-2}(\theta)h_0(\theta)\right)' + \underbrace{\dfrac{c\lambda}{D_\theta}}_{=:\xi}\cos(\theta) = 0 & h_0(0) = 0 \\ \sin^{2-d}(\theta)\left(\sin^{d-2}(\theta)h_1(\theta)\right)' + h_0(\theta)^2 = C_0 & h_1(0) = 0 \\ \sin^{2-d}(\theta)\left(\sin^{d-2}(\theta)h_2(\theta)\right)' + h_1(\theta)^2 + 2h_1(\theta)h_0(\theta) = C_1 & h_2(0) = 0 \\ C_0 = \int_0^\pi d\theta\, \sin^{d-2}(\theta)h_0^2(\theta) / \int_0^\pi d\theta\, \sin^{d-2}(\theta) \\ C_1 = \int_0^\pi d\theta\, \sin^{d-2}(\theta)\left(h_1^2(\theta) + 2h_1(\theta)h_0(\theta)\right) / \int_0^\pi d\theta\, \sin^{d-2}(\theta) \end{cases} \tag{147}$$

Then by construction, $f = e^{\int h}$ solves

$$\frac{-Lf}{f} = D_\theta\left(C_0 + C_1 + \underbrace{h_2(2h_0 + 2h_1 + h_2)}_{=\text{small, i.e. } O(\xi^5) \text{ (see later)}}\right) \tag{148}$$

The solution to (147) is given by

$$\begin{cases} h_0(\theta) = \frac{\xi}{d-1}\sin(\theta) & C_0 = \frac{\xi^2}{d(d-1)} \\ h_1(\theta) = \frac{\xi^2}{d(d-1)^2}\sin(\theta)\cos(\theta) & C_1 = \frac{\xi^4}{d^3(d-1)^3(d+2)} \\ h_2(\theta) = O(\xi^4) \end{cases}$$

Inserting (148) into the Rayleigh-Ritz quotient then yields a bound of the form

$$\kappa^* \leq -D_\theta\left(\frac{\xi^2}{d(d-1)} + \frac{\xi^4}{d^3(d-1)^3(d+2)}\right) + M\xi^5 \tag{149}$$

where the constant M can be estimated explicitly if the need would arise. Plugging (149) into (61) yields

$$0 \leq \alpha - v\lambda + \underbrace{\left(D_x + \frac{c^2}{d(d-1)D_\theta}\right)}_{=D_{\text{eff}}}\lambda^2 + \frac{c^4}{d^3(d-1)^3(d+2)D_\theta^3}\lambda^4 + M\frac{c^5}{D_\theta^4}\lambda^5 =: p_v(\lambda)$$

We can scan p_v along $\lambda = \frac{v}{2D_{\text{eff}}}$ (which is the minimum point of the parabolic part of p_v):

$$p_v(v/(2D_{\text{eff}})) = \alpha - \frac{v^2}{4D_{\text{eff}}} + \frac{c^4v^4}{16d^3(d-1)^3(d+2)D_\theta^3D_{\text{eff}}^4} + M\frac{c^5v^5}{32D_\theta^4D_{\text{eff}}^5}$$

The smallest root v_0 of this equation (which is a lower bound for $v_{\min}$) is

$$v_0^2 = 4\alpha D_{\text{eff}} + \frac{4\alpha^2c^4}{d^3(d-1)^3(d+2)D_\theta^3D_{\text{eff}}} + O\left(M\frac{\alpha^2c^4}{D_\theta^3D_{\text{eff}}}\frac{c}{\sqrt{\alpha D_{\text{eff}}}}\right) \tag{150}$$

One can in fact prove, by showing that the iteration (147) will in fact converge to the actual solution, that $v_{\min}$ agrees with v_0 to fourth order in c in the sense of the expression (150).

E The large-M limit

This Section is a compendium to Section 7.

Because M is large, the numerical analysis of the evolution of the scale factor is problematic. We can overcome this problem by considering the limit $M \to \infty$.

Before we consider this limit, note that for a solution $\{x(\tau), \psi(x,\tau)\}$ to (125) and (126), we have that [182]:

$$x(\tau) \equiv P_\tau^{-1}(P_0(x(0)))$$

where $P_\tau(x)$ is the cumulative probability distribution

$$P_\tau(x) := \int_x^\infty |\psi(x',\tau)|^2 \mathrm{d}x'$$

That is, trajectories correspond to the contours of the cumulative distribution function.

Consider now a Gaussian superposition (normalized over the real line)

$$\psi_M(x,\tau) = \sum_{j=1}^N \alpha_j \psi_{\bar{x}_j, v_j, \sigma_j, M} \tag{151}$$

It can be shown that the corresponding trajectories $x_M(\tau)$ of the rescaled scale factor converge uniformly to $x_\infty(\tau)$ under the limit $M \to \infty$ (with $\overline{x}_j$, σ_j, v_j constant), where $x_\infty(\tau)$ is the contour of the following cumulative probability distribution

$$\begin{aligned} P_{\tau,\infty}(x) &:= \lim_{M\to\infty} \int_x^\infty |\psi_M(x',\tau)|^2 \mathrm{d}x' \\ &= \sum_{j=1}^N |\alpha_j|^2 \lim_{M\to\infty} \int_x^\infty |\psi_{\bar{x}_j, v_j, \sigma_j, M}(x',\tau)|^2 \mathrm{d}x' \\ &= \sum_{j=1}^N |\alpha_j|^2 \int_x^\infty \frac{1}{\sigma_j\sqrt{\pi}} e^{-\frac{(x'-\bar{x}_j - v_j\tau)^2}{\sigma_j^2}} \mathrm{d}x' \end{aligned}$$

i.e.,

$$x_\infty(\tau) = P_{\tau,\infty}^{-1}(P_{0,\infty}(x_\infty(0))) \tag{152}$$

Assuming for simplicity that all the velocities v_j in (151) are different and letting $P_{\tau,M}$ be the cumulative distribution function associated to the wave function (151), we have that $P_{\tau,M}$ converges to (E), in the sense that $\|P_{\tau,M} - P_{\tau,\infty}\|_\infty \leq \frac{C}{M} \sup_{1\leq i<j\leq N} \frac{1}{|v_i - v_j|}$ for some parameter-independent $\mathcal{O}(1)$ constant C. Finally, it can be shown that a converging P_M gives rise to converging orbits x_M as $M \uparrow \infty$.

In conclusion, the error in numerically solving the trajectories made by replacing $M = 10^{120}$ with $M = \infty$ is indeed negligible, and we can use the far simpler recipe provided by (152).

F Construction of the Kolmogorov operators and the Feller semi-groups

We set out to construct the just-mentioned operators and semigroups by constructing the relevant resolvents first.

Definition F.1. *H^μ ($\mu > 0$) is the Hilbert space resulting from the closure of the vector-space of radial weakly differentiable functions $u : M \mapsto \mathbb{R}$ whose norm associated to the inner product*

$$(u, v)_{H^\mu} = \int_M \rho_0 \left(\nabla u \cdot \nabla v + \mu \frac{uv}{|y|^2} \right) dy$$

is finite and $\limsup_{y\to 0} \frac{|u(y)|}{|y|} = 0$. The closure is with respect to $(.,.)_{H^\mu}$.
Likewise $\hat{H}^\mu$ is the Hilbert space of weakly differentiable functions whose norm associated to the inner product

$$(u, v)_{\hat{H}^\mu} = (u, v)_{H^\mu} + (u, v)_{\mathscr{L}^2}$$

is finite.

Lemma F.1. *Let u, v be radial H^1-functions, then $f^i, g^i : M \mapsto \mathbb{R} : y \mapsto u(y)\hat{y}^i$ resp. $v(y)\hat{y}^i$ are in H^0. Conversely, if f, g are radial vectorfields with H^0-components, then $u, v : M \mapsto \mathbb{R} : y \mapsto f^i(y)\hat{y}_i$, $g^i(y)\hat{y}_i$ are in H^1. More precisely, one has the isometry*

$$(u, v)_{H^1} = (u\hat{y}^i,\, v\hat{y}_i)_{H^0}, \qquad (f^j\hat{y}_j,\, g^k\hat{y}_k)_{H^1} = (f^i,\, g_i)_{H^0} \tag{153}$$

For radial H^0-vectorfields f, g and radial H^1-functions u, one also has

$$F^i\partial_i u = 0 = g_j F^i \partial_i f^j. \tag{154}$$

Proof. Notice that

$$\partial_i \hat{y}^j = \partial_i \left(\frac{y^j}{|y|} \right) = \frac{\delta_i^j}{|y|} - \frac{y_i y^j}{|y|^3}. \tag{155}$$

Then $\hat{y}^i(\partial_i\hat{y}^j) = 0$ and $(\partial_i\hat{y}^j)(\partial^i\hat{y}_j) = \frac{1}{|y|^2}$ and it follows that

$$(f^j,\, g_j)_{H^0} = \int_M \partial_i(u(y)\hat{y}^j)\partial^i(v(y)\hat{y}_j)dy$$

$$= \int_M \left\{ (\partial_i u)(y)(\partial^i v)(y) + [v(y)(\partial_i u)(y) + u(y)(\partial_i v)(y)] \underbrace{\hat{y}^j \left(\frac{\delta^i_j}{|y|} - \frac{y_j y^i}{|y|^3} \right)}_{=0} \varphi(y) + \frac{u(y)v(y)}{|y|^2} \right\} dy$$

$$= \int_M \left\{ (\partial_i u)(y)(\partial^i v)(y) + \frac{u(y)v(y)}{|y|^2} \right\} dy$$

$$= (u,\, v)_{H^1}$$

which verifies the isometry (153). In (154), the first equality is trivial. For the second, one has (writing $f^i = u\hat{y}^i$ with u radial)

$$g_j F^i \partial_i f^j = g_j F^i \partial_i(u\hat{y}^j) = g_j u F^i \partial_i \hat{y}^j = 0$$

by (155) and since $g_i F^i = 0 = y_i F^i$. □

Definition F.2. *Let $\lambda \geq 0$ and define $B_{x,\epsilon,\lambda,\mu} : \hat{H}^\mu \times \hat{H}^\mu \to \mathbb{R}$ as the bilinear map which acts as*

$$(u, v) \mapsto \int \rho_0 \left\{ \left(\beta^{-1}\nabla u + \left(\nabla_y[U(x,y) - U(0,y)] + \epsilon F\right) u\right) \cdot \nabla v + \lambda\, uv + \beta^{-1}\mu \frac{uv}{|y|^2} \right\} dy$$

We also use the following auxiliary notations:

- $B_{x,\epsilon,\lambda} := B_{x,\epsilon,\lambda,\mu=0}$
- $B_\epsilon = B_{x=0,\epsilon,\lambda=0} := B_{x=0,\epsilon,\lambda=0,\mu=0}$
- $\tilde{B} = B_{x=0,\epsilon=0,\lambda=0,\mu=1}$

.

Lemma F.2. *(properties of $B_{x,\epsilon,\lambda,\mu}$)*

- *For all $u, v \in H^0$:*
$$B_{0,\epsilon,\lambda,\mu}(u, v) = B_{0,-\epsilon,\lambda,\mu}(v, u). \tag{156}$$
- *Let u and v be a pair of functions where one of the pair is smooth and compactly supported and the other is twice weakly differentiable, then*
$$(u,\, (\lambda + \frac{\mu}{\beta|y|^2} - l_{x,\epsilon})v) = B_{x,\epsilon,\lambda,\mu}(u, v). \tag{157}$$

Proof. The first result is straightforward and it requires the global antisymmetry of F as expressed in (94). (157) follows from a single partial integration (where the definition of weak differentiation is crucial, as is the compact support of one of the two functions since this ensures that there is no boundary term in the partial integration.) □

Lemma F.3. *There exists an increasing sequence of smooth, non-negative, compactly supported functions $(\chi_n)_n$ converging to 1 and for which $(\chi_n, \chi_n)_{H^0} \to 0$.*

Proof. Let $\eta : \mathbb{R} \to [0,1]$ be some non-negative smooth function whose support is $(-1,1)$, which is increasing in $(-1,0)$ and decreasing in $(0,1)$ and which has $\eta(0) = 1$. Now, define the auxiliary sequence

$$\eta_n(x) = \eta(x/n)$$

which is indeed increasing towards the constant function $x \mapsto 1$. Finally, define $\chi_n = \eta_n \circ U(x = 0)$. I.e.

$$\chi_n(y) = \eta_n(V(y)) = \eta(V(y)/n).$$

The property that χ_n has compact support follows from (87). Moreover

$$\begin{aligned}
(\chi_n, \chi_n)_{H^0} &= Z^{-1} \int_M \exp(-\beta V(y))(\partial_i \chi_n)(y)(\partial^i \chi_n)(y) dy \\
&= \int_M \exp(-\beta V(y)) \left(\eta'(V(y)/n)\right)^2 \frac{1}{n^2} (\partial_i V)(y)(\partial^i V)(y) \delta y \\
&\leq \left(\frac{\|\eta'\|_\infty}{n}\right)^2 \int_M \exp(-\beta V(y))(\partial_i V)(y)(\partial^i V)(y) dy \\
&\leq C/n^2
\end{aligned}$$

where the constant in the end is supplied by (89). □

The following calculation will turn out to be useful later: Let $\chi \geq 0$ be a function with $F^i \partial_i \chi = 0$. Then (94) implies

$$\begin{aligned}
&B_{x,\epsilon,\lambda}(\chi u, u) \\
&= \int_M \rho_0 \left(\beta^{-1} \nabla(\chi u) \cdot \nabla u + \chi u \nabla \left(U(x) - U(0)\right) \cdot \nabla u + \left[\lambda + \frac{\mu}{\beta |y|^2}\right] \chi u^2 \right) dy \quad (158) \\
&\geq \int_M \rho_0 \left(\beta^{-1} [\chi (\nabla u)^2 + u(\nabla \chi \cdot \nabla u)] - \chi k_1(x) |u \nabla u| + \left[\lambda + \frac{\mu}{\beta |y|^2}\right] \chi u^2 \right) dy \\
&\geq \int_M \rho_0 \left(\left[\beta^{-1}(\chi + \frac{\theta}{2}) + \frac{k_1(x)\chi}{2}\right] (\nabla u)^2 + \left[\lambda \chi + \frac{(\nabla \chi)^2}{2\theta} + \frac{\mu}{\beta |y|^2} \chi - \frac{k_1(x)\chi}{2}\right] u^2 \right) dy \quad (159)
\end{aligned}$$

where $\theta > 0$ is an arbitrary parameter.

In order to apply the Lax-Milgram theorem (see e.g. [183]) to the bilinear operator $B = B_{x,\epsilon,\lambda,\mu} : \hat{H}^\mu \times \hat{H}^\mu \to \mathbb{R}$, we need to show

Lemma F.4. *(coercivity of $B_{x,\epsilon,\lambda}$)*
For all $\lambda > \beta^{-1}$, there are positive constants c_i so that

$$\forall u, v \in \hat{H}^0 : |B_{x,\epsilon,\lambda}(u,v)| \leq c_1 \|u\|_{\hat{H}^0} \|v\|_{\hat{H}^0} \tag{160}$$

$$\forall u \in \hat{H}^0 : B_{x,\epsilon,\lambda}(u,u) \geq c_2 \|u\|^2_{\hat{H}^0} \tag{161}$$

$$\forall u, v \in H^0 : |B_\epsilon(u,v)| \leq c_3 \|u\|_{H^0} \|v\|_{H^0} \tag{162}$$

$$\forall u \in H^0 : B_\epsilon(u,u) \geq c_4 \|u\|^2_{H^0} \tag{163}$$

$$\forall u, v \in H^1 : |\tilde{B}(u,v)| \leq c_5 \|u\|_{H^1} \|v\|_{H^1} \tag{164}$$

$$\forall u \in H^1 : \tilde{B}(u,u) \geq c_6 \|u\|^2_{H^1} \tag{165}$$

Also the following bound (which is not required for the Lax-Milgram theorem but rather later to meet the requirements of the Hille-Yosida theorem) applies: $\exists c_7 \in \mathbb{R}$: $\forall u \in \hat{H}^0$

$$(c_7 + \lambda) \|u\|^2_{\mathscr{L}^2} \leq B_{x,\epsilon,\lambda}(u,u) \tag{166}$$

Proof. First, calculate

$$|B_{x,\epsilon,\lambda}(u,v)| =$$
$$\left| \int \rho_0 \left(\beta^{-1} \nabla u \cdot \nabla v + u \left(\nabla [U(x) - U(0)] + \epsilon F \right) \cdot \nabla v + \left[\lambda + \beta^{-1} \mu \frac{1}{|y|^2} \right] uv \right) dy \right|$$
$$\leq \beta^{-1} \left| \int \rho_0 \left(\nabla u \cdot \nabla v + \left[\beta\lambda + \mu \frac{1}{|y|^2} \right] uv \right) \right|$$
$$+ \int \rho_0 \left| \nabla [U(x) - U(0)] + \epsilon F \right| |u \nabla v| dy. \tag{167}$$

When $x = 0$, λ and v is radial ($F^i \partial_i v = 0$), the second term is zero and we can bound (167) by $\|u\|_{H^\mu} \|v\|_{H^\mu}$, thus obtaining (164). For the cases (160) and (162), we proceed with (167) (where we now put $\mu = 0$)

$$(167) \leq \max\left(\beta^{-1}, \lambda\right) \|u\|_{\hat{H}^0} \|v\|_{\hat{H}^0} + \int \rho \left| \nabla_y [U(x,y) - U(0,y)] + \epsilon F \right| |u \nabla v| dy$$
$$\leq \max\left(\beta^{-1}, \lambda\right) \|u\|_{\hat{H}^0} \|v\|_{\hat{H}^0} + \int \rho \left(\left| \nabla [U(x) - U(0)] \right| + \epsilon |F| \right) |u \nabla v| dy$$
$$\leq \max\left(\beta^{-1}, \lambda\right) \|u\|_{\hat{H}^0} \|v\|_{\hat{H}^0} + (k_1(x) + \epsilon C) \|u\|_{\mathscr{L}^2} \|v\|_{H^0}$$
$$\leq \left(\max\left(\beta^{-1}, \lambda\right) + k_1(x) + \epsilon C \right) \|u\|_{\hat{H}^0} \|v\|_{\hat{H}^0}$$

thus obtaining (160) and also (162) after noting that the Poincaré inequality implies that $\|u\|^2_{\hat{H}^0} \leq (1+c^{-2})\|u\|^2_{H^0}$.
Next, check (158) for $x = \lambda = 0$ and $\chi = 1$. The expression simply reduces to $\beta^{-1}\|u\|_{H^\mu}$ so that (163) and (165) is recovered. Otherwise we set $\mu = 0$, $\chi = 1$ and evaluate (159) for $\theta \to \infty$. The result:

$$B_{x,\epsilon,\lambda}(u,u) \geq \int_M \rho_0 \left(\left[\beta^{-1} - \frac{k_1(x)}{2} \right] (\nabla u)^2 + \left[\lambda - \frac{k_1(x)}{2} \right] u^2 \right) dy \tag{168}$$

To obtain (161), notice that rhs(168) $\geq (\min(\beta^{-1}, \lambda) - \frac{k_1(x)}{2}) \|u\|_{\hat{H}^0}$ which is positive for x sufficiently small. To obtain (166), notice that rhs(168) $\geq (\lambda - \frac{k_1(x)}{2}) \|u\|_{\mathscr{L}^2}$ provided x is small enough that $k_1(x) < 2\beta^{-1}$. □

Lemma F.5. *(Lax-Milgram: the boundedness of the 'external' linear functional) The linear functional $f_v : u \mapsto (u,v)_{\mathscr{L}^2}$ is bounded in the case that*

1. *$Dom(f_v) = \hat{H}^0$ and $v \in \mathscr{L}^2$.*
2. *$Dom(f_v) = H^0$ and $v \in \mathscr{L}^2$.*
3. *$Dom(f_v) = H^1$ and $v \in \mathscr{L}^2$ is radial.*

In case 1 and 3, the map $v \mapsto f_v$ is one-to-one. In case 2, the kernel of that map consist of the constant functions $\langle 1 \rangle$.

Proof. One has

$$|(u,v)_{\mathscr{L}^2}| \leq \|u\|_{\mathscr{L}^2}\|v\|_{\mathscr{L}^2}. \tag{169}$$

In general, the RHS is smaller than $\|u\|_{\hat{H}^0}\|v\|_{\mathscr{L}^2}$ which checks the first case. For the second case, one uses the Poincaré inequality to see that the RHS of (169) is smaller than $c^{-1}\|u\|_{H^0}\|v\|_{\mathscr{L}^2}$. In the third case, one uses the isometry (153) to obtain

$$|(u,v)_{\mathscr{L}^2}| = |(u\hat{y}^i, v\hat{y}_i)_{\mathscr{L}^2}| \leq \|u\hat{y}_i\|_{\mathscr{L}^2}\|v\hat{y}_i\|_{\mathscr{L}^2} \leq c^{-1}\|u\hat{y}\|_{H^0}\|v\hat{y}\|_{\mathscr{L}^2} = c^{-1}\|u\|_{H^1}\|v\|_{\mathscr{L}^2}.$$

Concerning the injectivity of $v \mapsto f_v$, it follows in case 1 and 3 from the density of $\hat{H}^0$ in $\mathscr{L}^2$ and H^1 in the radial $\mathscr{L}^2$-functions respectively. □

Combining Lemmata F.4 and F.5, we can use the Lax-Milgram Theorem to define the resolvents

Definition F.3. *For $\lambda > 0$, we define the resolvents $R_{x,\epsilon,\lambda} : \mathscr{L}^2 \to (\hat{H}^0 \subseteq)\mathscr{L}^2$ so that $w = R_{x,\epsilon,\lambda}v \in \hat{H}^0 \subseteq \mathscr{L}^2$ is the unique solution of the weak equation (which must hold for all $u \in \hat{H}^0$)*

$$B_{x,\epsilon,\lambda}(u,w) = (u,v)_{(\mathscr{L}^2)}.$$

Similarly, for $\lambda = 0$, $x = 0$ and $w = 0$ or 1, we define (respectively) the pseudo-inverses $R_\epsilon, \tilde{R} : \mathscr{L}^2 \to \mathscr{L}^2$ so that $w = R_\epsilon v \in H^0 \subseteq \mathscr{L}^2$ and $z = \tilde{R}v \in H^1 \subseteq \mathscr{L}^2$ is the unique solution of the weak equation (which must hold for all $u \in H^0$ resp. $\in H^1$)

$$B_\epsilon(u, w) = -(u, v) \qquad \tilde{B}(u, z) = -(u, v)$$

Proposition F.1. *(properties of the resolvents and pseudo-inverses)*

1. *The resolvents $R_{x,\epsilon,\lambda}$, R_ϵ and $\tilde{R}$ are one-to-one.*

2. *Considering the operator-norms of the resolvents, one has ($\forall \lambda > c_7$)*

$$\sup_{u \in \mathscr{L}^2} \frac{\|R_{x,\epsilon,\lambda} u\|_{\mathscr{L}^2}}{\|u\|_{\mathscr{L}^2}} \leq \frac{1}{c_7 + \lambda} \tag{170}$$

$$\sup_{u \in \mathscr{L}^2} c \frac{\|R_\epsilon u\|_{\mathscr{L}^2}}{\|u\|_{\mathscr{L}^2}} \leq \sup_{u \in \mathscr{L}^2} \frac{\|R_\epsilon u\|_{H^0}}{\|u\|_{\mathscr{L}^2}} \leq c_4^{-1} \tag{171}$$

   where $k_4(x) > 0$ is a constant independent of ϵ. Similar bounds hold for the operator norms of the pseudo-inverse R_ϵ, $\tilde{R}$

3. *There exists an unbounded operator $L_{x,\epsilon} : D \subseteq \mathscr{L}^2 \to \mathscr{L}^2$ whose resolvent is precisely $(\lambda I - L_{x,\epsilon})^{-1} = R_{x,\epsilon,\lambda}$. One has $\ker L_{x,\epsilon} = \langle 1 \rangle$.*

4. *$R_{x,\epsilon,\lambda}$ and $\tilde{R}$ map non-zero, non-negative functions to positive functions.*

5. *One has*

$$R_{x,\epsilon,\lambda} 1 = \lambda^{-1} 1. \tag{172}$$

6. *One has the identities*

$$\forall u \in \mathscr{L}^2 : L_{0,\epsilon} R_\epsilon u = P_H u \qquad \forall u \in D : R_\epsilon L_{0,\epsilon} = P_H u.$$

7. *The following adjoint properties hold when $x = 0$:*

$$\forall u, v \in \mathscr{L}^2 : (u, R_\epsilon v) = (R_{-\epsilon} u, v), \qquad \forall u, v \in D : (u, L_{0,\epsilon} v) = (L_{0,-\epsilon} u, v)$$

8. *When $v \in H^0$ is twice weakly-differentiable and $\ell_{x,\epsilon} v \in \mathscr{L}^2$, then $v \in D$ and*

$$L_{x,\epsilon} v = \ell_{x,\epsilon} v$$

Proof. 1. In the case of $R_{x,\epsilon,\lambda}$ and $\tilde{R}$, this follows from the Lax-Milgram Theorem and the fact that the functional $v \mapsto f_v$ ($f_v : u \mapsto (u, v)$) is one-to-one (see Lemma F.5). The case of R_ϵ is similar (in this case f_v is the zero functional only when v is a multiple of 1).

2. (170) follows from (161) and (166). Indeed, for all $u \in \mathscr{L}^2$ and denoting $v = \tilde{R}_{x,\epsilon,\lambda} u$

$$(v,\, u)_{\mathscr{L}^2} = B_{x,\epsilon}(v,\, v) \geq (c_7 + \lambda) \left\| v \right\|^2_{\mathscr{L}^2}$$

(171) follows from (163) and the Poincaré inequality in a similar fashion.

3. Let us first define the operator $L_\epsilon : (R_\epsilon^{-1}(\mathscr{L}^2) + \langle 1 \rangle) \subseteq \mathscr{L}^2 \to \mathscr{L}^2$ by requiring

$$\begin{cases} \forall u \in H :\ L_\epsilon R_\epsilon u = u \\ L_\epsilon 1 = 0 \\ L_\epsilon \text{ is linear.} \end{cases}$$

It is easy to see that one then has for all $u \in D := (R_\epsilon^{-1}(\mathscr{L}^2) + \langle 1 \rangle)$ that $R_\epsilon L_\epsilon u = u - 1(u, 1) = P_H u$. It is proved in item 8 that D includes all smooth and compactly supported functions which are dense in $\mathscr{L}^2$. Next, we define $L_{x,\epsilon} : D \subseteq \mathscr{L}^2 \to \mathscr{L}^2$ through the action

$$L_{x,\epsilon} v = L_\epsilon u - \nabla_y [U(x) - U(0)] \cdot \nabla v.$$

which maps to $\mathscr{L}^2$ because of 90 and D-functions are H^0-integrable. Notice that $\forall u \in \hat{H}^0$

$$(u, (\lambda I - L_{x,\epsilon}) v) = B_\epsilon(u, v) + \int_M \rho_0 \left(u \partial_i (U(0) - U(x)) \partial^i v + \lambda u v \right) dy = B_{x,\epsilon,\lambda}(u, v)$$

so that $R_{x,\epsilon,\lambda}(\lambda I - L_{x,\epsilon}) v = v$. Since $R_{x,\epsilon,\lambda}$ is one-to-one and bounded, this means that $R_{x,\epsilon,\lambda}$ is the resolvent of $L_{x,\epsilon}$.

4. Let us fix a nested sequence $(C_n \subseteq M)_n$ of compact subsets of M with a smooth boundary (e.g. origin-centered disks with radius $< R$) such that $\cup_n C_n = M$. On the disk C_n let us solve the auxiliary boundary-value problem

$$\begin{cases} (\lambda + \frac{\mu}{\beta |y|^2}) - \ell_{x,\epsilon} u_n = v \\ \lim_{y \to x \in \partial C_n} u_n(y) = 0 \\ \text{ if } \mu \neq 0 \text{:}\ \lim_{y \to 0} u_n(y) = 0 \end{cases}$$

for a given smooth, compactly supported and non-negative $v \neq 0$ (we denote $r = \sup_{y \in \text{ supp } v} |y|$). This problem is standard and a strong C^∞ solution u_n exists provided the coefficients of $\ell_{x,\epsilon}$ are smooth ([184] p.70-73, [183]). In addition, the maximum principle implies that $u_n \geq 0$ (and is zero only at the boundary ∂C_n provided $C_n \cap \text{supp } v \neq \emptyset$) and

$$\left\| u_n \right\|_\infty \leq \frac{1}{\lambda + \frac{\mu}{\beta r^2}} \| v \|_\infty. \tag{173}$$

Moreover, the same maximum principle implies that $(u_n)_n$ is non-decreasing in n and therefore converges point-wisely to a positive function u_∞. Let us presently continue with the case $\mu = 0$ (and prove the statement about $R_{x,\epsilon,\lambda}$, the statement about $\tilde{R}$ is proved similarly).

It is a straightforward calculation to verify that u_∞ still solves $(\lambda I - \ell_{x,\epsilon})u_\infty = v$ in the weak sense. Elliptic regularity then again implies that $u_\infty \in C^\infty$. Now the equation

$$B_{x,\epsilon,\lambda}(\xi, u_\infty) = (\xi, v)$$

holds for every smooth, compactly supported ξ. But that set of functions is dense in $\hat{H}^0$ (Lemma F.6), so by the definition of $R_{x,\epsilon,\lambda}$ and (160) we can conclude that $u_\infty = R_{x,\epsilon,\lambda}v$ after verifying that $u_\infty \in \hat{H}^1$. But $\chi_n u_\infty$ (with χ_n specified as in Lemma F.3) is smooth and compactly supported, while by inspection of the expression (159) one can see $B_{x,\epsilon,\lambda}(\chi_n u_\infty, u_\infty) \to B_{x,\epsilon,\lambda}(u_\infty, u_\infty) + \frac{\theta}{2}(u_\infty, u_\infty)$. So we let $\theta \to 0$ and (161) implies

$$\begin{aligned} c_2\|u_\infty\|^2_{\hat{H}^0} \leq B_{x,\epsilon,\lambda}(u_\infty, u_\infty) = \limsup_{n\to\infty} B(\chi_n u_\infty, u_\infty) = \limsup_{n\to\infty}(\chi_n u_\infty, v) \\ \leq \|\chi_n u_\infty\|_{\mathscr{L}^2}\|v\|_{\mathscr{L}^2} \leq \|u_\infty\|_\infty \|v\|_\infty \leq \lambda^{-1}\|v\|^2_\infty \end{aligned}$$

(where we used (173) for the last inequality). So $R_{x,\epsilon,\lambda}v = u_\infty > 0$. This finishes the proof that $R_{x,\epsilon,\lambda}$ maps smooth, compactly supported, non-negative functions to positive functions. Since $R_{x,\epsilon,\lambda}$ is a continuous operator and because of Lemma (F.6), the assumption of v being smooth and compactly supported can be dropped by a density argument: A non-zero, non-negative function $v \in \mathscr{L}^2$ is the $\mathscr{L}^2$-limit of an increasing sequence $(v_n)_n$ of non-negative, smooth, compactly supported functions. Since $R_{x,\epsilon,\lambda}v_n$ is, by the foregoing, itself an increasing sequence of positive functions, the limit $R_{x,\epsilon,\lambda}v$ is positive as well.

5. Proved already during the proof of item 3.

6. Proved already during the proof of item 3.

7. One has (for all $u \in \mathscr{L}^2$, $v \in H^0$)

$$\forall u \in \mathscr{L}^2,\, v \in H^0 : (R_\epsilon u, v) = B_{-\epsilon}(R_\epsilon u, R_{-\epsilon}v) \underbrace{=}_{(156)} B_\epsilon(R_{-\epsilon}v, R_\epsilon u) = (R_{-\epsilon}v, u)$$

But H^0 is dense in H and $(R_\epsilon u, 1) = 0 = (1, R_{-\epsilon})$ so that $(R_\epsilon u, v) = (u, R_{-\epsilon}v)$ holds true for all $v \in \mathscr{L}^2$

$$\forall u, v \in D : (u, (\lambda I - L_{0,\epsilon})v) = B_{0,\epsilon,\lambda}(u, v) = B_{0,-\epsilon,\lambda}(v, u) = (u, (\lambda I - L_{0,-\epsilon})v)$$

8. It follows from (157) that for all u smooth and compactly supported

$$(u,\, \ell_{0,\epsilon})v) = -B_\epsilon(u, v). \tag{174}$$

But since the compactly supported smooth functions are dense in $\hat{H}^0$ and because of (160), (174) holds for all $u \in \hat{H}^0$. In particular,

(a) (174) holds for all $u \in H^0$.

(b) $(1,\, \ell_{0,\epsilon}v) = -B_\epsilon(1, v) = 0$

therefore $\ell_{0,\epsilon}v = L_{0,\epsilon}v$. But through the way we have defined $L_{x,\epsilon}$, also the equality $\ell_{x,\epsilon}v = L_{x,\epsilon}v$ follows.

□

Corollary F.1. *(Feller semigroup) The operator $L_{x,\epsilon}$ generates a positive, strongly-$\mathscr{L}^2$-continuous contraction semi-group $(S_{x,\epsilon}(t))_{t\geq 0}$. In addition, probability-conservation holds:*

$$S(t)1 \equiv 1$$

Proof. From (170) we deduce that the resolvent of $L_{x,\epsilon}$, is bounded in accordance with the assumptions of the Hille-Yosida Theorem for strongly-continuous contraction semigroups. That implies the existence and uniqueness of the generated semigroup S. Positivity of this semigroup (i.e. $\forall t \geq 0 :\ f(\in \mathscr{L}^2) \geq 0 \Rightarrow S_{x,\epsilon}(t)f \geq 0$) follows from the Hille-Yoshida identity

$$S_{x,\epsilon}(t) = \lim_{\lambda\to\infty} e^{-\lambda t} e^{\lambda^2 t R_{x,\epsilon,\lambda}} \tag{175}$$

the positivity of the resolvents (item 2 of Theorem (F.1)) and the Taylor-formula for the exponential of a bounded operator. The probability-conservation property follows again from (172), (175) and the Taylor formula for the exponential. □

Lemma F.6. *The set of smooth, compactly supported functions is dense in $\hat{H}^0$.*

Proof. It suffices to prove the following three steps:

1. For every $u \in \hat{H}^0$, there is a sequence $(u_n)_n$ of bounded $\hat{H}^0$-functions converging to u.

2. For every bounded $\hat{H}^0$-function v there is a sequence of compactly supported $\hat{H}^0$-functions (v_n) converging to v.

3. A compactly supported $\hat{H}^0$-function can be approximated by smooth counterparts.

The first step is proved as follows: consider a sequence $\kappa_n : \mathbb{R} \to \mathbb{R}$ of compactly supported functions with $\kappa_n \to Id : s \mapsto s$ as $n \to \infty$ and moreover $s\kappa_n(s) > 0$ unless $s = 0$. This sequence is tuned in such a way that $s \mapsto (\kappa_n'(s)-1)^2$ is uniformly bounded by some $K > 0$. Then for any $u \in \hat{H}^0$, $u_n := \kappa_n \circ u$ is bounded and

$$\|u_n - u\|^2_{\hat{H}^0} = \int_M \rho_0 \left\{(\kappa_n'(u) - 1)^2(\nabla u)^2 + (\kappa_n(u) - u)^2\right\} dy \tag{176}$$

The integrand in the RHS is pointwise bounded by the integrable function $K(\nabla u)^2 + u^2$, so that the dominated convergence theorem implies that (176) converges to zero.
The second step is proved as follows: approximate the bounded $\hat{H}^0$-function u by $\chi_n u$ where $(\chi_n)_n$ is the sequence constructed in Lemma (F.3). It is straightforward to prove that $\|u - \chi_n u\|_{\hat{H}^0} \to 0$.
The third step is standard and treated in many standard PDE textbooks.
Virtually the same proof applies for H^1 after one identifies that space with the radial vectorfields with components in H^0 (lemma (F.1)). The only required modification is that in (176) one uses the $\|\|_{H^0}$ norm so that the second term of the RHS is not there. □

Proposition F.2. *Let φ be a radial $\mathscr{L}^2$-function, then $f^i = \varphi\hat{y}^i$ is in $\mathscr{L}^2$ and $(\forall \epsilon \in \mathbb{R})$*

$$\hat{y}_i(R_0 f^i)(y) \equiv (\tilde{R}\varphi)(y)$$

Proof. Pick any H^1-function u, by lemma F.1 $\tilde{R}\varphi \in H^1 \Rightarrow (\tilde{R}\varphi)\hat{y}^i \in H^0$ and therefore

$$\tilde{B}(u,\, \tilde{R}\varphi) = (u, \varphi) = (u\hat{y}_i,\, \varphi\hat{y}^i) = B_0(u\hat{y}_i,\, R_\epsilon(\varphi\hat{y}^i)) = \beta^{-1}(u\hat{y}_i,\, R_\epsilon(\varphi\hat{y}^i))_{H^0}$$
$$\underbrace{=}_{(153)} \beta^{-1}(u,\, \hat{y}_i R_\epsilon(\varphi\hat{y}^i))_{H^1} = \tilde{B}(u,\, \hat{y}_i R_\epsilon(\varphi\hat{y}^i)),$$

so that

$$\tilde{B}(u,\, [(\tilde{R}\varphi) - \hat{y}_i(R_\epsilon f^i)]) = 0$$

Taking $u = \tilde{R}\varphi - \hat{y}_i(R_\epsilon f^i)$ (which is radial of course) and considering (165) then yields the desired result. □

G Proof of Theorem 6.3

Proof. Let us first prove that $\nu_{x,\epsilon}$ is well-defined and in $H^0 \cap \mathscr{L}^2$. Note that

$$\left\|L_{0,-\epsilon}^{-1}F_x\right\|_{H^0} := \sup_{u\in H^0}\frac{\left\|L_{0,-\epsilon}^{-1}F_x u\right\|_{H^0}}{\|u\|_{H^0}} \leq \left(\sup_{u\in\mathscr{L}^2}\frac{\left\|L_{0,\epsilon}^{-1}u\right\|_{H^0}}{\|u\|_{\mathscr{L}^2}}\right)\left(\sup_{v\in H^0}\frac{\|F_x v\|_{\mathscr{L}^2}}{\|v\|_{H^0}}\right) \leq k_4(x)k_F(x) =: k_S(x).$$

This together with $L_{-\epsilon}^{-1}F_x 1 \in H^0$ implies that

$$\left\|(L_{-\epsilon}^{-1}F_x)^n 1\right\|_{H^0} \leq (k_S(x))^{n-1}\left\|L_{-\epsilon}^{-1}F_x 1\right\|_{H^0}.$$

So define the radius $R_\rho > 0$ so that $\forall x \in B(0,\epsilon) : |x| < R_\rho \Rightarrow k_S(x) < 1$. Then for $x \in B(0,R_\rho)$, the partial sums associated to the sequence (100) constitute a Cauchy sequence in H^0. H^0 is a Hilbert space and therefore the limit $\nu_{x,\epsilon} \in H^0$. By the Poincaré inequality (95) $\nu_{x,\epsilon} \in \mathscr{L}^2$.

To prove the stationarity (101), it suffices to prove the more general identity

$$B_{x,\epsilon}(\nu_{x,\epsilon}, u) = 0 \tag{177}$$

for all $u \in \hat{H}^0$. Note that F_x was defined in such a way that when u is smooth and compactly supported and $v \in H^0$, then

$$B_{x,\epsilon}(v,u) - B_{0,\epsilon}(v,u) = -(F_x v, u)$$

Therefore, sticking to u smooth and compactly supported

$$\begin{aligned}
B_{x,\epsilon}(\nu_{x,\epsilon},u) &= B_{x,\epsilon}\left(\lim_{N\to\infty}\sum_{n=0}^{N}(L_{-\epsilon}^{-1}F_x)^n 1,\, u\right) = \lim_{N\to\infty}\sum_{n=0}^{N}B_{x,\epsilon}\left((L_{-\epsilon}^{-1}F_x)^n 1,\, u\right)\\
&= \lim_{N\to\infty}\sum_{n=0}^{N}\left\{B_{0,\epsilon}\left((L_{-\epsilon}^{-1}F_x)^n 1,\, u\right) - \left(F_x(L_{-\epsilon}^{-1}F_x)^n 1,\, u\right)\right\}\\
&= \lim_{N\to\infty}\left\{\sum_{n=1}^{N}B_{0,-\epsilon}\left(u,\,(L_{-\epsilon}^{-1}F_x)^n 1\right) - \sum_{n=0}^{N}\left(F_x(L_{-\epsilon}^{-1}F_x)^n 1,\, u\right)\right\}\\
&= \lim_{N\to\infty}\left\{\sum_{n=1}^{N}\left(u,\,(F_x L_{-\epsilon}^{-1})^{n-1}F_x 1\right) - \sum_{n=0}^{N}\left(F_x(L_{-\epsilon}^{-1}F_x)^n 1,\, u\right)\right\}\\
&= -\lim_{N\to\infty}(F_x(L_{-\epsilon}^{-1}F_x)^N 1,\, u) = 0.
\end{aligned}$$

Since (177) holds for all u smooth and compactly supported, lemma F.6 and (160) imply that the identity holds for all $u \in \hat{H}^0$.

Finally, to check (102), note that

$$\left\|\nu_{x,\epsilon} - 1 - L_{-\epsilon}^{-1}F_x 1\right\|_{\mathscr{L}^2} \leq c^{-1}\left\|\nu_{x,\epsilon} - 1 - L_{-\epsilon}^{-1}F_x 1\right\|_{H^0} \leq c^{-1}\sum_{n=2}^{\infty}\left\|(L_{-\epsilon}^{-1}F_x 1)^n\right\|_{H^0} \leq c^{-1}k_S(x)$$

So far we have achieved establishing that $\nu_{x,\epsilon}$ solves (177) and is therefore stationary. To prove that it is unique in this respect,
suppose there were another density $\tilde{\rho}_{x,\epsilon}$ such that $\frac{\tilde{\rho}_{x,\epsilon}}{\rho_0} \in \mathscr{L}^2$ and

$$\left(\frac{\tilde{\rho}_{x,\epsilon}}{\rho_0},\, L_{x,\epsilon}u\right)$$

for all $u \in D$.
Then $\exists \lambda \in \mathbb{R}$ such that

$$\nu_{x,\epsilon} := \frac{\tilde{\rho}_{x,\epsilon}}{\rho_0} + \lambda \frac{\rho_{x,\epsilon}}{\rho_0} \in H$$

Suppose (seeking a contradiction) that $\nu_{x,\epsilon} \neq 0$ and define $v = L_\epsilon^{-1}\nu_{x,\epsilon}$. Then $\nu_{x,\epsilon} = L_\epsilon v$ and therefore

$$(\nu_{x,\epsilon}, L_\epsilon v) = (\nu_{x,\epsilon}, \nu_{x,\epsilon}) > 0.$$

But since

$$\|(L_{x,\epsilon} - L_\epsilon)v\|_{\mathscr{L}^2} = \|\nabla\left(U(x) - U(0)\right) \cdot \nabla v\|_{\mathscr{L}^2} \leq k_1(x)\|v\|_{H^0},$$

we then obtain

$$\begin{aligned}(\nu_{x,\epsilon}, L_{x,\epsilon}v) \geq (\nu_{x,\epsilon}, L_\epsilon v) - k_1(x)\|\nu_{x,\epsilon}\|_{\mathscr{L}^2}\|v\|_{H^0} = (\nu_{x,\epsilon}, \nu_{x,\epsilon}) - k_1(x)\|\nu_{x,\epsilon}\|_{\mathscr{L}^2}\|L_\epsilon^{-1}\nu_{x,\epsilon}\|_{H^0} \\ \geq (1 - k_1(x)k_4(x))\|\nu_{x,\epsilon}\|^2_{\mathscr{L}^2}.\end{aligned}$$

For x sufficiently small, the RHS (and therefore the LHS is positive). But we then arrive at the following contradiction

$$0 < (\nu_{x,\epsilon}, L_{x,\epsilon}v) = \left(\frac{\tilde{\rho}_{x,\epsilon}}{\rho_0},\, L_{x,\epsilon}v\right) - \lambda\left(\frac{\rho_{x,\epsilon}}{\rho_0},\, L_{x,\epsilon}v\right) = 0.$$

□